INFORMATION TO USERS

This manuscript has been reproduced from the microfilm master. UMI films the text directly from the original or copy submitted. Thus, some thesis and dissertation copies are in typewriter face, while others may be from any type of computer printer.

The quality of this reproduction is dependent upon the quality of the copy submitted. Broken or indistinct print, colored or poor quality illustrations and photographs, print bleedthrough, substandard margins, and improper alignment can adversely affect reproduction.

In the unlikely event that the author did not send UMI a complete manuscript and there are missing pages, these will be noted. Also, if unauthorized copyright material had to be removed, a note will indicate the deletion.

Oversize materials (e.g., maps, drawings, charts) are reproduced by sectioning the original, beginning at the upper left-hand corner and continuing from left to right in equal sections with small overlaps.

Photographs included in the original manuscript have been reproduced xerographically in this copy. Higher quality 6" x 9" black and white photographic prints are available for any photographs or illustrations appearing in this copy for an additional charge. Contact UMI directly to order.

Bell & Howell Information and Learning
300 North Zeeb Road, Ann Arbor, MI 48106-1346 USA

UMI®
800-521-0600

Control of Flexible–Link Manipulators Using Nonlinear H_∞ Techniques

Mohammad J. Yazdanpanah

A Thesis

in

The Department

of

Electrical and Computer Engineering

Presented in Partial Fulfillment of the Requirements

for the Degree of Doctor of Philosophy at

Concordia University

Montréal, Québec, Canada

August 1997

ABSTRACT

Control of Flexible–Link Manipulators Using Nonlinear H_∞ Techniques

Mohammad J. Yazdanpanah

Most engineering systems encountered in practice exhibit significant nonlinear behavior. For control of systems exhibiting nonlinearities, the normal design procedure is to construct a linearized approximation of the process model followed by the application of a linear control methodology. This procedure, however, can yield unsatisfactory performance, especially when the system is highly nonlinear and undergoes large motions, that is, it operates over wide nonlinear dynamical ranges, as is often the case in the problems of attitude control, advanced aircraft control, and the control of robotic manipulators. Furthermore, most systems are seldom completely known and therefore, their mathematical models should include some uncertain parts. The control of an uncertain system is required to be *robust* with respect to modeling uncertainties. *Robust control* strives to characterize the uncertainty in the model of the plant and to evaluate the degrees of freedom left to achieve the control task within specified bounds.

This dissertation is concerned with the control of a highly complicated and nonlinear system, namely, a flexible-link manipulator. The general procedure taken in this regard is to develop, design and analyze nonlinear H_∞ techniques applied to flexible-link manipulators.

For the purpose of robust control of an uncertain model of the flexible-link manipulator two types of modeling are studied. In the first type, uncertainty is due to parameter variations of the manipulator while performing a task or when its

configuration is changing. The uncertainties considered in this regard may be L_2 bounded and/or constant. In the second type of modeling, a new look at the notion of flexibility in robotic manipulators is presented. Based on this interpretation, flexible structures exhibit two kinds of behavior, one of which may be treated as a disturbance acting on the modeled dynamics.

For designing the nonlinear H_∞ controller, the approximate polynomial solution of the Hamilton-Jacobi-Isaacs (HJI) inequality for a general nonlinear system is derived. Also by exploiting the stability properties of perturbed systems, qualitative behavior of nonlinear H_∞ controllers is considered.

ACKNOWLEDGEMENTS

During my graduate studies at Concordia, I have had the assistance of many people.

First and foremost among them have been Professors K. Khorasani and R.V. Patel, my advising supervisors. I wish to express my sincere gratitude and profound appreciation to them for their great enthusiasm, precious guidance and constructive criticism in the course of my doctoral research at Concordia.

I would like to extend a special note of thanks to the other members of my examining committee for their valuable comments, which improved the quality of the final version of the thesis.

I am also grateful to my friends in the Department of ECE with whom I have had useful discussions on the subject.

Finally, my heartfelt thanks to my family for their wholehearted support and encouragement throughout this endeavor.

TABLE OF CONTENTS

LIST OF FIGURES

LIST OF TABLES

LIST OF SYMBOLS

$M(\theta, \delta)$	Positive-definite symmetric inertia matrix
θ	Vector of joint variables
δ	Vector of modal amplitudes
$n_1(\theta, \dot{\theta}, \delta, \dot{\delta})$	Coriolis forces
$n_2(\theta, \dot{\theta}, \delta, \dot{\delta})$	Centrifugal forces
F_c	Coulomb friction
F_h	Hub damping
F_g	Gravity effect
K_s	Stiffness matrix
u	Control input
L_0	Length of the link
A_0	Link cross-sectional area
ρ	Mass per unit length of the link
E	Young's modulus of elasticity of the material of the link
I	Moment of inertia of the cross section of the link (Z-axis)
M_L	Payload mass
J_L	Payload inertia
m_b	Link mass
I_0	Joint actuator inertia
J_0	Link inertia relative to the joint
$\xi = \eta / L_0$	Normalized position along the link
$w(\xi, t)$	Deflection of the link at position ξ and time t
$\phi(\xi)$	Normalized clamped-free eigenfunction
$\phi'(\xi)$	Derivative of $\phi(\xi)$ with respect to ξ
$\Phi(\xi)$	Vector of ϕ's
m	Number of deflection modes

C_{coul}	Amplitude of the sigmoid function in F_c
$\hat{\kappa}$	Slope of the sigmoid function in F_c
$[f, g, k, h]$	System vector fields and functions (nonlinear)
$[F, G, K, H]$	System matrices (linear)
$V(x)$	Storage (value) function
$s(u, y)$	Supply rate
γ	Attenuation level
$p^T(x)$	Gradient of $V(x)$ with respect to x, i.e., $V_x(x)$
$H(x, p, w, u)$	Hamiltonian function
w^*, u^*	Saddle point of the Hamiltonian function
$(.)^{[d]}$	d^{th}–order truncated polynomial of (.)
$(.)^{(d)}$	d^{th}–order polynomial component of (.)
$\hat{w}$	L_2 bounded uncertainty in the flexible link manipulator
(ω_i, ξ_i)	Frequency and damping ratio of the ith deflection mode
$\frac{1}{\beta}$	Total inertia about the armature
$RRH_\infty C$	Robust regulation with an H_∞ constraint
$RRGBU$	Robust regulation in the presence of gain-bounded uncertainty

Chapter 1

Introduction

The field of control theory has a rich heritage of intellectual depth and practical achievements. From a simple temperature regulator, to the space probes and the automated manufacturing plants of today, control systems have played a key role in technological and scientific advancements.

In engineering and decision-making systems, the paradigm of feedback control addresses the problem of using the information about the output (effect) to design or modify the input (cause) for a given task. Tasks range from controlling a robotic manipulator to grasping an object to stabilizing a large space structure. The complexity of control for even a small-scale system such as a compact disk drive may be due to the very stringent accuracy and speed requirements. In large-scale systems, the task of meeting rigorous performance requirements is much more challenging because of the uncertainty of the system model and its environment.

Most engineering systems encountered in practice exhibit significant nonlinear behavior. For systems exhibiting nonlinearities, the normal design procedure is to employ a linearized approximation of the process model followed by the application of a linear control methodology. However, this procedure can yield unsatisfactory performance, especially when the system is highly nonlinear and undergoes large motions, and thus operates over wide nonlinear dynamical regimes, as is often the

case in the problems of attitude control, advanced aircraft control, and the control of robot manipulators. During the past fifteen years, there has been considerable progress in the understanding of *nonlinear systems*, primarily due to the application of mathematical concepts derived from the field of differential geometry. There has been substantial work on qualitative concepts, such as controllability and observability for nonlinear systems. Techniques for the control of nonlinear systems described by nonlinear mathematical models were difficult to find until a major breakthrough occurred during the past decade with the development of solutions to such problems as *disturbance decoupling, input-output decoupling,* and *feedback linearization.* Feedback linearization utilizes state and feedback transformations to transform a nonlinear system into an equivalent linear system so that the standard well-known linear control tools may be used for design. This technique has been successfully applied to very difficult problems such as controlling aircraft with multi-axis nonlinear dynamics and tracking in robot manipulators that have highly nonlinear dynamics.

In addition to being nonlinear, most realistic systems are seldom completely known. Control theorists are now challenged to expand their concepts and schemes to be applicable to incompletely modeled nonlinear systems. A control theory for incompletely known systems and systems described by non-traditional models will produce a wider repertoire of control laws, algorithms, and strategies.

In the presence of model uncertainty and unmeasurable disturbances it has been found that the use of *feedback control* can satisfy performance specifications, whereas open-loop control simply cannot meet stringent command-following and/or disturbance rejection requirements. Thus the most fundamental reason for using *feedback* is to guarantee good performance in the presence of *uncertainty*; also, feedback is used to enable operating conditions, i.e., to stabilize unstable plants. Care must be exercised so that feedback system is *reliable*, i.e., that it should continue to operate in the presence of hardware and software failures.

Uncertainty and achievable performance tend to oppose each other, even though

the very reason for using feedback is to obtain better performance over open-loop control. The controller is required to be *robust* with respect to modeling uncertainty and to *adapt* to slow changes in the system dynamics. *Robust control* strives to characterize the uncertainty in the model of the plant to be controlled and to evaluate the degrees of freedom left to achieve the control task within specified bounds. Considerable efforts have been made in the literature to satisfy the *stability robustness* requirement, that is to guarantee closed-loop stability under a wide range of plant variations and disturbances. Bounds under which stability can be preserved have been derived and a rigorous mathematical theory has been developed to minimize sensitivity with respect to disturbances and norm-bounded uncertainty. More research is under way to reduce the conservatism of available stability robustness results. Specifically, the "directional information" [1, 2] should be exploited to decrease the conservatism of results. The payoff will be improved performance, because in the linear systems, for instance, stability robustness tends to limit the bandwidths of the closed-loop system, and thereby deteriorate command-following and/or disturbance-rejection performance.

A new and relevant topic in this respect is the notion of *performance-robustness*. This issue is concerned with the characterization of and feedback design in the presence of the so called "structured" and/or "unstructured" uncertainties to meet predefined performance specifications. Meanwhile, it should be guaranteed that these performance specifications will be met by a fixed controller for any value of the plant "structured/unstructured" uncertainty in *a prior* known plant set which is defined in an appropriate topology.

One of the important classes of plants is the class of *distributed parameter* systems in which the variables of importance depend on both spatial and time variations. Such systems are usually modeled by partial or integro-differential equations. Large flexible space structures and flexible robots are examples of such systems. Although there has been considerable progress in understanding the stabilization

of distributed parameter systems, and in the development of fast algorithms and computational schemes specifically for control of systems governed by partial and integro-differential equations, there remains a number of theoretical and practical problems that must be considered before distributed parameter control becomes a systematic tool for the design of these complex systems.

The development of models specifically suited for control design and analysis is an important area of current research. for example, the sensors and actuators which may be used on flexible structures can strongly affect the dynamic performance of the structure, and this must be taken into account both in the design of the structure and in the design of the control system.

Due to infinite dimensional nature of distributed parameter models, and since inherent damping is small in the applications mentioned above, it is essential to develop new identification schemes, robustness criteria, and easily implementable control algorithms.

This dissertation is concerned with the control of a typical example of a distributed parameter system, namely, a flexible-link manipulator. The general procedure taken in this regard is the H_∞ technique in its nonlinear setting. The dissertation is organized as follows. The next section of this chapter presents a review of and a general perspective on the related work that has appeared so far in the literature on the control of flexible-link manipulators. Chapter 2 presents a dynamical model of a flexible-link manipulator. Analytical models of a single-link as well as multi-link flexible manipulators are derived. Chapter 3 introduces the problem of nonlinear H_∞ control. Connections of the topic to some basic notions like dissipativeness, differential games, and the Hamiltonian function are discussed. An approximate solution of Hamilton-Jacobi-Isaacs inequality is also obtained. In Chapter 4 the domain of validity of nonlinear H_∞ control is discussed. Using a Lyapunov technique, it is shown that the nonlinear feedback controller always results in a larger domain of validity than its linearized counterpart. Uncertainty compensation for

a flexible-link manipulator is the subject of Chapter 5. For the purpose of robust control, constant as well as L_2-bounded deviations of parameters from their nominal values are considered as uncertainties. Chapter 6 deals with a new methodology for modeling a flexible-link manipulator with an arbitrarily large (infinite) number of deflection modes. In this regard, a part of dynamics representing flexibility is treated as *uncertainty*. In Chapter 7, nonlinear robust regulation based on the new modeling approach is studied which is an extension of the results of the previous chapter. Chapter 8 concludes the dissertation by specifying several directions for future work.

1.1 Perspective

In many industrial applications, robots are designed to achieve precise positioning of the end-effector with relatively simple control algorithms. For example, in applications such as welding, spray painting and laser cutting, the controller is typically supposed to be capable of accurately reproducing pre-planned smooth trajectories [3]. This accuracy is guaranteed by current robots at the expense of a rigid and massive mechanical structures. Recently, the use of lightweight flexible arms has been proposed as offering potential benefits such as increased payload-to-arm mass ratio, faster executable motions and lower energy consumption [4]. Flexible mechanisms are important in space structure applications, where large, lightweight robots are utilized in a variety of tasks, including deployment, spacecraft servicing, space station maintenance, etc. Flexibility is not designed into the mechanism; it is usually an undesirable characteristic which results from trading off mass and length requirements in optimizing the mechanical structure of a robot [5]. Although a robot with lightweight links has intrinsically compliant behavior allowing smooth contacts, the flexibility of lightweight links cannot be neglected, and this makes the control problem much more complex.

One of the early papers to discuss some fundamental issues in flexible structure control is by Gevarter [6]. The paper illustrates the crucial role of the location of the actuator and sensor in a flexible structure. In flexible structure control parlance, when the sensor and actuator are at the same spatial location, the setup is referred to as colocated control and when sensing and actuation occur at different locations, the scheme is called noncolocated control. In the noncolocated case, the system's zero dynamics [7] are unstable. If a linear version of the system is considered, this situation corresponds to a transfer function whose inverse dynamics represent an unstable system. Colocated proportional derivative (PD) control at either end of the structure ensures stability to parametric variations within a certain bound. This type of control, however, just adds damping to the rigid mode while other modes remain relatively unaffected [8].

Different approaches are available for deriving the dynamics of flexible manipulators. The model may be obtained from the distributed parameter model of the flexible robot [9], from a discrete model in space and in time [10], or from a discrete model in space and continuous in time as performed in the current literature. This last method may be divided into four major categories: Euler-Bernoulli and modal expansion [11], Lagrange equations and modal expansion [12], Hamiltonian and energy equations [13] and finite elements [14, 15, 16].

In this dissertation, a dynamical model is considered for a single-link flexible manipulator using the Euler-Bernoulli beam theory as studied in [17, 18, 19, 20, 21]. One way of minimizing the effect of the elastic displacements of large amplitude in flexible manipulators is to choose, for instance, materials which are able to stiffen the structure or to damp the vibrations [22]. Another solution consists of developing open-loop elastic displacements of the structure [23, 24]. In these methods, however, it is not possible to take disturbances into account.

A variety of control techniques have been used by researchers to control flexible manipulators. The results vary in accuracy and robustness to parameter variations

and exogenous inputs. Among these techniques, one finds linear quadratic Gaussian (LQG) and linear quadratic regulator (LQR) [11], PID [25], optimal control [26], adaptive control [27, 28, 29, 30], singular perturbation [31, 32, 33, 34, 35] and H_∞ [36, 37, 38, 39].

It is worth noting that in spite of its many attractive properties, the LQG compensators do not yield good robustness and performance. In fact, it was shown in [40] that LQG designs can exhibit poor stability margins. Moreover, even when coupled with loop transfer recovery (LTR), the resulting LQG/LTR does not work well with non-minimum phase systems [41].

It should be mentioned that the recent work in the area of two-time scale (singular perturbation) approaches for vibration suppression in flexible mechanical structures shows promise [42, 43, 44]. The control objective in this investigation and the primary focus are on the rejection of small deflections after larger slew motions are complete. In [42] a linear mathematical model of a flexible-link manipulator is expressed in a standard singularly perturbed form. The concept of the integral manifold is utilized to design a dynamical composite control strategy to guarantee a minimum-phase closed-loop system restricted to the manifold, resulting in controlling the tip position to an arbitrary degree of accuracy by just measuring the hub angle and the tip position. The authors of [44] develop a nonlinear control strategy for approximate tip-position tracking of a class of flexible multi-link manipulators based on the concept of integral manifolds and singular perturbation theory. The development is along the lines stated in [42] and [43] which is applicable to the linear dynamics of a single-link flexible arm. The approach is based on the more appropriate *nonlinear* framework, and is applicable to a class of multi-link flexible manipulators. The conditions that guarantee small tracking errors and closed-loop system stability are given. Inherent in the singular perturbation technique is the need for accurate models of the system dynamics.

Other recent approaches to the problem of flexible robot control include the

work in [45] for the use of linear (state feedback) techniques where a fast state estimator is employed in small-angle movements and in [46] where gross-motion movements for a single flexible-link are studied in the case of adaptation for payload tasks. A different form of "output redefinition" by "feedthrough" compensation to assign transmission zeros and the experimental verification of the results are given in [20]. In [47], the authors develop a nonlinear adaptive control scheme for a discrete-time model of a single-link flexible manipulator. The discrete-time model of the system is derived using a forward difference method (Euler approximation). The output re-definition method is used so that the resulting zero dynamics is guaranteed to be exponentially stable. It is assumed that the "payload mass" is unknown but its upper bound is known *a priori.*

The controller developed in [48] uses a nonlinear inversion (feedback linearization) control law for rigid dynamics, with separate loops for flexure effects. The study in [49] investigated and compared time-domain and frequency domain identification techniques on a single-link robot, and the work in [50, 51] developed time- and frequency-domain identification and control schemes for payload adaptation, which were later employed on a two-link apparatus [52].

An inverse dynamics control strategy for tip position tracking of flexible multi-link manipulators is presented in [53]. This paper presents an inverse dynamics control strategy to achieve small tracking errors for a class of multi-link structurally flexible manipulators. This is done by defining new outputs near the end points of the arms as well as by augmenting the control inputs by terms which ensure stable operation of the closed-loop system under specific conditions. In [54], the authors present an observer-based inverse dynamics control strategy that results in small tip-position tracking errors for a class of multi-link structurally flexible manipulators. The control strategy developed in [53] requires measurements of rates of change of flexible modes with time that are not conveniently measurable. The observer-based controller alleviates this difficulty. The work reported in [55] focuses

on the experimental implementation of an observer-based decoupling control strategy for tip-position tracking of a class of multi-link flexible manipulators. Since the rates of change of flexible modes are required, a nonlinear observer is implemented to estimate these variables. Inverse dynamics sliding control of flexible multi-link manipulators is reported in [56]. Motivated by the concept of a *sliding surface* in variable structure control, a robustifying term is developed to drive the nonlinear plant's error dynamics onto a sliding surface. On this surface, the error dynamics are then independent of parametric uncertainties. In order to avoid over excitation of higher frequency flexural modes due to control chattering, the discontinuous functions normally used in classical sliding mode control are replaced by saturation nonlinearities at the outset. This also facilitates analysis by the standard Lyapunov techniques.

In the recent work of [8], the authors present an LQG/H_∞ controller synthesis for a flexible single-link manipulator with noncolocated sensing. In the inner-loop an LQG controller provides adequate damping to the flexible modes while the outer-loop H_∞ controller provides stability in the face of unstructured perturbations.

In [57] authors report experimental results for the end-effector control of a single flexible robotic arm using several approaches: PD, feedback linearization, linear quadratic regulator (LQR), singular perturbation and sliding modes techniques. Comparison is made based on computational complexity, sensitivity to disturbances, complexity of tuning and damping of the flexible variables. Although this study is not concerned with theoretical issues, it roughly infers that singular perturbation and sliding modes control result in better performance compared to the other methods.

A feed-forward design methodology to compensate for unstable zeros in linear discrete-time systems with tracking objectives is considered in [58]. Based on this methodology, an experimental study for end-point tracking of a flexible beam is performed. The method exploits the fact that non-causal expansion of unstable

inverse dynamics is convergent in the region of the complex plane encompassing the unit circle.

Another technique for flexible robot control is input command shaping, where the system inputs (e.g., motor voltages) are "shaped" in such a manner that minimal energy is injected into the flexible modes of the system [59]. Some results using input-shaping with outer-loop disturbance rejection controller for a two-link robot were reported in [60]). In [61] experimental verifications of input shaping schemes for controlling the endpoint movement of a large two-link robot were addressed and in [62] an adaptive algorithm was implemented on a single-link apparatus. In [63] forcing functions are developed to produce vibration-free motions in flexible systems. These forcing functions are constructed from ramped sinusoid basis functions so as to minimize excitation in a range of frequencies surrounding the system natural frequency. It is well known, however, that the primary difficulty of such schemes lies in the fact that they are open-loop strategies and require relatively precise knowledge of the system dynamics. Any attempt to improve robustness to uncertainties (such as placing the shaper in the loop or increasing the filter order) results in delays in the system response, which may or may not be tolerable.

While most of the work to date for control of flexible-link robotic systems has used conventional control techniques, there has been recent interest in the literature in using intelligent control strategies. Fuzzy logic and neural networks have been investigated for flexible robotic mechanisms. For example the paper [64] uses fuzzy logic for a fast-moving single-link apparatus, focusing on smooth, rigid body motion control. In [65] a fuzzy learning control approach is used for the same laboratory test bed. The focus there is on automatic synthesis of a direct fuzzy controller and its subsequent tuning when there are payload variations. In [66, 67] a fuzzy logic supervisory level is used for lower-level conventional controller selection and tuning. Motivated by the success of these studies, the control schemes in [5] builds on the idea of supervising lower level controllers in a hierarchy so as to improve on

all previous results by using rule-based controllers at the lower level (this paper is actually an expanded version of the work reported in [68]).

In the area of application of neural networks for controlling a flexible-link manipulator one may refer to [69] and [70]. The former presents a design methodology for an on-line self-turning adaptive control of a single flexible-link manipulator using back-propagation neural networks. The particular problem discussed is the on-line system identification of a flexible-link manipulator using back-propagation neural networks and the on-line self-turning adaptive control of a flexible-link manipulator using a separate neural network as a controller. A finite-element model of a flexible-link manipulator is used. The pseudo-link concepts developed in [71, 72] are used to determine on-line angular displacement of the end effector of the flexible-link manipulator. The object of the latter is to achieve tracking control of a partially known flexible-link robot arm. It is shown how to stabilize the internal dynamics by selecting a physically meaningful modified performance output for tracking. The controller is composed of a singular-perturbation-based fast control and an outer-loop slow control. The slow subsystem is controlled by a neural network for feedback linearization, plus a PD outer-loop for tracking, and a robustifying term to assure the closed-loop stability. Experimental evaluation of neural network-based controllers for tip position tracking of a flexible-link manipulator is reported in [73]. The control is designed by using the output re-definition approach. Three different neural network schemes are examined. None of the schemes requires full state measurements.

It should be noted that although intelligent control techniques may present some interesting results from an engineering point of view, their theoretical foundations (e.g., stability and reachability analysis) need further investigation.

Having reviewed the above mentioned techniques for controlling flexible-link manipulators, we may divide these methods into three major categories: Linear, intelligent and nonlinear. It is a fact that linear control techniques even for nonlinear

plants, may result in some desirable performance. However, the convergence and stability properties are restricted to a particular region in the state-space. Intelligent control-based techniques, on the other hand, suffer from a sound theoretical justification. Nonlinear control techniques offer more reliable results as compared to the other methods. Although these results may not be global, the region of desirable operation is larger than that provided by linear controllers. Exact knowledge of the plant is one of the main limitations in applying most nonlinear techniques. If the dynamics are not precisely known and/or the mathematical model for synthesis is somehow different from that of the actual plant, the controller should be responsible for operating in such a manner that can cover a variety of plants in a neighborhood of the nominal plant with respect to the relevant topology. The above discussion opens the avenue for developing robust nonlinear control which is the subject of the present dissertation.

Chapter 2

A Flexible-Link Manipulator Model

The purpose of this chapter is to provide a dynamical model for a flexible-link manipulator. Although affine, the dynamical model for a flexible-link manipulator is highly nonlinear. Therefore, the synthesis of a nonlinear controller based on such model is very complicated. The design, however, may be simplified if certain state-dependent functions are zero or constant. For this purpose, a nonlinear dynamical model of a flexible-link manipulator that is more effective in designing nonlinear controllers is derived. The methodology considered in this thesis can be applied to a multi-link flexible manipulator. However, for the purpose of numerical simulations, the design technique is applied to a single-link flexible manipulator. Towards this end, the analytical model of a single-link flexible manipulator is derived in configuration space. By using a nonlinear transformation, the resulting model in state-space is transformed to a model which has a constant *input vector field.* The resulting model is more suitable for design and simulation purposes as compared to the conventional nonlinear model.

2.1 Analytical Model of a Multi-Link Flexible Manipulator

A robot arm consists of a number of links connected by rotational or translational joints, with the last link equipped with some end-effector. The dynamics of an n-link rigid robot arm can be expressed by a set of n equations [74],

$$M(\theta)\,\ddot{\theta} + n_1(\theta,\ \dot{\theta}) + F_c(\dot{\theta}) + F_h\dot{\theta} = u \tag{2.1}$$

where θ is an n-dimensional vector describing the joint positions of the robot, n_1 represents the Coriolis and centrifugal forces, F_c denotes the Coulomb friction, F_h is the hub damping, and u is the vector of joint torques.

The dynamics of a flexible-link manipulator can be derived by using the assumed modes method [17]. By considering a finite number m of modal terms, the dynamic equations for the flexible-link manipulator are derived following a Lagrangian approach:

$$M(\theta,\delta)\begin{bmatrix}\ddot{\theta}\\ \ddot{\delta}\end{bmatrix} + \begin{bmatrix} n_1(\theta,\dot{\theta},\delta,\dot{\delta}) \\ n_2(\theta,\dot{\theta},\delta,\dot{\delta})\end{bmatrix} + \begin{bmatrix} F_c(\dot{\theta}) + F_h\dot{\theta} + F_g(\theta,\delta) \\ K_s\delta + F_s\dot{\delta}\end{bmatrix} = \begin{bmatrix} u \\ 0\end{bmatrix} \tag{2.2}$$

where $M(\theta,\delta)$ is the positive-definite symmetric inertia matrix. Let n and m_i ($i = 1\ ...\ n$) be the number of joints and deflection modes of the ith link, respectively. Then the inertia matrix $M(\theta,\delta)$ would be an $r \times r$ matrix, where $r = n + \sum_{i=1}^{n} m_i$, $\delta_i = [\delta_{i_1}\ \ ...\ \ \delta_{m_i}]^T$ is the vector of modal amplitudes, n_1 and n_2 are Coriolis and centrifugal terms respectively, F_c denotes the Coulomb friction, F_h is the hub damping, F_g is the gravity effect, K_s represents the stiffness matrix, F_s is the structural damping matrix, and u is the vector of joint control torques.

A simple comparison between (2.1) and (2.2) reveals that the number of control inputs in a rigid manipulator, i.e., n is the same as the number of mechanical degrees of freedom, whereas this is not the case in a flexible manipulator where the number of mechanical degrees of freedom is $n + \sum_{i=1}^{n} m_i$. Hence, a flexible-link manipulator

is an under-actuated system in which the control is to be designed so that the rigid displacements as well as the flexible deflections have simultaneously certain desired behaviors. This limitation makes the control problem of a flexible-link manipulator significantly more complicated than the same problem for a rigid manipulator.

In the next section the analytical model for a single-link flexible manipulator is derived.

2.2 Analytical Model of a Single-Link Flexible Manipulator

Similar to most contributions in the field, in this dissertation the control strategies are developed for a single-link flexible manipulator as a first step towards general multi-link flexible manipulators. As shown in Figure 2.1, the flexible-link is connected to a motor at one end (hub) and is driven by a torque u. The other end is free to move and has a small mass M_L as a payload. The reference frame $X_o - Y_o$ is without any movement while the origin of $X - Y$ frame is attached to the actuator. It is assumed that the length of the beam is much greater than its width, thus restricting the beam to oscillate in the horizontal direction. The effects of rotary inertia and shear deformation are ignored by assuming that the cross-sectional area of the link is small in comparison with its length. Using the assumed modes approach and Euler-Bernoulli beam theory the single-link flexible manipulator may be modeled according to the equation [75]

$$EI\frac{\partial^4 w(\xi,t)}{\partial \xi^4} + \rho L_0^4 \frac{\partial^2 w(\xi,t)}{\partial t^2} = 0$$

where $\xi = \eta/L_0$ is the normalized position along a link of length L_0, A_0 is the link cross-sectional area and I is the area moment of inertia of the cross section about the z-axis, E is Young's modulus of elasticity of the material and ρ is the mass per unit length of the link. Assuming separability in time and space [76], one may set

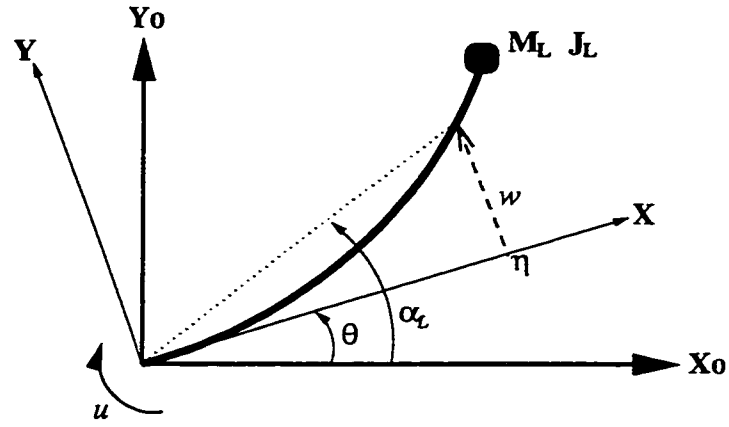

Figure 2.1: *Single-link flexible manipulator.*

$$w(\xi, t) = \phi(\xi)\delta(t),$$

where $\delta(t)$ is the modal amplitude and $\phi(\xi)$ is the normalized clamped-free eigenfunction as defined in [77] and [35]. Using modal analysis results in the following general solution

$$\delta(t) = e^{j\omega t}, \qquad \omega^2 = \frac{\beta_\omega^4 EI}{\rho L_0^4} \tag{2.3}$$

$$\phi(\xi) = C_1 \sin(\beta_\omega \xi) + C_2 \cos(\beta_\omega \xi) + C_3 \sinh(\beta_\omega \xi) + C_4 \cosh(\beta_\omega \xi) \tag{2.4}$$

The boundary conditions to the problem specify an infinite set of admissible values for the parameter β_ω, each of which determines an associated eigenfrequency ω of the beam. The following clamped-mass boundary conditions are imposed on the eigenfunction $\phi(\xi)$:

$$clamped: \quad \phi(\xi)\Big|_{\xi=0} = 0, \qquad \frac{d\phi(\xi)}{d\xi}\Big|_{\xi=0} = 0 \tag{2.5}$$

$$\begin{aligned} mass: \quad \frac{d^2\phi(\xi)}{d\xi^2}\Big|_{\xi=1} &= \frac{J_L\beta_\omega^4}{\rho L_0^3}\frac{d\phi(\xi)}{d\xi}\Big|_{\xi=1} \\ \frac{d^3\phi(\xi)}{d\xi^3}\Big|_{\xi=1} &= -\frac{M_L\beta_\omega^4}{\rho L_0}\phi(\xi)\Big|_{\xi=1} \end{aligned} \tag{2.6}$$

where M_L and J_L are, respectively, the load mass and the load inertia. The clamped conditions at the joint yield $C_3 = -C_1$ and $C_4 = -C_2$ while the mass conditions at the end-point lead to

$$[Q(\beta_\omega)] \begin{bmatrix} C_1 \\ C_2 \end{bmatrix} = 0$$

where the frequency equation is given by setting to zero the determinant of the 2×2 matrix $Q(\beta_\omega)$. It can be shown that the positive values of β_ω are given by the solutions of the equation

$$1 + \cos\beta_\omega \cosh\beta_\omega = 0. \tag{2.7}$$

Substituting the boundary conditions (2.5) and (2.6) into (2.4) yields the following expression for $\phi(\xi)$:

$$\phi(\xi) = C_1 \left(\sin(\beta_\omega \xi) - \sinh(\beta_\omega \xi) - \frac{\sin(\beta_\omega \xi) + \sinh(\beta_\omega \xi)}{\cos(\beta_\omega \xi) + \cosh(\beta_\omega \xi)} [\cos(\beta_\omega \xi) - \cosh(\beta_\omega \xi)] \right)$$

The individual mode functions $\phi_i(\xi)$ are found by substituting the values β_{ω_i} determined from the transcendental frequency equation (2.7) and by substituting the coefficients $\bar{c}_i$ for C_1:

$$\phi_i(\xi) = \bar{c}_i \left(\sin(\beta_{\omega_i} \xi) - \sinh(\beta_{\omega_i} \xi) - \frac{\sin(\beta_{\omega_i} \xi) + \sinh(\beta_{\omega_i} \xi)}{\cos(\beta_{\omega_i} \xi) + \cosh(\beta_{\omega_i} \xi)} [\cos(\beta_{\omega_i} \xi) - \cosh(\beta_{\omega_i} \xi)] \right)$$

The $\phi_i(\xi)$ are normalized by choosing $\bar{c}_i$ to satisfy $\int_0^1 \phi_i^2(\xi)\, d\xi, \qquad i = 1, \ldots, m.$

The dynamic equations for a planar single-link flexible manipulator ($F_g = 0$) are now given by (2.2) where the elements of the inertia matrix are as follows:

$$\begin{aligned}
m_{11} &= J_0 + J_L + M_L L_0^2 + I_0 + M_L (\Phi_e^T \delta)^2 \\
m_{1j} &= M_L L_0 \phi_{j-1,e} + J_L \phi'_{j-1,e} + \sigma_{j-1}, \qquad j = 2, \ldots, m+1 \\
m_{ii} &= m_b + M_L \phi_{i-1,e}^2 + J_L \phi_{j-1,e}'^2, \qquad i = 2, \ldots, m+1 \\
m_{ij} &= M_L \phi_{i-1,e} \phi_{j-1,e} + J_L \phi'_{i-1,e} \phi'_{j-1,e}, \qquad i = 2, \ldots, m+1, \quad j \neq i
\end{aligned} \tag{2.8}$$

with

$$\begin{aligned}
\Phi_e^T &= \Phi^T \Big|_{\xi=1} = [\phi_1 \quad \dots \quad \phi_m] \Big|_{\xi=1}, & \phi_{ie} &= \phi_i(\xi) \Big|_{\xi=1} \\
\Phi_e'^T &= \left[\phi'_{1e} \quad \dots \quad \phi'_{me}\right], & \phi'_{ie} &= \frac{d\phi_i(\xi)}{d\xi} \Big|_{\xi=1} \\
\sigma_i &= \rho L_0^2 \int_0^1 \phi_i(\xi)\xi \, d\xi, & i &= 1, \ \dots, \ m
\end{aligned}$$

where m_b is the link mass, I_0 is the joint actuator inertia, and J_0 is the link inertia relative to the joint.

The interaction between the rigid and flexible dynamics may be studied through the inertia matrix. The inertia matrix $M(\delta, \theta)$ may also be partitioned as

$$M(\delta, \theta) = M(\delta) = \begin{bmatrix} m_{11} & \mathbf{m_2^T} \\ \mathbf{m_2} & \mathbf{M_3} \end{bmatrix}$$

where

$$\mathbf{m_2} = \begin{bmatrix} \rho L_0^2 \int_0^1 \phi_1(\xi)\xi \, d\xi + J_L \phi_1(1)' + M_L L_0 \phi_1(1) \\ \vdots \\ \rho L_0^2 \int_0^1 \phi_m(\xi)\xi \, d\xi + J_L \phi_m(1)' + M_L L_0 \phi_m(1) \end{bmatrix}$$

is an m–tuple vector and $\mathbf{M_3}$ is an $m \times m$ matrix whose elements are given in (2.8). With reference to (2.2), now suppose that the Coriolis and centrifugal forces are negligible and $\mathbf{m_2}$ defined above is zero. Then there is no coupling between the rigid (θ) and flexible (δ) dynamics. As a result, one may realize that the vector $\mathbf{m_2}$ represents the coupling between the rigid and flexible dynamics. From the expression of $\mathbf{m_2}$ it is apparent that any increase in the value of parameters ρ, M_L, J_L and L_0 will strengthen the coupling effect. This means that in the case of a strong coupling any change in the joint variable will affect the behavior of the flexible modes. On the other hand based on (2.3), increasing L_0 for instance will lower the value of the eigenfrequencies implying a more flexible system.

The nonlinear terms n_1 and n_2 can be computed by differentiation of the elements of the inertia matrix resulting in

$$n_1(\dot{\theta}, \delta, \dot{\delta}) = 2M_L \dot{\theta}(\Phi_e^T \delta)(\Phi_e^T \dot{\delta})$$

$$n_2(\dot{\theta}, \delta) \;=\; -M_L \dot{\theta}^2 (\Phi_e \Phi_e^T)\delta$$

The matrices K_s and F_s are given by [17]

$$K_s \;=\; \text{diag}\{k_1, \; ..., k_m\}, \qquad k_i = \frac{EI}{L_0^3}\int_0^1 \left[\frac{d^2\phi_i(\xi)}{d\xi^2}\right]^2 d\xi$$

$$F_s \;=\; \text{diag}\{f_{s1}, \; ..., f_{sm}\}, \qquad f_{si} = 0.2\sqrt{k_i}$$

The Coulomb friction, F_c, is modeled as a sigmoidal function (instead of a pure signum function which has a discontinuity at the origin). The sigmoid function is given by

$$F_c(\dot{\theta}) = C_{coul}\left(\frac{2}{1+e^{-\hat{\kappa}\dot{\theta}}} - 1\right)$$

The value of hub damping F_h may be obtained from an experimental test [78]. With reference to Figure 2.1, the angle α_L formed by a generic point along the link can be expressed with respect to η as

$$\alpha_L(\eta) = \theta + \arctan\left(\frac{w(\eta)}{\eta}\right)$$

For small deflections, the position of any point along the link can be given as the linearized version of α_L , i.e.,

$$y(\eta) = \theta + \frac{w(\eta)}{\eta} = \theta + \frac{\Phi^T(\eta/L_0)}{\eta}\delta \tag{2.9}$$

This parameterization is convenient, since for $\eta = 0$ the joint position is recovered and for $\eta = L_0$ the tip-position is obtained. It is worth noting that $y(L_0)$ based upon (2.9) is expressed in *radians*. To convert the position to *meters*, one may consider $L_0\theta + \Phi^T(1)\delta$ as the tip-position.

2.3 Model Construction

The parameters used to construct a suitable model for the purpose of computer simulations are all based on an actual experimental set-up in the Robotics Laboratory at the ECE Department of Concordia University. These parameter values were determined in an earlier work [78]. The link data are given in Appendix A.

2.3.1 State-Space Model

For the purpose of design, we first derive a state-space model for the flexible-link manipulator. By choosing $[\theta_1^T, \delta_1^T, \theta_2^T, \delta_2^T]^T = [\theta^T, \delta^T, \dot{\theta}^T, \dot{\delta}^T]^T$ as the state vector, and the tip-position as the output, the state-space equations are obtained as

$$\begin{aligned} \dot{\theta}_1 &= \theta_2 \\ \dot{\delta}_1 &= \delta_2 \\ \dot{\theta}_2 &= f_3(\theta_1, \theta_2, \delta_1, \delta_2) + g_3(\theta_1, \delta_1)\, u \\ \dot{\delta}_2 &= f_4(\theta_1, \theta_2, \delta_1, \delta_2) + g_4(\theta_1, \delta_1)\, u \\ y &= \theta_1 + K_{tip}\, \delta_1 \end{aligned} \tag{2.10}$$

where $K_{tip} = \frac{\Phi_c^T}{L_0}$.

A nonlinear design for the above problem is in general complicated. However, the design may be simplified if certain state-dependent functions are zero or constant. Specifically, we apply a nonlinear transformation so that the resulting model has a constant input term. Namely, by using the *nominal* transformation

$$\begin{bmatrix} \hat{\theta}_2 \\ \hat{\delta}_2 \end{bmatrix} = M(\theta, \delta) \begin{bmatrix} \theta_2 \\ \delta_2 \end{bmatrix} \tag{2.11}$$

and noting that the (i,j)-th element of the matrix $\dot{M}$ may be computed as

$$\dot{M}_{ij}(\theta_1,\ \delta_1,\ \hat{\theta}_2,\ \hat{\delta}_2) = \frac{\partial M_{ij}}{\partial(\theta_1, \delta_1)} \begin{bmatrix} \dot{\theta}_1 \\ \dot{\delta}_1 \end{bmatrix} = \frac{\partial M_{ij}}{\partial(\theta_1, \delta_1)} M^{-1} \begin{bmatrix} \hat{\theta}_2 \\ \hat{\delta}_2 \end{bmatrix},$$

and accordingly

$$\begin{aligned} \begin{bmatrix} \ddot{\hat{\theta}}_2 \\ \ddot{\hat{\delta}}_2 \end{bmatrix} &= \dot{M} \begin{bmatrix} \theta_2 \\ \delta_2 \end{bmatrix} + M \begin{bmatrix} \dot{\theta}_2 \\ \dot{\delta}_2 \end{bmatrix} \\ &= \dot{M} D \begin{bmatrix} \hat{\theta}_2 \\ \hat{\delta}_2 \end{bmatrix} + M \begin{bmatrix} f_3 + g_3\, u \\ f_4 + g_4\, u \end{bmatrix} \Bigg|_{\substack{\theta_2 = \hat{f}_1 \\ \delta_2 = \hat{f}_2}} \end{aligned}$$

where

$$\begin{aligned} D(\theta_1,\ \delta_1) &= M^{-1}(\theta_1,\ \delta_1) \\ \hat{f}_1 &= D_{11}\hat{\theta}_2 + D_{12}\hat{\delta}_2 \\ \hat{f}_2 &= D_{21}\hat{\theta}_2 + D_{22}\hat{\delta}_2 \end{aligned}$$

we can obtain the state-space equations in the form

$$\begin{aligned} \dot{\theta}_1 &= \hat{f}_1(\hat{\theta}_2, \delta_1, \theta_1, \hat{\delta}_2) \\ \dot{\delta}_1 &= \hat{f}_2(\theta_1, \hat{\theta}_2, \delta_1, \hat{\delta}_2) \\ \dot{\hat{\theta}}_2 &= \hat{f}_3(\theta_1, \hat{\theta}_2, \delta_1, \hat{\delta}_2) + u \\ \dot{\hat{\delta}}_2 &= \hat{f}_4(\theta_1, \hat{\theta}_2, \delta_1, \hat{\delta}_2) \\ y &= \theta_1 + K_{tip}\ \delta_1 \end{aligned} \tag{2.12}$$

which has a constant input term.

The dynamics of a single flexible-link manipulator were computed by a computer code using MAPLE that automatically generates the corresponding M-File for use in MATLAB [79]

2.4 Preamble to Control

The objective of robot control is to produce fast, efficient and robust transportation of a payload. In a manipulator, the actuator acts by causing the tip to move from an initial position to a specified destination position. For a rigid manipulator, the tip trajectory is completely defined by the trajectory of the joint. Effective control of the joint is synonymous with good control of the tip. In a flexible-link manipulator, however, the situation is different. The system is characterized by a number of flexible modes as well as rigid modes. If flexible modes are ignored in the control design, they can lead to a significant deterioration of the closed-loop performance. Specifically, the control design for a flexible-link manipulator is difficult for a number

of reasons: Nonminimum-phase behavior, unmodeled and/or inaccurately modeled dynamics, model truncation, control spillover and observation spillover.

In terms of the transfer function of the linearized model of the manipulator, the tip-position zeros lie along the positive real axis [80]. This is the characteristic pattern for a non-colocated system and the transfer function is clearly nonminimum-phase. In time domain a non-minimum phase system introduces an undershoot in the start of the response to a step input. Such a system would require careful control design to avoid migration of the poles towards the right-half plane zeros resulting in unstable behavior.

Control spillover is the excitation of the residual modes (those not considered in the reduced-order model) by the control action and *observation spillover* is the contamination of the sensor readings by the residual modes. The effect of spillover on a pole placement regulator is studied in [80].

Another important issue in the control of flexible-link manipulators is the speed of maneuver of the tip. Generally, manipulator motions may be divided into two groups in terms of motion: 1) fine motion and 2) gross motion [81]. In fine motion, the manipulator tip moves in a small region of the workspace. Despite high closed-loop bandwidth, absolute velocities do not become very large since the motion occurs in a small region. Therefore, the nonlinear dynamic forces (Coriolis and centrifugal) are generally negligible. In gross motion, the manipulator tip makes large rotational maneuvers in the workspace. Large rotation of joints relative to each other are the main source of the complicated nonlinear dynamic coupling between the generalized coordinates [82]. Absolute velocities may become large during the fast, large maneuvers to the point that nonlinear dynamic forces become very dominant [83]. Any given manipulator can be moved slowly enough so that structural flexibility will not cause any significant deviation from the intended motion. Similarly, it can also be moved fast enough so that structural flexibility will become very apparent in the response of the manipulator (presuming the availability of actuators that can

deliver sufficiently high torque/force levels.

The fundamental challenge in the control of industrial and space robots is to provide high-speed, high-precision motion, despite large variations in payload and other task conditions. It is desirable to have a controller that will achieve the following performance criteria:

1. Good transient and steady-state tracking of a desired motion trajectory
2. High-speed and -precision manipulation in gross and fine motions (high closed-loop bandwidth) relative to structural flexibility
3. Good performance and stability robustness against unknown task variations.

Chapter 3

Nonlinear H_∞ Control

The dynamics of a flexible-link manipulator are highly nonlinear. In practice, the system parameters cannot be assumed to be known exactly *a priori*. For example, the payload may vary while performing a task, or the coefficients of friction and damping may change in different configurations. Therefore, there may be significant uncertainty in a robot's dynamic model. *Robust control* strives to characterize the uncertainty in the model of the plant to be controlled and to evaluate the degrees of freedom left to achieve the control task within specified bounds. Considerable effort has been made in the literature to satisfy the *stability robustness* requirement, that is, to guarantee closed-loop stability under a wide range of plant variations and disturbances. A linear robust controller may yield unsatisfactory performance, especially when the system is highly nonlinear and undergoes large motions, and thus operates over wide nonlinear dynamical regimes, as is often the case in the problems of robot manipulators. In this chapter the recent results on the subject of nonlinear H_∞ control are reviewed. Connections of the topic to some basic notions like dissipativeness, differential games, and the Hamiltonian function are discussed. An approximate solution of Hamilton-Jacobi-Isaacs inequality in the case of a general nonlinear system is also obtained.

3.1 Perspective

The development of H_∞ control has been one of the major concentrated activities in the control theory in the past decade. This area addresses the issue of worst-case controller design for dynamical systems subject to unknown disturbances including the problem of disturbance attenuation, model matching and tracking; see [84] and the references therein.

The mathematical symbol "H_∞" in its linear setting stands for the Hardy space of all complex-valued functions of a complex variable, which are analytic and bounded in the open right-half complex plane. The H_∞ control problem may be stated as follows. Assume that we have a system with two kinds of inputs and two kinds of outputs. The first type of input is an *exogenous input* representing the references (to be tracked) and/or disturbances (to be rejected). The other type of input is the *control input*. The *controlled output* represents a penalty variable, which may include a tracking error, as well as a cost of the control input needed to achieve the prescribed goal. The other type of output is the *measurement* that is made on the system. This is used to generate the control input, which in turn is the tool we have to minimize the effect of the exogenous input on the controlled output. A constraint we impose is that the mapping from *measurement* to *control input* should be such that the closed loop system is internally stable. The effect of the *exogenous input* on the *controlled output* after closing the loop is measured in terms of the energy and the worst-case disturbance. Our measure is the closed-loop H_∞ norm which is simply the L_2 induced norm (from the input time-functions to the output time-functions for zero initial state).

Although, the H_∞ technique was originally proposed for linear systems, this approach has also been studied for nonlinear systems. By appropriate formulations, H_∞ can provide the robustness property in controller design. By robustness, we mean that the stability of the system (or other goals) will be preserved in the presence of perturbations arising due to structured uncertainties (in the parameters

value) or unstructured uncertainties (unmodeled dynamics). In the classic approach to this issue i.e. the Linear Quadratic Gaussian (LQG) theory, the uncertainty is modeled as a white Gaussian noise process added as an extra input to the system. The major problem of this approach is that our uncertainties cannot always be modeled as white noise. While measurement noise can be quite well described by a random process, this is not the case with parameter uncertainty or unmodeled dynamics. The resulting error due to these uncertainties is deterministic but unknown.

The first systematic use of the work of Hill-Moylan [85] on dissipative systems in nonlinear H_∞ control was by Van der Schaft [86] who gave a general theory of the Hamilton-Jacobi-Isaacs equations for input affine systems with state feedback. In the state -space formulation, the problem of reducing the H_∞ norm of the closed-loop system is viewed as a two- person, zero-sum, differential game [87].

Although the direction of H_∞ optimal control for nonlinear systems is very new, it has attracted a lot of attention during recent years. The development of a systematic analysis of nonlinear H_∞ control was initiated by Ball and Helton [88, 89], Basar and Bernhard [87] and Van der Schaft [86, 90]. More recent contributions to this area of research are the works of Isidori and Astolfi [91], and Isidori and Tarn [92].

These papers all consider the necessary and/or sufficient conditions for solving the problem of disturbance attenuation and robust regulation for affine nonlinear systems. In the work of Isidori and Kang [93], however, the problem is studied for general nonlinear systems. Before reviewing the final results in [93], we present the basic definitions in H_∞ control from a general viewpoint. The main concepts for analysis and synthesis of nonlinear systems may be found in [7, 94].

For a vector-valued function $z(t)$, we say that $z : (0,T) \to \mathbb{R}^k$ is in $L_2(0,T)$ if $\int_0^T \|z(t)\|^2 dt < \infty$ where $\|z(t)\|^2 = z^T z$. Now, consider a smooth nonlinear system

of the form

$$\begin{aligned} \dot{x} &= f(x,u) \qquad u \in \mathbb{R}^m \\ y &= h(x) \qquad y \in \mathbb{R}^p \end{aligned} \tag{3.1}$$

where $x = (x_1, ..., x_n)$ are local coordinates for a smooth state-space manifold denoted by M. We assume the existence of an equilibrium $x_0 \in M$, i.e. $f(x_0, 0) = 0$, and without loss of generality we assume that $h(x_0) = 0$.

Let $\gamma \geq 0$. The system (3.1) is said to have L_2-gain less than or equal to γ if

$$\int_0^T \|y(t)\|^2 \, dt \leq \gamma^2 \int_0^T \|u(t)\|^2 \, dt$$

for all $T \geq 0$ and all $u \in L_2(0, T)$.

3.2 Connection to Dissipativeness

The nonlinear system (3.1) is said to be dissipative near $(x, u) = (0, 0)$, with respect to a given supply rate $s(u, y)$, if there exists a smooth function $V(x)$, which is non-negative and vanishes at $x = 0$ such that

$$\frac{\partial V}{\partial x} f(x,u) - s(u, h(x)) \leq 0$$

for all (x, u) in a neighborhood of $(0, 0)$. If (3.1) is locally asymptotically stable (at the equilibrium $x = 0$) and locally dissipative with respect to the supply rate

$$s(u,y) = \gamma^2 \|u(t)\|^2 - \|y(t)\|^2 \tag{3.2}$$

then its output response to any sufficient small input, from the initial state $x(0) = 0$, satisfies

$$0 \leq V(x(t)) \leq \int_0^T \gamma^2 \|u(s)\|^2 \, ds - \|y(s)\|^2 \, ds$$

for all $T > 0$. As a consequence, the following expressions for system (3.1) are equivalent

- the system has finite gain (or is dissipative with respect to (3.2)).
- the system has H_∞ (or L_2 induced) norm less than or equal to γ.

3.3 Connection to Differential Games

Consider the system

$$\begin{aligned} \dot{x} &= f(x,w,u) \\ z &= Z(x,u) \\ y &= Y(x,w) \end{aligned} \tag{3.3}$$

where w is the *exogenous input*, z is the *controlled output* and y is the *measured output*. For system (3.3), we want to design a *controller* of the form

$$\begin{aligned} \dot{\xi} &= \eta(\xi,y) \\ u &= \theta(\xi,y) \end{aligned}$$

to achieve two goals: closed-loop stability and attenuation of the effect of the exogenous input w on the controlled output z. Note that state feedback is a special case of the above controller. Define T_{wz} as the map from w to z. Clearly, this map is a function of x, w and u. Suppose the worst case disturbance, due to the maximum effort of w occurs at w_*, i.e.

$$T(w_*,u) := \sup_w \frac{\|T(w,u)\ w\|}{\|w\|}$$

Now, the control u has to minimize this value, i.e.

$$T(w_*,u_*) := \inf_u\ T(w_*,u).$$

Therefore, we have the following min-max problem

$$T(w_*,u_*) := \inf_u \sup_w\ T(w,u).$$

It is seen that the problem has a game-structure with two players: u and w. The first player , w, wishes to maximize $T(w,u)$, while the second player, u, wants to minimize it, or equivalently to maximize $-T$. So, in a unified structure, the sum of these two costs, i.e. T and $-T$ is zero and hence such an optimization problem is referred to as a *two-player zero-sum game.* Since this optimization is restricted to a dynamical system characterized by a set of differential equations, the associate game is a *differential game.* [95, 96]

3.4 Connection to Hamiltonian Functions

For system (3.3), now define the following Hamiltonian

$$H(x,p,w,u) = p^T f(x,w,u) - s(u,h(x)).$$

where $p^T = V_x := \frac{\partial V}{\partial x}$ is the costate vector, and $V(x)$ is the storage function (in the context of dissipativeness) or is the value function (in the context of a two-person zero-sum differential game). Now, if the finite gain property from w to z is sought, then

$$\begin{aligned} H(x,p,w,u) &= p^T f(x,w,u) - s(w,z) \\ &= p^T f(x,w,u) - \gamma^2 \|w\|^2 + \|z\|^2. \end{aligned}$$

So, if $H(x,p,w,u) \leq 0$, the system would have H_∞ norm less than or equal to γ.

Now, suppose the function $V(x)$ is positive and satisfies the inequality

$$H(x,p,w_*,u_*) < 0 \tag{3.4}$$

for each x in a neighborhood of zero. Then the resulting closed-loop system based on the control u_* is dissipative and locally asymptotically stable [93]. The inequality (3.4) is called a Hamilton-Jacobi-Isaacs inequality and in fact has a partial differential form. Finding the closed-form solution for such an inequality depends on each

particular problem and usually is too difficult. Thus a practical way is to approximate the solution up to a prescribed order by means of a polynomial approximation method. For system (3.3), assume that $f(0,0,0) = 0$, and let

$$\begin{aligned} \dot{x} &= Fx + Kw + Gu \\ y &= Jx + Mw \end{aligned} \tag{3.5}$$

be its linearization about $(x, w, u) = (0, 0, 0)$. Let $\hat{V}(x)$ be a negative-definite function and define

$$\hat{H}(x, p, w, u) = H(x, p, w, u) - \hat{V}(x) = 0. \tag{3.6}$$

Therefore, the solution $p^T = V_x$ of (3.6) satisfies that of (3.4) and hence to find the appropriate $V(x)$, we can proceed to solve (3.6). With an abuse of notation, for simplicity, we write H, instead of $\hat{H}$.

3.5 Approximate Solution of HJI Inequality

For affine nonlinear systems the approximate solution is given by Van der Schaft [90]. Here, we derive the approximate polynomial solution of HJI inequality associated with a general nonlinear system up to a prescribed order. Without loss of generality, we assume $M = 0$. Following [97, 93], set

$$\begin{aligned} V(x) &= \sum_{d=1}^{\infty} V^{[d+1]}(x) \\ w_* &= \sum_{d=1}^{\infty} w_*^{[d]}(x) \\ u_* &= \sum_{d=1}^{\infty} u_*^{[d]}(x) \end{aligned}$$

in which the superscript "$[d]$" implies that a function or the components of a vector are polynomials of degree d.

The function $V^{[2]}(x)$ is determined by the linearized model of (3.5) , i.e. $V^{[2]}(x) = x^T P x$, where P is the positive semi-definite solution of the following algebraic Riccati inequality

$$F^T P + PF + P(\frac{1}{\gamma^2} K K^T - G G^T) P + J^T J < 0 \tag{3.7}$$

from which the first-order approximations of u and w may be computed as

$$u_*^{[1]} = \frac{-1}{2} G^T P x \tag{3.8}$$

$$w_*^{[1]} = \frac{1}{2\gamma^2} K^T P x \tag{3.9}$$

The higher-order terms of $V(x)$ can be determined recursively. To this end, an expansion of f about $(u_*^{[1]}, w_*^{[1]})$ results in

$$\begin{aligned} H &= p^T[F_* x + K(w - \frac{1}{2\gamma^2} K^T P x) + G(u + \frac{1}{2} G^T P x) + \hat{f}(x, w, u)] + \\ &\quad \|u\|^2 + \|y\|^2 - \gamma^2 \|w\|^2. \end{aligned} \tag{3.10}$$

where $F_* = F + \frac{1}{2\gamma^2} K K^T P - \frac{1}{2} G G^T P$, $z = [y^T, u^T]^T$, and $\hat{f}$ contains higher-order terms. Now, a saddle point (w_*, u_*) of $H(x, p, w, u)$ necessarily satisfies the conditions

$$\frac{\partial H}{\partial u}(w_*, u_*) = 0 \qquad \frac{\partial H}{\partial w}(w_*, u_*) = 0$$

As a result, we have

$$\frac{\partial H}{\partial u} = 0 \quad \Rightarrow \quad G^T p + \hat{f}_u^{\ T} p + 2u = 0 \tag{3.11}$$

$$\frac{\partial H}{\partial w} = 0 \quad \Rightarrow \quad K^T p + \hat{f}_w^{\ T} p - 2\gamma^2 w = 0 \tag{3.12}$$

where $\hat{f}_q$ stands for the derivative with respect to q. Defining the value of H at the saddle point (w_*, u_*) as H_* in (3.10), and setting $H_* = 0$ we get

$$\begin{aligned} -p^T F_* x &= p^T[K(w_* - \frac{1}{2\gamma^2} K^T P x) + G(u_* + \frac{1}{2} G^T P x) + \hat{f}(x, w_*, u_*)] + \\ &\quad \|u_*\|^2 + \|y\|^2 - \gamma^2 \|w_*\|^2. \end{aligned}$$

The m_o^{th}–order terms $V^{(m_o)}(x)$ of $V(x)$ can now be computed inductively for $m_o = 3, 4, ...$, as follows

$$-V_x^{(m_o)} F_* x = R(x) \tag{3.13}$$

where

$$\begin{aligned} R(x) \;=\; & \sum_{k=2}^{m_o-1} V_x^{(k)}[K(w_* - \frac{1}{2\gamma^2}K^T P x) + G(u_* + \frac{1}{2}G^T P x) + \hat{f}(x, w_*, u_*)]^{(m_o+1-k)} + \\ & (\|u_*\|^2 + \|y\|^2 - \gamma^2\|w_*\|^2)^{(m_o)} \end{aligned}$$

Accordingly, by using (3.11), (3.12) and (3.13) the higher-order terms of u and w may be updated as

$$u_*^{[k]} \;=\; \frac{-1}{2}\left(G^T p^{(k+1)} + \sum_{j=1}^{k-1} \hat{f}_u^{T^{(j)}}(x, w_*^{[k-1]}, u_*^{[k-1]}) p^{(k-j+1)}\right) \tag{3.14}$$

$$w_*^{[k]} \;=\; \frac{1}{2\gamma^2}\left(K^T p^{(k+1)} + \sum_{j=1}^{k-1} \hat{f}_w^{T^{(j)}}(x, w_*^{[k-1]}, u_*^{[k-1]}) p^{(k-j+1)}\right) \tag{3.15}$$

Note that the function $\hat{V}(x)$ in (3.6) is an arbitrary negative-definite function.

One of the important issues in H_∞ control is the amount of attenuation provided by the control. For different values of gain there may or may not exist a positive semi-definite solution to the HJI inequality. As shown in [90], for a nonlinear system the maximum attenuation of disturbance that corresponds to the smallest γ has the same value as for its linearization. Therefore, the optimal H_∞ gain may be computed by using a search algorithm similar to the one presented in [98].

The procedure of how to utilize MAPLE and MATLAB to design a nonlinear H_∞ controller is described in [79].

Chapter 4

Domain of Validity of Nonlinear H_∞ Control

In this chapter, certain properties of controllers designed using nonlinear H_∞ technique are studied. It is well known that the explicit solution of the Hamilton-Jacobi-Isaacs (HJI) inequality is generally not feasible. By applying the polynomial approximation method, approximate expressions of the co-state and the two players of the game are considered. Using a Lyapunov technique, we prove the conjecture by van der Schaft [99] that the nonlinear feedback controller always results in a larger domain of validity than its linearized controller. Effects of attenuation level and weighting the controlled output on the domain of validity are also discussed. In this connection, a fictitious autonomous system derived from the original system and its HJI inequality is first introduced. The effect of approximation is then represented by introducing a perturbation term. It is shown that the domain of validity for the HJI inequality may be related to the domain of attraction of the equilibrium point of the fictitious system.

4.1 Introduction

In the time-domain formulation, the problem of minimizing the H_∞ norm (or, equivalently, the L_2 gain) of a closed-loop system is viewed as a two-person, zero-sum, differential game and, thus, the existence of the desired controller can be related to the existence of a solution of the algebraic Riccati equation arising in linear quadratic differential game theory [100].

Although H_∞ techniques were originally proposed for linear systems, the approach has also been studied for nonlinear systems. The development of a systematic analysis of nonlinear H_∞ control was initiated by Ball and Helton [88], and van der Schaft [90]. In the nonlinear setting, the Riccati equation is replaced by a particular type of Hamilton-Jacobi equation, the Hamilton-Jacobi-Isaacs (HJI) equation [91]. In particular, it has been shown that the existence of a solution to HJI equation is a sufficient condition for the existence of a full-information feedback law providing disturbance attenuation in the sense of the L_2 gain [86, 101]. In addition, it has also been shown that under appropriate assumptions, the existence of a solution is a necessary condition for the solvability of the problem [90]. The relation between Zubov's theory and the Hamilton-Jacobi equation is studied in [102].

In nonlinear H_∞ control, the goal is to attenuate the effect of an exogenous input on the controlled output in a stable manner. Instrumental in this regard is the solution of a PDE type inequality referred to as HJI inequality. The design of a nonlinear H_∞ controller proceeds by approximating the solution of the HJI equation. Various methods have been proposed in the literature for solving the HJI equation. Perhaps the most useful method is the power series method [90, 93]. The approximate solutions of the co-state vector V_x, the best control strategy u_* and the worst-case disturbance w_* can be obtained up to an arbitrary prescribed order of accuracy. Intuitively, using a low-order controller sacrifices certain features of the closed-loop performance. In particular, we show in this chapter that a nonlinear

feedback control law will always result in a larger domain of validity than its linearized counterpart. Furthermore, it is shown that weighting the controlled output and or changing the attenuation level can affect the domain of validity. In [103], numerical simulations on an aircraft model show that the nonlinear H_∞ control obtains a more reliable domain of attraction.

Consider a nonlinear system modeled by equations of the form

$$\begin{aligned} \dot{x} &= f(x) + g(x)u + k(x)w \\ z &= \begin{pmatrix} h(x) \\ u \end{pmatrix} \end{aligned} \tag{4.1}$$

where $x \in \mathbb{R}^n$ is the state vector, $w \in \mathbb{R}^r$ is the *exogenous input*, $u \in \mathbb{R}^p$ is the *control input* and $z \in \mathbb{R}^s$ is the *controlled output*. All the mappings introduced are assumed to be smooth. We assume that $f(0) = 0$ and $h(0) = 0$. The notation used in this chapter is the same as that in [90, 93].

4.2 Hamilton-Jacobi-Isaacs Equation

The goal of H_∞ control is to design a state feedback controller to achieve two objectives: Closed-loop stability and attenuation of the effect of the exogenous input w on the controlled output z which in turn is equivalent to a min-max type optimization problem

$$J_I = \min_u \max_w \int_0^T (\|z(t)\|_2^2 - \gamma^2 \|w(t)\|_2^2)\, dt \leq 0, \quad \forall\, T \geq 0$$

The HJI equation with the finite gain property associated with (4.1) has the form

$$H(x, p, w, u) = p^T(f(x) + g(x)u + k(x)w) + \frac{1}{2}(\|z\|_2^2 - \gamma^2 \|w\|_2^2) \tag{4.2}$$

where $p^T = V_x := \frac{\partial V}{\partial x}$ is the co-state vector, and $V(x)$ is the storage function (in the context of dissipative-ness) or is the value function (in the context of a two-person,

zero-sum, differential game). A saddle point (w_*, u_*) of $H(x, p, w, u)$ satisfies the condition $\frac{\partial H}{\partial(u,w)}(w_*, u_*) = 0$, yielding

$$u_* = -g^T(x)V_x^T(x), \qquad w_* = \frac{1}{\gamma^2}k^T(x)V_x^T(x)$$

Substituting u_* and w_* in (4.1) yields an asymptotically stable system [99]

$$\dot{x} = f(x) + g(x)u_* + k(x)w_* \tag{4.3}$$

which we refer to it as the *worst-case closed-loop system.*

Let $V(x)$ be non-negative in which case $V(0) = 0$ results in $V_x(0) = 0$, which in turn implies $u_*(0) = 0$ and $w_*(0) = 0$. The value of the Hamiltonian in the saddle point is given by

$$\begin{aligned} H_*(x,p) := H(x,p,w_*,u_*) \;\; &= \;\; V_x(f(x) + g(x)u_* + k(x)w_*) + \\ &\quad \frac{1}{2}(\|u_*\|_2^2 + \|h(x)\|_2^2 - \gamma^2\|w_*\|_2^2) \end{aligned} \tag{4.4}$$

If $H_*(x,p) \leq 0$, the system would have H_∞ norm less than or equal to γ. If in addition the function $V(x)$ is positive definite and

$$H_*(x,p) < 0 \tag{4.5}$$

for each nonzero x in a neighborhood of zero, then the resulting closed-loop system based on the control u_* is dissipative as well as asymptotically stable [90, 93]. The inequality (4.5) is referred to as the HJI inequality and in fact has a partial differential form. An explicit closed-form solution for the above inequality is problem dependent and is generally *not* feasible. A notion that is closely related to the HJI inequality is that of domain of validity defined formally as follows.

Definition 4.1 A region of state-space that satisfies the HJI inequality and guarantees asymptotic stability of the system is referred to as the *domain of validity.*

Domain of validity may be related to the domain of attraction, i.e., a region in state-space in which all trajectories originating there would evolve towards the equilibrium point.

A practical way for solving the inequality (4.5) would be to approximate the solution up to a prescribed order by means of a polynomial method. Suppose the exact solution to the H_∞ control problem can be represented by an infinite series in the form

$$V(x) = \sum_{d=1}^{\infty} V^{[d+1]}(x), \quad w_* = \sum_{d=1}^{\infty} w_*^{[d]}(x), \quad u_* = \sum_{d=1}^{\infty} u_*^{[d]}(x) \tag{4.6}$$

where the superscript "$[d]$" implies that a function or the components of a vector are polynomials of degree d.

Note that even the first order controller can provide local closed-loop stability and attenuation of disturbances on the controlled output. However, the use of higher order controllers, as shown in this chapter, can provide a larger domain of attraction for the closed-loop system. Towards this end, we seek a suitable framework in which the above advantage of nonlinear control laws may be demonstrated.

The approach in this chapter for analyzing the above problem is based on a perturbation technique. Therefore, in the next section, we briefly review the stability properties of perturbed systems.

4.3 A Perturbation Framework

In order to show the advantage of nonlinear feedback control over its linearized control, we construct a nominal system with a perturbation term. Towards this end, we review the asymptotic stability of a nonlinear system perturbed by a vanishing perturbation. Consider the system

$$\dot{x} = f_1(x) + g_1(x) \tag{4.7}$$

where $g_1(x)$ may be considered as a perturbation on the nominal system $\dot{x} = f_1(x)$. Let $g_1(0) = 0$. Suppose $x = 0$ is an asymptotically stable equilibrium of the nominal system. Let $V(x) > 0$ be a Lyapunov function for the nominal system that satisfies

the following condition in a ball with radius r_c

$$\dot{V}(x) = V_x f_1 < -c_1 \phi(x)^2 \tag{4.8}$$

$$\|V_x\|_2 < c_2 \phi(x) \tag{4.9}$$

for some positive constants c_1 and c_2, where $\phi : \mathbb{R}^n \to \mathbb{R}$ is positive definite and continuous. Suppose the perturbation term $g_1(x)$ satisfies

$$\|g_1(x)\|_2 \leq c_3 \phi(x)$$

where c_3 is a positive constant. Then the equilibrium point of (4.7) is locally asymptotically stable in a domain specified by $\dot{V}$, c_1, c_2 and c_3 [104]. As mentioned in the Introduction, one of our objectives is to relate the domain of validity to the domain of attraction. For this, we need the following lemma.

Lemma 4.1 *[105]: Suppose that $V(x)$ is positive definite for all x and $\dot{V}$ is negative definite along the system's trajectories in the vicinity of the origin. Let $c := V_{min}$ be the lowest value of $V(x)$ on the surface $\dot{V} = 0$. If the region about the origin defined by*

$$D = \{ x \in \mathbb{R}^n \mid V(x) \leq c \} \tag{4.10}$$

is bounded, then it is a conservative estimate of the domain of attraction.

Now, suppose that an estimate of the domain of attraction for the equilibrium point of (4.7) is provided by the set (4.10). Since the nominal system is asymptotically stable, there is a ball $B_{r_1} = \{ x \in \mathbb{R}^n \mid \|x\|_2 \leq r_1 \}$ in which $\dot{V}(x)$ is negative definite. Given B_{r_1}, the set D is obtained such that $D \subset B_{r_1}$ by choosing

$$c < \min_{\|x\|_2 = r_1} V(x) \tag{4.11}$$

The value of c is computed by finding a lower bound on the functional $V(x)$. From (4.6), we can write

$$\|V(x) - V^{[2]}(x)\|_2 \leq \sum_{i=3}^{\infty} \alpha_i \|x\|_2^i$$

Since $\|V(x) - V^{[2]}(x)\|_2$ is a scalar we may re-write the result in the form

$$\frac{|V(x) - V^{[2]}(x)|}{\|x\|_2} \leq \sum_{i=2}^{\infty} \alpha_i \|x\|_2^i$$

from which we can conclude that

$$\frac{|V(x) - V^{[2]}(x)|}{\|x\|_2} \to 0 \quad \text{as} \quad \|x\|_2 \to 0$$

By an argument similar to the one given in [104, pp. 131], it follows that for any $\gamma_1 > 0$ there exists an $r_2 > 0$ such that

$$|V(x) - V^{[2]}(x)| < \gamma_1 \|x\|_2, \qquad \forall \ \|x\|_2 < r_2$$

Consequently,

$$V(x) > V^{[2]}(x) - \gamma_1 \|x\|_2 > \frac{\lambda_{min}(P)}{2} \|x\|_2^2 - \gamma_1 \|x\|_2, \qquad \forall \ \|x\|_2 < r_2$$

where $V^{[2]}(x) = x^T P x$.

Now, let $\gamma_1 < \frac{\lambda_{min}^2(P)}{16\mu}$ where $\mu > 0$. It follows that

$$\frac{\lambda_{min}(P)}{2} \|x\|_2^2 - \gamma_1 \|x\|_2 > \mu \|x\|_2^3, \qquad \forall \ \|x\|_2 < r_3 = \frac{\lambda_{min}(P)}{4\mu} + \frac{1}{\mu} \sqrt{\frac{\lambda_{min}^2(P)}{16} - \gamma_1 \mu}$$

Therefore, we can choose c such that

$$c < \mu r^3, \qquad r = \min\{r_1, r_2, r_3\} \tag{4.12}$$

in order to construct the domain D in (4.10).

4.4 Domain of Validity

When the solution to the HJI inequality is obtained by using the approximation method certain aspects of performance of the closed-loop system will be compromised. In this section, we will show that the lower the order of the controller, the smaller the domain of validity of the controller.

4.4.1 Effect of Approximate Solution

The purpose of constructing a perturbed fictitious system will be shown to be useful in relating the domain of attraction to the domain of validity of the solution of the HJI inequality. As we will see in the sequel, the domain of attraction of the equilibrium of (4.7) is a subset of the domain of validity of the HJI inequality of (4.14). Let us define a fictitious system of the form

$$\dot{x} = f_1(x) := f(x) + g(x)u_* + k(x)w_* + \frac{1}{2}\hat{m}(x)(\|u_*\|^2 + \|h(x)\|^2 - \gamma^2\|w_*\|^2) \quad (4.13)$$

where $\hat{m}(x)$ is a function with the property that $V_x\ \hat{m}(x) = 1$ for each nonzero x with $V(x)$ such that (4.5) is satisfied. Note that constructing an $\hat{m}(x)$ to satisfy the above equation is always possible. To wit since the row vector $V_x(x)$ for each nonzero x is not identically zero, we can assume that at least one of its element, say the ith element, namely v_i is non-zero. We can now define the jth element of $\hat{m}(x)$, namely $\hat{m}_j$ as follows

$$\hat{m}_j = \begin{cases} 0 & \text{if } i \neq j \\ \frac{1}{v_i} & \text{if } i = j \end{cases}$$

The time derivative of $V(x)$ along trajectories of f_1 is

$$\frac{dV}{dt} = V_x(f(x) + g(x)u_* + k(x)w_*) + \frac{1}{2}(\|u_*\|^2 + \|h(x)\|^2 - \gamma^2\|w_*\|^2) < 0 \quad (4.14)$$

The negative-definiteness of (4.14) follows from (4.5). Therefore, $V(x)$ is an appropriate Lyapunov function that guarantees the asymptotic stability of the equilibrium of (4.13), which is the origin by assumption. Consider (4.13) as the nominal system that satisfies the following conditions in a ball of radius r_c

$$\begin{aligned} \dot{V}(x) &= V_x\ (f(x) + g(x)u_* + k(x)w_*) + \frac{1}{2}(\|u_*\|^2 + \|h(x)\|^2 - \gamma^2\|w_*\|^2) \\ &< -c_1\ \phi(x)^2 \quad (4.15) \\ \|V_x\| &< c_2\ \phi(x) \quad (4.16) \end{aligned}$$

It is clear that (4.15) results in (4.14), i.e., the HJI inequality. Since a conservative estimate of the domain of attraction is contained in the region satisfying condition (4.15) and Lemma 4.1, the domain of attraction is a subset of the domain of validity for the HJI inequality. Let us treat system (4.13) as a nominal system on which the following perturbation is acting

$$\begin{aligned} g_1(x) = & - (g(x)\sum_{d=s}^{\infty} u_*^{[d]} + k(x)\sum_{d=s}^{\infty} w_*^{[d]}) \\ & - \frac{1}{2}\hat{m}(x)(\|u_*\|^2 + \|h(x)\|^2 - \gamma^2\|w_*\|^2), \quad s \geq 2 \end{aligned} \tag{4.17}$$

The resulting perturbed system can then be represented according to

$$\begin{aligned} \dot{x} &= f_0(x) := f_1(x) + g_1(x) \\ &= f(x) + g(x)u_* + k(x)w_* - g(x)\sum_{d=s}^{\infty} u_*^{[d]} - k(x)\sum_{d=s}^{\infty} w_*^{[d]}, \quad s \geq 2 \end{aligned} \tag{4.18}$$

Note that the terms containing $\hat{m}(x)$ are canceled out. Therefore, to study the domain of attraction of the nominal system $\dot{x} = f_1(x)$ perturbed by $g_1(x)$, it suffices to consider the simplified model introduced in (4.18). Note that the role of $\hat{m}(x)$ is to justify how the domain of attraction of the fictitious system is related to the domain of attraction of the perturbed system.

In fact the perturbed system (4.18) represents the dynamics of the worst-case closed-loop system with u_* and w_* being replaced by their first $s-1$ terms. Setting $s = 2$, for instance, cancels out all the nonlinear terms of u_* and w_* and gives a closed-loop system based on a linear control strategy of the original nonlinear controller. In other words, by appropriately setting the parameter s, it is possible to obtain an approximation to the worst-case closed-loop system up to order $s-1$. Thus, the purpose of the perturbation term $g_1(x)$ is to cancel out certain parts of the dynamics in order to yield a desired approximated system.

Note that the perturbation thus introduced with $s = 2$ does not affect the stability property of the perturbed system since the closed-loop system in the first approximation is known *a priori* to be asymptotically stable. In fact in this case,

the set $\{ x \in \mathbb{R}^n \mid \|x\|_2 < r,\ V(x) > 0,\ \dot{V}(x) < 0 \}$ -with r defined as in (4.12)- is not empty. However the domain in which the trajectories approach towards the equilibrium point is not specified yet. As we will see in the sequel, the effect of the perturbation term in this framework is to change the domain of attraction of the equilibrium point.

The following theorem presents the main result of this section.

Theorem 4.1 *Let the equilibrium point of (4.18) be asymptotically stable. Then the size of the domain of attraction D depends on the parameter s. In particular, the smaller (larger) the parameter s, the smaller (larger) will be the domain D. Furthermore, suppose the approximate solution of the H_∞ control problem for (4.1) is given by a power series expansion in the form*

$$w_* = \sum_{d=1}^{s-1} w_*^{[d]}(x), \quad u_* = \sum_{d=1}^{s-1} u_*^{[d]}(x), \qquad s \geq 2 \tag{4.19}$$

Then, the domain of validity of the controller corresponding to $s = s_0$ is larger than or equal to the domain of validity for all $s < s_0$.

Proof: The time derivative of $V(x)$ along $\dot{x} = f_0(x)$ is given by

$$\frac{dV}{dt} = V_x(f(x) + g(x)u_* + k(x)w_*) + V_x\ g_2(x) \tag{4.20}$$

where $g_2(x)$ is defined as

$$g_2(x) = -g(x)\sum_{d=s}^{\infty} u_*^{[d]} - k(x)\sum_{d=s}^{\infty} w_*^{[d]}, \qquad s \geq 2 \tag{4.21}$$

It is known that the vector field $f(x)+g(x)u_*+k(x)w_*$ is asymptotically stable [99]. As a result, $V_x(f(x) + g(x)u_* + k(x)w_*) < 0$. This implies that there exists some $k_1 > 0$ and $\rho_1 > 0$ such that

$$V_x(f(x) + g(x)u_* + k(x)w_*) < -k_1\|x\|_2^2, \qquad \forall\ \|x\|_2 < \rho_1. \tag{4.22}$$

Therefore, condition (4.8) is satisfied with $\phi(x) = \|x\|_2$. To see if (4.9) is also satisfied, observe that it is possible to find an upper bound for the slope of $\|V_x\|_2$ in

the coordinates of $(\|V_x\|_2, \|x\|_2)$. From (4.6), we have

$$\|V_x\|_2 \leq \alpha_1\|x\|_2 + \sum_{i=2}^{\infty} \alpha_i \|x\|_2^i$$

Therefore,

$$\frac{\|V_x\|_2 - \alpha_1\|x\|_2}{\|x\|_2} \leq \sum_{i=2}^{\infty} \alpha_i \|x\|_2^i$$

which results in

$$\frac{\|V_x\|_2 - \alpha_1\|x\|_2}{\|x\|_2} \to 0 \quad \text{as} \quad \|x\|_2 \to 0$$

Consequently, for any $\alpha_0 > 0$ there exists $\rho_2 > 0$ such that

$$\|V_x\|_2 - \alpha_1\|x\|_2 < \alpha_0\|x\|_2, \qquad \forall\ \|x\|_2 < \rho_2$$

or

$$\|V_x\|_2 < (\alpha_0 + \alpha_1)\|x\|_2 := c_2\ \|x\|_2, \quad \forall\ \|x\|_2 < \rho_2 \tag{4.23}$$

As a result, (4.22) and (4.23) are satisfied in a ball with radius $r_c = \min\{\rho_1, \rho_2\}$. Now to get a condition on negative-definiteness of $\dot{V}$ along the trajectories of the perturbed system consider the effect of $V_x\ g_2(x)$. The contribution of this term can be incorporated via its norm according to

$$\|V_x\ g_2(x)\|_2 \ < \ a\|x\|_2^2 \sum_{j=s-2}^{\infty} \|x\|_2^j, \qquad a > 0, \quad s \geq 2 \tag{4.24}$$

$$< \ a\|x\|_2^2 \sum_{j=s-2}^{\infty} k_0^j, \qquad \forall\ \|x\|_2 < k_0 < \rho_1 \tag{4.25}$$

Consequently, equation (4.20) on a certain domain of state-space yields

$$\begin{aligned} \dot{V} \ &< \ -k_1\|x\|^2 + \|V_x\ g_2(x)\|_2 \\ &< \ (a \sum_{j=s-2}^{\infty} k_0^j - k_1)\|x\|_2^2, \qquad \forall\ \|x\|_2 < k_0 \end{aligned} \tag{4.26}$$

In order to find the domain D, it is necessary to have,

$$a \sum_{j=s-2}^{\infty} k_0^j < k_1, \quad s \geq 2 \tag{4.27}$$

which may be considered as an inequality in terms of k_0. Since the smaller the value of s, the less precise is the approximation to the HJI inequality, therefore it follows from (4.27) that the smaller the value of s, the smaller the radius k_0. Let the least upper bound on the values of k_0 satisfying (4.27) be represented by

$$\hat{k}_0(s) = \sup\{\ k_0 \mid a \sum_{j=s-2}^{\infty} k_0^j < k_1\ \}, \quad s \geq 2 \tag{4.28}$$

Before completing the proof of Theorem 4.1, note that according to Lemma B.1 stated in the Appendix the function $\hat{k}_0(s)$ just introduced is a monotonic function of s. Since k_0 determines the domain of attraction for a locally asymptotically stable system without lose of any generality, we assume that $k_0 < 1$. This is due to the fact that it is always possible to transform the state in such a way that $\|x\| < a$ (with $a > 1$) results in $\|Tx\| < 1$ where T represents the transformation.

Note that according to (4.26) the value of k_0 determines the largest ball in which $\dot{V} < 0$. Considering (4.12) and (4.28), we may express the estimate of the domain of attraction as a function of s

$$D(s) = \{\ x \in I\!R^n \mid V(x) \leq \mu \hat{k}_0^3(s)\ \}, \quad s \geq 2 \tag{4.29}$$

As a consequence of the above results, two important observations may now be presented.

1. The dependency of D on s reveals that the higher-order approximations result in a larger domain of attraction for the equilibrium point. This statement is true regardless of the choice of Lyapunov function since the function $\hat{k}_0(s)$ resulting from the above analysis is a monotonic function of s. In other words, a larger value of s, regardless of the choice of the Lyapunov function, always results in a larger $\hat{k}_0(s)$ which in turn results in a larger D.

2. After some algebraic manipulations it is possible to show that the nominal system (f_1) with the original perturbation term (g_1) does also satisfy the conditions of asymptotic stability of a perturbed system. Consequently, the above

computations may originally be performed on (f_1, g_1). However, the computations in this case are far more involved than the ones developed above.

Based on Lemma 4.1, estimation of the domain of attraction may proceed in two steps: First one finds a region in which $\dot{V} < 0$, and then constructs a set on which $V \leq c$. Note that the expansion $\dot{V} = V_x f_1 < 0$ is exactly identical to the HJI inequality of the original system. Hence, the relation (4.29) –which resulted directly from $\dot{V} = V_x f_1 < 0$– represents the HJI inequality. As a result, the larger the value of s in (4.29), the larger the domain of validity of HJI inequality. Construction of the domain of validity of the controller, on the other hand, also needs the second requirement, i.e., $V \leq c$. Therefore, the value of s also affects the domain of validity of the controller, implying that the larger the value of s, the larger the domain of validity of the designed controller. $\triangle$

Remark 4.1 Our approach for qualitatively analyzing the behavior of the H_∞ controlled closed-loop system is based on a Lyapunov technique. Given that in general, Lyapunov methods can only provide an estimate of the domain of attraction for a nonlinear system, therefore, it is not feasible to explicitly obtain the *exact* domain of validity of a nonlinear system by using this technique. In other words the purpose of the chapter is *not* to explicitly *compute* the *exact* domain of validity; rather, the objective is to provide a methodology for *comparing* the estimates of domains of validity obtained by using different approximations of the nonlinear system. The result given in Lemma 1 does not provide a basis for explicitly computing the exact domain of attraction. As pointed out above, although the study of domains of attraction through Lyapunov methods is in general qualitative in nature; nevertheless, it should be emphasized that it is possible to *compare* the size of the estimated regions, quantitatively. Note that the approach adopted in the proof of Theorem 1 uses the *same* Lyapunov function, the *same* value of k_1 for constructing the upper bound for $\dot{V}$, the *same* balls with radii ρ_1 and ρ_2, and the same c_2. The only difference in the analysis is the order of the approximation that is used for the nonlinear

system which is specified by the parameter s. The above remarks also apply to the rescaling of the state vector of the system discussed previously.

Remark 4.2 The analysis used in the proof of Theorem 4.1 is based on the explicit solution of $V(x)$. This assumption, however, does not restrict the use of the above analysis. This is due to the fact that as far as the approximate worst-case closed-loop system is concerned, only the approximations of u_* and w_* are needed. Although these approximations are related to the approximations of $V(x)$, nevertheless, $V(x)$ was considered for both the nominal as well as the perturbed systems, simultaneously. In other words, if we consider only the approximations of $V(x)$ together with u_* and w_*, the above analysis holds, of course, with different values for c_1 and c_2 in (4.15) and (4.16), respectively.

4.4.2 Effect of the Attenuation Level (γ)

One of the important issues in H_∞ control is the level of attenuation provided by the control law. It turns out that different values of gain may or may not guarantee the existence of a positive (semi)definite solution to the HJI inequality. As shown in [90], for a nonlinear system the maximum attenuation of disturbance that corresponds to the smallest γ has the same value as for its linearized model. Therefore, the optimal H_∞ gain may be computed by using a search algorithm similar to the one presented in [98]. In addition to the maximum level of attenuation other issues regarding the role of this factor can be investigated. In fact one can investigate whether or not the attenuation level can affect the domain of validity as well as the rate of convergence in a nonlinear H_∞ control problem. In the following sections, these two issues are further investigated. The following theorem states that higher attenuation of the exogenous input may result in smaller domain of validity for the HJI inequality.

Theorem 4.2 *Let the worst-case closed-loop system corresponding to (4.1) be given by (4.3), in which the effect of the exogenous input w on the controlled output z is*

attenuated by γ, i.e.,

$$\frac{\int_0^T \|z(t)\|^2\,dt}{\int_0^T \|w(t)\|^2\,dt} < \gamma$$

Let the HJI inequality corresponding to this problem be given by (4.5). Then, the larger(smaller) γ, the larger(smaller) the domain of validity of the HJI inequality.

Proof: The HJI inequality can be written in the form

$$H_*(x,p) = V_x(f(x)+g(x)u_*) + \frac{1}{2}(\|u_*\|^2 + \|h(x)\|^2) + \frac{1}{2\gamma^2}V_x k(x)k^T(x)V_x^T(x)$$

As before, let us construct a fictitious system to study the problem. Consider the system $\dot{x} = f_o(x) := f_1(x) + g_1(x)$ with f_1 and g_1 defined as

$$\begin{aligned} f_1(x) &= f(x) + g(x)u_* + \frac{1}{2}\hat{m}(x)(\|u_*\|^2 + \|h(x)\|^2) \\ g_1(x) &= \frac{1}{2\gamma^2}k(x)k^T(x)V_x^T(x) \end{aligned}$$

where $\hat{m}(x)$ is defined as before, i.e., $V(x)\ \hat{m}(x) = 1$. In this framework, the nominal system $\dot{x} = f_1(x)$ is asymptotically stable; since $\dot{V}_1(x) = V_x\ f_1(x) = V_x(f(x) + g(x)u_*) + \frac{1}{2}(\|u_*\|^2 + \|h(x)\|^2)$ corresponds to the HJI inequality with no exogenous input. Therefore, $\dot{V}_1(x) = V_x\ f_1(x) < 0$. This implies that there exists some $k_1' > 0$ and $\rho_1' > 0$ such that

$$V_x(f(x)+g(x)u_*) + \frac{1}{2}(\|u_*\|^2 + \|h(x)\|^2) < -k_1'\|x\|_2^2, \qquad \forall\ \|x\|_2 < \rho_1'. \quad (4.30)$$

Now, since $g_1(x)$ satisfies

$$\frac{\|g_1(x)\|_2}{\|x\|_2} \to 0 \quad \text{as} \quad \|x\|_2 \to 0,$$

it turns out that for any $\hat{\alpha} > 0$, there exists $r_\alpha > 0$ such that

$$\|g_1(x)\|_2 < \hat{\alpha}\|x\|_2, \qquad \forall\ \|x\|_2 < r_\alpha$$

By defining $\dot{V}_2(x) = V_x\ g_1(x)$, it is easy to show that

$$\|V_x\| < a'\|x\|_2 \sum_{d=1}^{s-1}(k_o')^d, \qquad a' > 0, \quad s \geq 2, \qquad \forall\ \|x\|_2 < k_o' \quad (4.31)$$

where $s-1$ is the order of the approximation. The time derivative of $V(x)$ along $g_1(x)$ is then bounded by

$$\|V_x\ g_1(x)\| < \frac{\hat{\alpha}}{\gamma^2}\|x\|_2^2 \sum_{d=1}^{s-1}(k_o')^d, \qquad \forall\ \|x\|_2 < k_0' < \rho_1' \tag{4.32}$$

Thus we have

$$\dot{V} = V_x\ f_o = \dot{V}_1 + \dot{V}_2 < (\frac{\hat{\alpha}}{\gamma^2} \sum_{d=1}^{s-1}(k_o')^d - k_1')\|x\|_2^2, \qquad \forall\ \|x\|_2 < k_0' \tag{4.33}$$

By invoking the same reasoning as in the previous section, it may be shown that for a given value of s, if a smaller value of γ is selected, then a smaller value of k_o results. Consequently, decreasing γ for the purpose of further attenuation yields a smaller domain of validity. $\triangle$

4.4.3 Weighting the Controlled Output

As in other optimal control algorithms the controlled output may be weighted with respect to the disturbance to get a faster response. Given that the cost function is of quadratic type, increasing the weighting on output would result in a more damped response. More emphasis on rise time, however, may result in a smaller domain of validity for the relevant HJI inequality. In this section we study the effect of such weightings on the domain of validity of the HJI inequality. In this section, we also construct a fictitious system to study the problem. Consider the system $\dot{x} = f_o(x) := f_1(x) + g_1(x)$ with f_1 and g_1 defined as

$$\begin{aligned} f_1(x) &= f(x) + g(x)u_* + \frac{1}{2}\hat{m}(x)(\|u_*\|^2 - \gamma^2\|w_*\|) \\ g_1(x) &= \frac{\theta^2}{2}\ \hat{m}(x)\|h(x)\|^2 \end{aligned}$$

where $\hat{m}(x)$ is defined as before, i.e., $V(x)\ \hat{m}(x) = 1$ and $\theta > 1$ is a weighting factor on the first component of the controlled output. In this framework the nominal system $\dot{x} = f_1(x)$ is asymptotically stable; since this corresponds to a controlled output including only the control input u. After some algebraic manipulation and

using the arguments used in the proof of Theorem 4.1 (cf. equations (4.26)-(4.29)), it can be shown that there exist some $k_0'' > 0$ and $k_1'' > 0$ such that

$$\dot{V} = V_x \; f_o = \dot{V}_1 + \dot{V}_2 < (\frac{\theta^2}{2} \sum_{d=1}^{s-1} (k_o'')^{d-1} - k_1'') \|x\|_2^2, \qquad \forall \; \|x\|_2 < k_0'' \tag{4.34}$$

Consequently, it now follows that the larger (smaller) θ, regardless of the value of s, the smaller (larger) k_o''. As a result, weighting with a factor greater than one can shrink the domain of validity. The result of this subsection is now summarized in the following lemma. The details of the proof are omitted due to space limitations.

Lemma 4.2 *Consider the problem of nonlinear H_∞ control for (4.1) in which the controlled output is replaced by*

$$z = A \begin{pmatrix} h(x) \\ u \end{pmatrix} \tag{4.35}$$

where A is a weighting matrix. Then, the domain of validity of the HJI inequality for the system having (4.35) as its controlled output is larger (smaller) than the corresponding domain for the HJI inequality of (4.1) if $\|A\| < 1$ ($\|A\| > 1$).

4.5 Example

The method of analysis posed in this chapter, as indicated previously, does not yield an actual domain of validity of the HJI inequality. It qualitatively provides, however, a good evidence and justification as to why nonlinear control is potentially superior to the linearized control.

Consider the scalar system [99]

$$\begin{aligned} \dot{x} &= u + \arctan(x)\; w \\ z &= \begin{pmatrix} x \\ u \end{pmatrix} \end{aligned}$$

It is shown in [99] that the *exact* domain of validity for the corresponding HJI inequality is $|\arctan(x)| \leq \gamma$. By applying the linear controller, the HJI inequality is shown to be valid for all x satisfying $|\arctan(x)| < \frac{\sqrt{2}}{2}\gamma$. If we choose $\gamma = 1$, the linear controller results in the exact domain $|x| < 0.85$. By applying the procedure proposed in Section 4 and by choosing $\gamma = 1$ and $k_1 = 0.5$ in (4.28), the estimate of domain of validity for $s = 2$ (linear control), $s = 4$, and $s = 8$ are obtained as $|x| < 0.71 < 0.85$, $|x| < 0.91$, and $|x| < 0.96$, respectively. This clearly shows that as the order of the controller is increased the estimate of domain of validity is also increased. Note that our result for the linear controller is conservative as compared to the exact domain due to the fact that our analysis for the estimate of domain of validity is based on Lyapunov theory. This conservative property is also present for higher order approximations of the controller.

4.6 Concluding Remarks

Qualitative behavior of nonlinear H_∞ controllers was considered. The effects of (i) the approximate solutions, (ii) attenuation level, and (iii) weighting the controlled output on the domain of validity of the HJI inequality were investigated. It is shown that (i) utilizing lower order approximations, (ii) increasing the attenuation level, and (iii) weighting the controlled output may result in a smaller domain of validity. The method used in this chapter has exploited the stability properties of perturbed systems. Although the results of this chapter have revealed certain performance properties of nonlinear feedback controllers, they cannot provide any explicit quantitative measure for the above mentioned issues.

Chapter 5

Uncertainty Compensation for a Flexible-Link Manipulator

In a flexible-link manipulator, in general the effect of some parameters such as payload, friction amplitude and damping coefficients cannot be exactly measured. One possibility is to consider the above as part of the system uncertainty. In this chapter, constant as well as L_2-bounded deviations of parameters from their nominal values are considered as uncertainties. These uncertainties make it difficult for a linear controller to achieve desired closed-loop performance. To remedy this problem, a nonlinear dynamical model of a flexible-link manipulator that is linear with respect to the control input is derived. Based on recent results in nonlinear robust regulation with an H_∞ constraint, a nonlinear controller is designed for the flexible-link manipulator. The contribution of this chapter is in demonstrating that the nonlinear controller has a larger domain of attraction than the linearized controller. In fact, for the single-link flexible manipulator considered in this chapter, the linear H_∞ controller results in *instability* for step changes in the desired output greater than 3.6 *rads*, whereas the nonlinear H_∞ controller yields desired step changes of 2π *rads*. Simulation results demonstrating the advantages and superiority of the nonlinear H_∞ controller over the linear H_∞ controller are presented.

5.1 Introduction

Flexible manipulators exhibit many advantages over rigid manipulators as they require less material, have less (link) weight, consume less power, are more maneuverable, require smaller actuators, and are more easily transportable. However, they have not been widely used in industrial operations due in part to the fact that manipulators have to satisfy strict accuracy requirements in the response of the manipulator's end-effector to the joint control input commands. This task is severely complicated by structural deformations in the manipulator. Traditionally, the vibrations have been eliminated by increasing the rigidity of the links. However, in many situations, this option is not available especially if the advantages associated with lightweight manipulators are not to be sacrificed. Consequently, this leaves us with the only other available alternative which is to design effective and advanced control strategies for these systems.

The control problem for a flexible-link manipulator is complicated by the fact that the dynamics of the system are highly nonlinear and complex. The dynamics are basically described by a system of partial differential equations where for the purpose of control, the integro-partial differential type equations are reduced to ordinary differential equations.

5.2 Uncertainties in a Flexible-Link Manipulator

As pointed out earlier, nonlinear control techniques offer more reliable solutions in comparison to the above methods. Although, the nonlinear techniques may not in general yield global results; however, the region of desirable operation is larger than that provided by linear controllers. Precise knowledge of the plant is one of the main limitations in applying most of nonlinear control techniques.

In particular for a flexible-link manipulator in general, the system parameters are not known *a priori*. For example, the load may vary while performing a task,

or the coefficients of friction and damping may change as the configurations vary. Thus, there may be significant uncertainty in a robot's dynamic model. These uncertainties should be compensated for by designing an appropriate robust controller. Applications of linear H_∞ control theory to rigid and flexible-link manipulators have been studied in [39, 37]. To the best of our knowledge, nonlinear H_∞ control, on the other hand, has been applied only to rigid-link robots [106].

5.3 Incorporation of Uncertainties in the Flexible-Link Manipulator Model

The dynamics of a flexible-link manipulator were derived in Chapter 2. To incorporate the effect of uncertainties due to load variations, friction and damping characteristics, one may rewrite (2.12) in the form

$$\begin{aligned}
\dot{\theta}_1 &= \hat{f}_1(\hat{\theta}_2, \delta_1, \theta_1, \hat{\delta}_2, \hat{w}) \\
\dot{\delta}_1 &= \hat{f}_2(\theta_1, \hat{\theta}_2, \delta_1, \hat{\delta}_2, \hat{w}) \\
\dot{\hat{\theta}}_2 &= \hat{f}_3(\theta_1, \hat{\theta}_2, \delta_1, \hat{\delta}_2, \hat{w}) + u \\
\dot{\hat{\delta}}_2 &= \hat{f}_4(\theta_1, \hat{\theta}_2, \delta_1, \hat{\delta}_2, \hat{w}) \\
y &= \theta_1 + K_{tip}\, \delta_1 \\
z &= [y^T, u^T]^T
\end{aligned} \tag{5.1}$$

where $\hat{w}$ is the vector of uncertainties that represents the deviations of parameters from their nominal values. For instance, the inertia matrix is a function of the load mass M_L. Therefore, in deriving the state-space equations (5.1) , we need to take into account that the uncertainty on the load mass does indeed propagate throughout the system dynamics. Specifically, to consider this uncertainty, one may assume that $M_L = M_{L0}(1+\hat{w}_1)$ where M_{L0} is the nominal value of the load mass and $\hat{w}_1$ is an L_2-bounded disturbance acting on it. By a similar reasoning, we assume

that

$$P_i = P_{i0}(1 + \hat{w}_i) \tag{5.2}$$

where P_i stands for every parameter in the system (2.12) having an uncertain value. Note that there could be a number of parameters that may have uncertain values. For instance, the amplitude of a sigmoidal function that is commonly used to model the Coulomb friction or the value of hub damping for each joint and/or the value of structural damping due to link flexibility are some examples to name.

The design methodology in this chapter is based on the nonlinear H_∞ control technique where the objective is to attenuate the effects of disturbances on the controlled output. Therefore, any bounded signal with a compact support can enter the system as a disturbance. Consequently, in the non-affine model (5.1) with respect to the exogenous input $\hat{w}$, all deviations must be L_2-bounded. Based on the assumption of boundedness of $\hat{w}$ one may apply the nonlinear H_∞ technique developed in [93] to design a controller that attenuates the effect of $\hat{w}$ on the controlled output. It should be noted, however, that not all parameter perturbations are necessarily L_2-bounded. Constant deviations from the nominal values of the parameters are very common in practice. Obviously, constant deviations are not L_2-bounded. As a matter of fact, model (5.1) cannot handle constant deviations from the nominal values of the parameters. To circumvent this difficulty, one may rewrite model (2.12) into the form

$$\dot{x} = \bar{f}(x) + \Delta\bar{f}(x) + (G + \Delta G)\, u \tag{5.3}$$

where $x = [y, \delta_1^T, \hat{\theta}_2^T, \hat{\delta}_2^T]^T$, is a coordinate change, $\Delta\bar{f}$, ΔG denote the deviations of $\bar{f}$ and G from their nominal values, respectively and

$$\bar{f}(x) = \begin{pmatrix} \bar{f}_1(x) \\ \bar{f}_2(x) \\ \bar{f}_3(x) \\ \bar{f}_4(x) \end{pmatrix}, \quad G = \begin{pmatrix} 0 \\ 0 \\ 1 \\ 0 \end{pmatrix} \tag{5.4}$$

Since $\bar{f}(0) = 0$, the resulting model may be expressed in the form

$$\dot{x} = \bar{f}(x) + G\, u + v \tag{5.5}$$

where

$$v = (\Delta G \;\; \Delta(x)) \begin{pmatrix} u \\ x \end{pmatrix} \quad \text{and} \quad \Delta(x) := \int_0^1 \frac{\partial\, \Delta\bar{f}(\lambda x)}{\partial x}\, d\lambda \tag{5.6}$$

and the formula on page 51 in [107] is used in defining (5.6). The main idea is shown schematically in Figure 5.1, where $z_1 = (u^T, x^T)^T$ and $e = y - y_{ref}$, where y_{ref} is the desired tip position reference trajectory. Let Δ_p represent the map from z_1 to v in Figure 5.1. Let also the L_2-gain of the closed-loop system from v to z_1 –with Δ_p block disconnected– be γ. Then by virtue of the small-gain theorem as used in [108], the overall closed-loop system subject to the presence of Δ_p remains stable for all Δ_p's having L_2-gain less than or equal to $1/\gamma$. Note that as long as $\|\Delta_p\|_\infty$ is bounded, the setup introduced in Figure 5.1 can also handle L_2-bounded deviations. It is clear that the possible range of uncertainties introduced by Δ_p may be extended by designing a controller that makes the value of γ as small as possible. This is indeed possible by utilizing the H_∞ control technique to attenuate the effect of v on z_1.

The above proposed design technique is now applied to a single-link flexible manipulator with one deflection mode. The dynamics of a single-link flexible manipulator were computed by using MAPLE to automatically generate the corresponding M-Files for use in MATLAB. In this chapter, we only consider set point regulation by using the approach developed in [109].

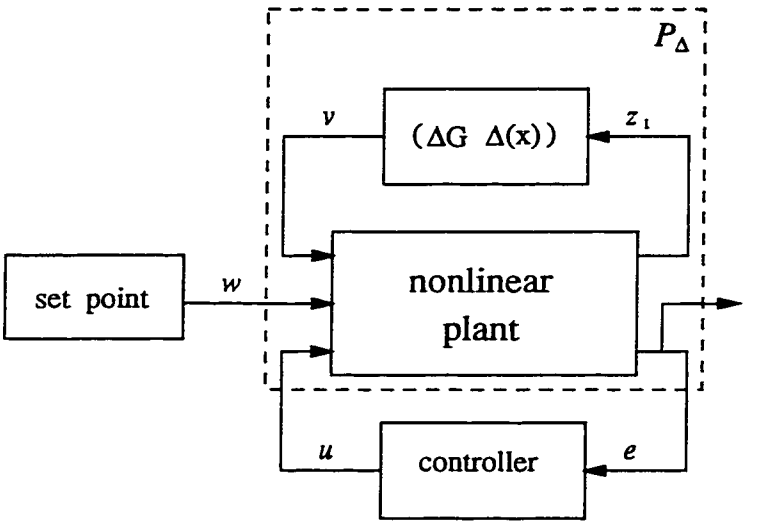

Figure 5.1: *Problem setup for robust regulation in the presence of parametric uncertainty.*

5.4 Zero-State Detectability of the Flexible-Link Model

Recall from [110] that system (2.12) is zero-state detectable if any bounded trajectory satisfying $z = 0$, $\forall t > 0$, is such that $\lim_{t\to\infty} x(t) = 0$. In [100] it is shown that the linear version of this condition is equivalent to

$$\text{rank } L = \text{rank} \begin{bmatrix} F - j\omega I & G \\ J & 0 \end{bmatrix} = 1 + n, \quad \forall \omega \in \mathbb{R} \tag{5.7}$$

where n is the model order, and F, G and J are the matrices of the *certain* linearized model of (5.5) about $(x, v, u) = (0, 0, 0)$, namely

$$\begin{aligned} \dot{x} &= Fx + Kv + Gu \\ y &= Jx \end{aligned} \tag{5.8}$$

It is well known [80] that for a single-link flexible manipulator, the tip position zeros lie along the real axis and are non-zero. As a result, the linear model $[F, G, J, 0]$ does not have any transmission zeros on the imaginary axis. This indicates that

condition (5.7) is satisfied for our system. The rank condition in (5.7) together with continuity of $\bar{f}$ guarantee that the nonlinear model (5.5) is locally zero-state detectable. The zero-state detectability property is a sufficient condition for the existence of an asymptotically stable closed-loop system as stated in the next section.

5.5 Application to a Single-Link Flexible Manipulator

As discussed above, the H_∞ control technique can be applied to design a robust regulator for a flexible-link manipulator. Towards this end, we first augment the dynamics of the exosystem with the manipulator dynamics, and then define the error as the difference between the regulated output and the exosystem output. Since in this chapter we only consider set-point regulation, therefore an integrator can represent the dynamics of the exosystem as stated in [111]. For simplicity of control design, the first state is taken as the output, i.e., the tip position. Following [109] and by considering (5.5) and noting the definition of v from Figure 5.1, we may write the dynamics of the manipulator augmented with the exosystem according to

$$\dot{x} = \bar{f}(x) + G\,u + v \tag{5.9}$$

$$\dot{\xi} = e = y - y_{ref} = [1\ 0_{2\times m+1}]\,x - y_{ref} \tag{5.10}$$

$$z = [e, u]^T \tag{5.11}$$

where ξ denotes the state of the internal model of the exosystem. Note that the error e is deriving the internal model of the exosystem. In the case of set-point regulation, the dynamics of the internal model correspond to a pure integrator. Using the above problem setup, robust regulation is now achieved by designing a controller that renders $\|T_{z_1 v}\|_\infty < \gamma$ while the regulated output e converges to zero as time tends to infinity, i.e., $\lim_{t\to\infty} e(t) = 0$.

5.5.1 Constrained Disturbance Attenuation

The dynamic equations (5.9)-(5.10) may be represented in the form

$$\dot{X} = F(X) + G_1\, v + G_2\, u \tag{5.12}$$

where $X = (x^T, \xi)^T$ and

$$F(X) = F(x) = \begin{pmatrix} \bar{f}(x) \\ x_1 \end{pmatrix}, \quad G_1 = \begin{pmatrix} I_4 \\ 0 \end{pmatrix}, \quad G_2 = \begin{pmatrix} G \\ 0 \end{pmatrix} \tag{5.13}$$

where I_4 is a 4×4 identity matrix (model order n=4). The corresponding HJI inequality (3.4) for this system becomes [91]

$$W_{(x,\xi)}F(x,\xi) + y^2 + \frac{1}{4}W_{(x,\xi)}(\frac{1}{\gamma^2}G_1G_1^T - G_2G_2^T)W_{(x,\xi)}^T \leq 0 \tag{5.14}$$

where

$$W_{(x,\xi)} = \begin{pmatrix} \frac{\partial W(x,\xi)}{\partial x} & \frac{\partial W(x,\xi)}{\partial \xi} \end{pmatrix}$$

It is shown in [109] that the solution of (5.14) may be obtained in terms of $V(x)$; namely from the solution of the HJI inequality for (5.9), we get

$$V_x\bar{f}(x) + y^2 + \frac{1}{4}V_x(\frac{I_4}{\gamma^2} - GG^T)V_x^T \leq 0$$

In fact

$$W(x,\xi) = V(x) + \|\xi - \lambda(x)\|^2$$

where $\lambda(x)$ is a solution of the partial differential equation

$$\begin{pmatrix} \frac{\partial \lambda(x)}{\partial x} & -1 \end{pmatrix} F^*(x,\xi)_{\xi=\lambda(x)} = 0, \quad \lambda(0) = 0$$

with

$$F^*(x,\xi) = \begin{pmatrix} \bar{f}(x) + \frac{1}{2}(\frac{I_4}{\gamma^2} - GG^T)V_x^T \\ x_1 \end{pmatrix}$$

After obtaining $W(x,\xi)$, one can find the following feedback law that renders the L_2-gain of the corresponding closed-loop system (5.9)-(5.11) less than or equal to the prescribed number γ, namely

$$u = -\frac{1}{2}(W_{(x,\xi)}\ G_2)^T$$

5.6 Simulation Results and Discussions

As mentioned earlier, the main objective is to robustly control the tip position of a single-link flexible manipulator whose dynamic specifications are derived in (5.5) . The data for the link are given in Appendix A. In this set of computer simulations only the first deflection mode eigenfrequency is considered. In this section two separate issues are considered. The first issue deals with parametric uncertainty and the second one with compensating the hub friction.

5.6.1 Presence of Parametric Uncertainty

For the purpose of defining an uncertainty set, we consider parameter deviations according to (5.2). In particular, *four* parameters are assumed uncertain, viz., payload mass, hub damping, structural damping and the amplitude of the sigmoidal function used to model the Coulomb friction. The disturbances w_i in (5.2) are taken as sine functions with amplitude 0.2, i.e., the deviation from the nominal values of the parameters vary in time by maximally 20%. Note that this kind of disturbance is *not* L_2-bounded. The simulation results presented here are based on the model whose state vector is $x = [y, \delta_1^T, \hat{\theta}_2^T, \hat{\delta}_2^T]^T$. To relate the simulation results of these states to the state vector $\hat{x} = [y, \delta_1^T, \theta_2^T, \delta_2^T]^T$, it is sufficient to use the *nominal* transformation (2.11).

The approximate solution of the HJI inequality is analytically given in ([90], under expression (83)). It is worth noting, however, that the solution based on such time integration is too time consuming in MAPLE. Therefore, we use a polynomial

approximation to $V(x)$ where the coefficients of the expansion are determined recursively. This is accomplished by first defining a polynomial for $V(x)$ whose order is the same as that of the approximation for $V(x)$. Algebraic re-arrangement of all the terms involved results in a linear matrix equality in terms of the unknown coefficients.

Based on the results developed in the preceding sections a nonlinear controller was designed to attenuate the effect of disturbances on the controlled output for the flexible-link manipulator described above. The procedure of designing a nonlinear robust regulator for a flexible-link manipulator is as follows:

1. Construct the state-space model as in (5.1).
2. Obtain the linear model of the system as in (5.8).
3. Solve the algebraic Riccati inequality (3.7) for P.
4. Compute the linear part of the controller from (3.8) and (3.9).
5. Solve (3.13) for $V^{(m)}(x)$ $(m \geq 2)$ by means of the polynomial approximation technique described above.
6. Obtain the higher-order terms of the controller from (3.14) and (3.15).

When solving the HJI inequality in Step 5 of the above procedure one finds that the transformed model (5.1) can efficiently reduce the complexity of the HJI inequality.

It is natural to expect that if, instead of the exact solution of the HJI equality, we use only its truncated polynomial approximation, certain performance features will be compromised. In particular, the closer the controller is to its exact solution, the larger will be the region of attraction of the equilibrium point. Note, however, that increasing the order of approximation by one, may not necessarily result in a significant improvement. In our specific application, it turned out that the performance of the controller did not improve considerably from the linear controller

by utilizing the second-order controller. The third-order controller, however, did have a significant effect on the performance. The fourth- and fifth-order controllers performed identically to the third-order controller. Simulation results revealed that the third-order controller, in this application, has the ability of performing a 2π *rad* maneuver in a stable manner. The complete rotation (2π *rad* set-point) of a flexible-link manipulator, in our view demonstrates the advantage of the proposed nonlinear controller over its linearized controller which becomes unstable beyond a 3.6 *rad* maneuver. It turns out that the higher-order controllers do not make a significant improvement in the performance of the closed-loop system. In other words, the third-order controller in this application is a sufficiently good approximation to the exact controller.

Note that near the equilibrium point, the results for both linear and nonlinear controllers should be close to each other. This statement is verified in Figure 5.2 by showing the results for a step input with an amplitude of 0.1. It follows that for small inputs, the results for the linear controller and a third-order nonlinear controller are practically identical (indistinguishable in the figure).

The advantage of the third-order nonlinear controller over its linear counterpart becomes apparent from the results shown in Figure 5.3. The main reason for the difference between the results in Figures 5.2 and 5.3 is due to the larger amplitude of the step input.

The attenuation factor, γ, is one of the controlling parameters affecting the performance of the closed-loop system. As pointed out earlier, the maximum level of attenuation is limited. This is due to the fact that the algebraic Riccati equation for the linearized model has a positive semi-definite solution for only a particular range of γ. Moreover, the higher the attenuation factor, i.e., the larger the value of γ, the smaller the region of attraction. Figure 5.4 shows the effect of the attenuation factor on the performance of the closed-loop system.

As in other optimal control algorithms the controlled output may be weighted

with respect to the disturbance for obtaining a faster response. Since the cost function is of quadratic type, increasing the weighting on the output should result in a more damped response. More emphasis on rise time, however, may result in a smaller region of attraction. Figure 5.5 shows two cases with $10y$ and $5y$ as the controlled outputs.

As mentioned earlier, the nonlinear controller has the ability of extending the region of attraction. One particular feature of this region is the dependence of the stability margin on the input amplitude. By using the same attenuation level and weighting of the output, the linear controller *fails* to achieve a stable response to inputs whose amplitudes exceed a certain level. In the simulations shown in Figure 5.6, the maximum allowable amplitude for the linear controller is 3.6 *rads*. Beyond this limit the closed-loop system becomes unstable. The nonlinear controller, however, provides in a stable manner a complete rotation of the link, i.e., for inputs with 2π *rad* amplitudes.

5.6.2 Compensation for Hub Friction

In this section, we show that the nonlinear controller is capable of handling the effect of hub friction more effectively than the linearized controller. For this purpose, the design procedure was repeated in the absence of friction while simulations were performed where the Coulomb friction is present. It should be noted that for low input torque amplitudes, the simulation results for the linear and nonlinear controllers are almost the same. However, by increasing the torque amplitude the limitations of both controllers become evident. Although, the nonlinear controller can still handle much higher amplitudes as compared to the linear controller. Figure 5.7 depicts the simulation results for the nonlinear controller. The linear controller, for this level of torque amplitude results in instability.

5.7 Concluding Remarks

A dynamical model that is linear with respect to the joint control torques for a flexible-link manipulator was obtained. In general, in a flexible-link manipulator, the system parameters may not be known exactly *a priori*. Consequently, this will introduce significant uncertainties in the robot's dynamic model. The uncertainties considered in this chapter are due to deviations of parameters from their nominal values. These deviations may be L_2-bounded and/or constant. The problem of robust set-point regulation in the presence of norm-bounded uncertainties was formulated as the problem of constrained disturbance attenuation. For the purpose of designing the nonlinear H_∞ controller, an approximate polynomial solution of the Hamilton-Jacobi-Isaacs inequality was used. The properties of the resulting controller were also discussed. It was observed that the nonlinear feedback controller has a larger domain of attraction than its linear counterpart (the size of this region for the nonlinear controller is almost twice that of the linearized controller for the application considered in this chapter). Furthermore, it was observed that the nonlinear controller is capable of compensating the hub friction more effectively as compared to its linearized controller. Although the design technique used in this chapter is based on full state feedback, the extension to the case of output feedback should be feasible and is is a topic for future work. The proposed control methodology is based on minimizing the effect of the disturbances on the tip position. It was found that the performance quality is influenced by input amplitude, attenuation level, and the relative weighting of the controlled output with respect to the disturbance. It was observed that the above factors also affect the region of attraction. Therefore, achieving a desirable performance may require a compromise among them. The symbolic software package MAPLE was used to implement and design the nonlinear controller with an arbitrary order of approximation. Simulations were carried out using both linear and nonlinear controllers. The results clearly show the advantages and superiority of the nonlinear controller over its linearized counterpart.

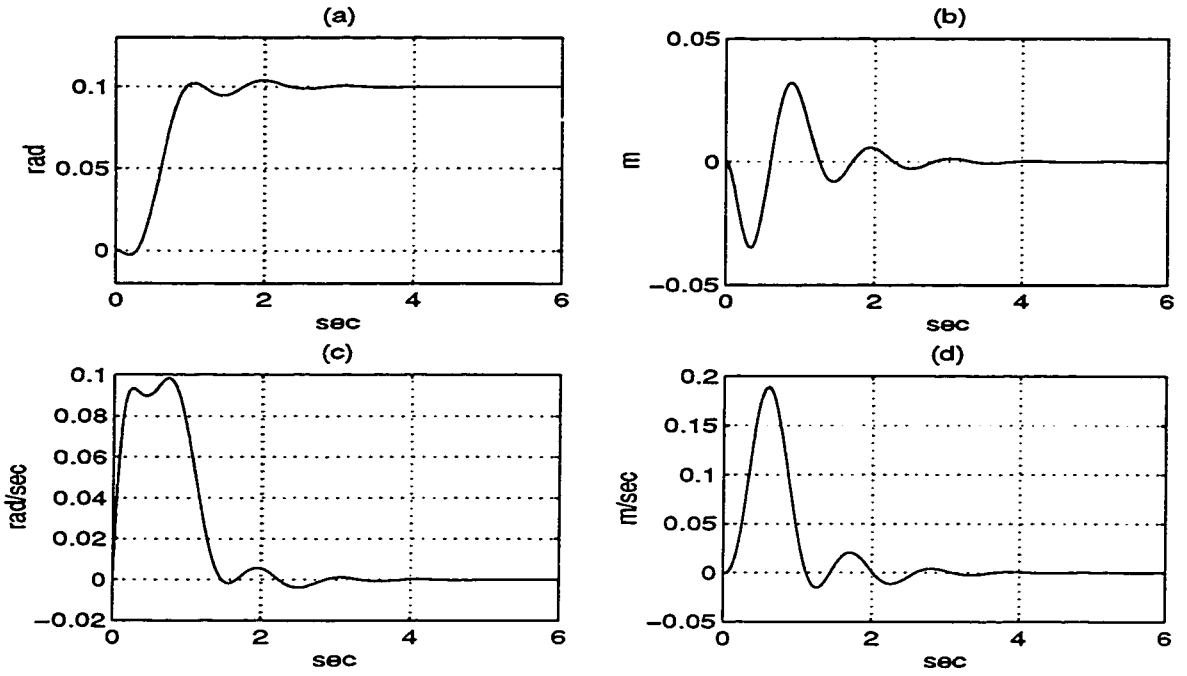

Figure 5.2: *Comparison between the linear (dashed) and nonlinear (solid) controllers for small inputs: (a) tip position y, (b) tip deflection δ, (c) $\hat{\theta}_2$, and (d) $\hat{\delta}_2$.*

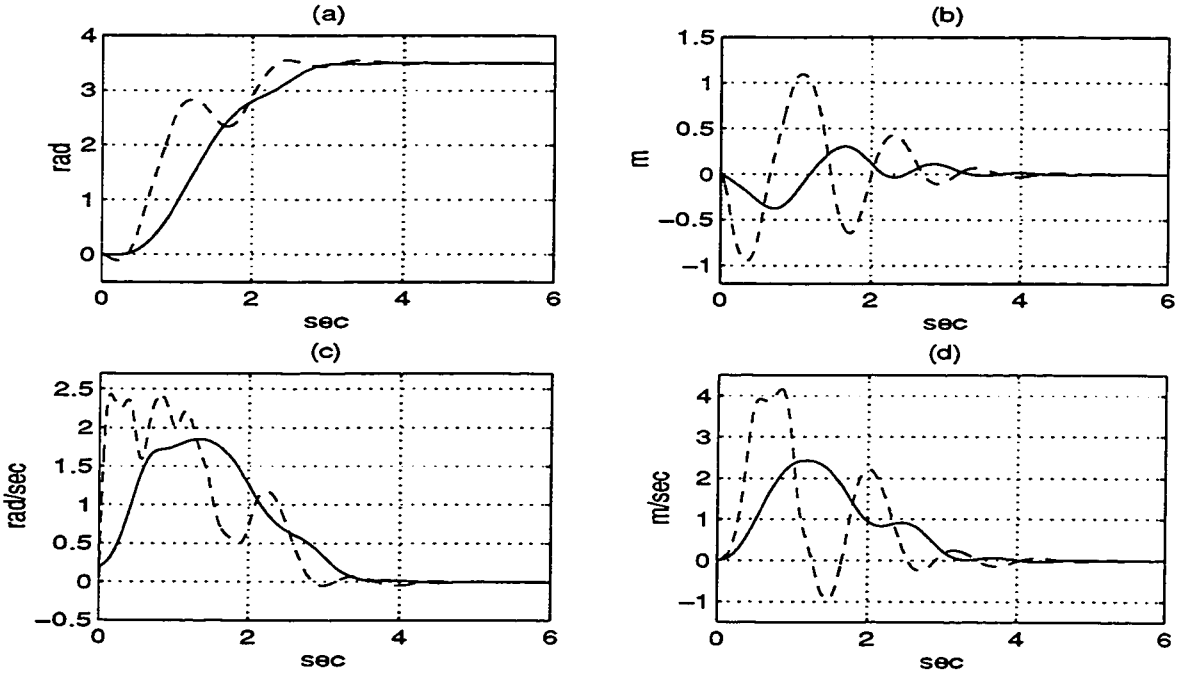

Figure 5.3: *Comparison between the linear (dashed) and nonlinear (solid) controllers for large inputs: (a) tip position y, (b) tip deflection δ, (c) $\hat{\theta}_2$, and (d) $\hat{\delta}_2$.*

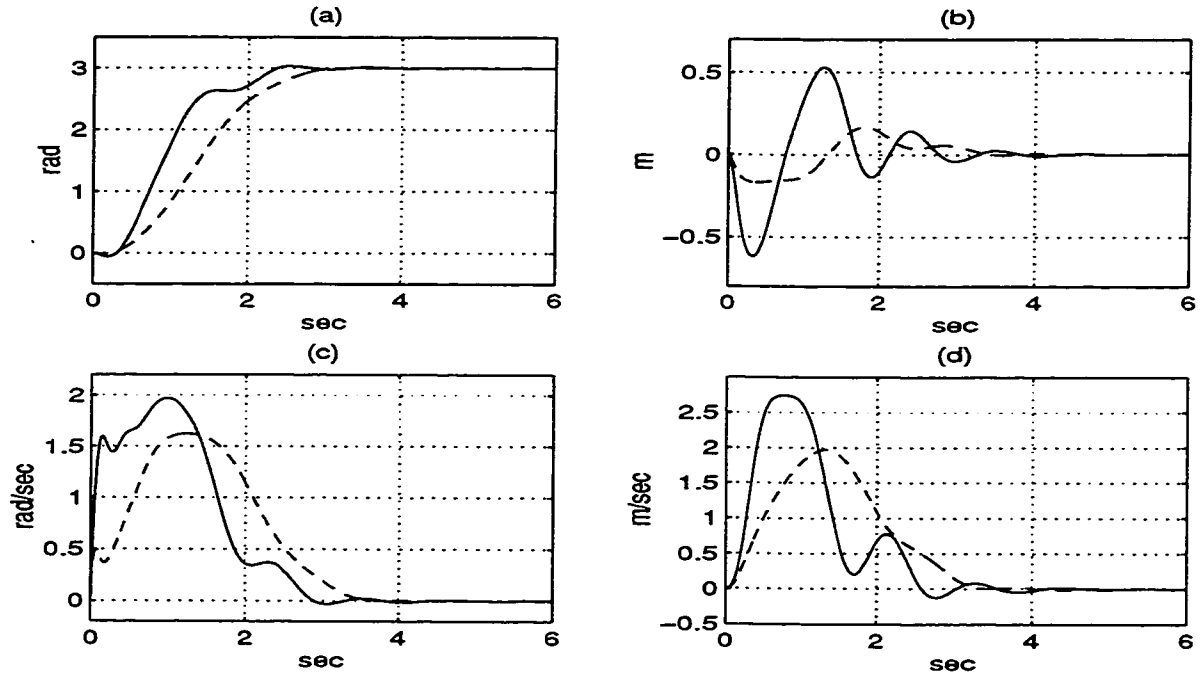

Figure 5.4: *The influence of gain on the performance:* $\gamma = 3$ *(dashed) and* $\gamma = 10$ *(solid): (a) tip position* y*, (b) tip deflection* δ*, (c)* $\hat{\theta}_2$*, and (d)* $\hat{\delta}_2$*.*

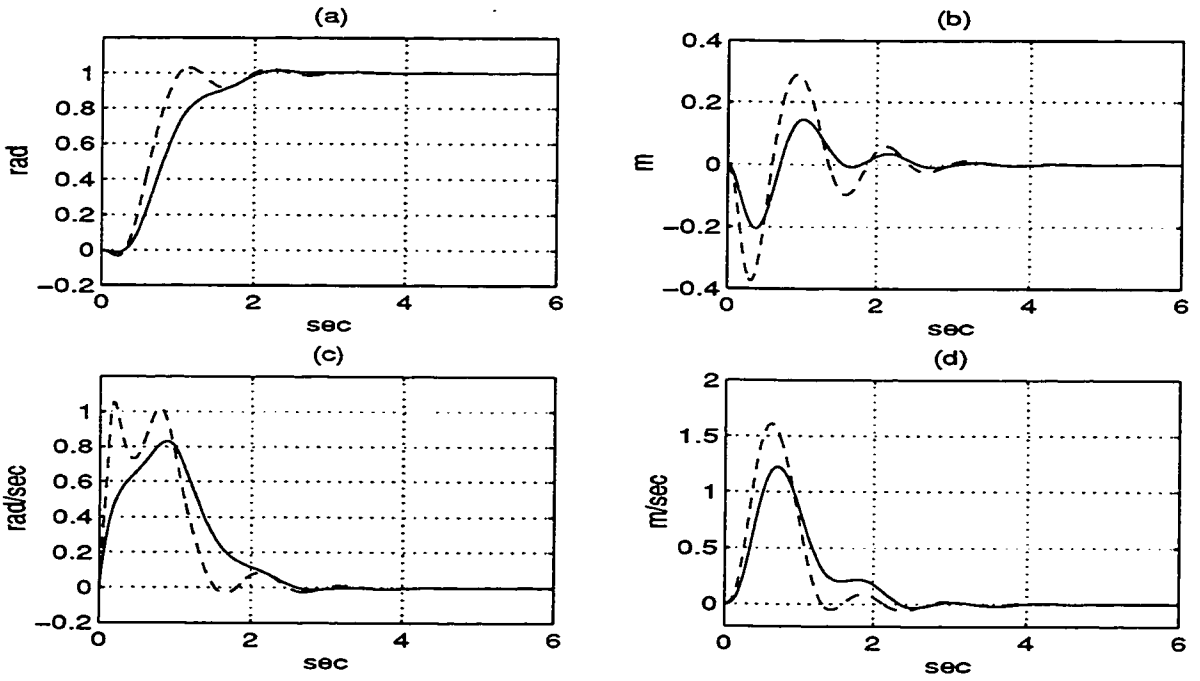

Figure 5.5: *The effect of weights on the controlled output:* $z = 5y$ *(solid) and* $z = 10y$ *(dashed): (a) tip position* y*, (b) tip deflection* δ*, (c)* $\hat{\theta}_2$*, and (d)* $\hat{\delta}_2$*.*

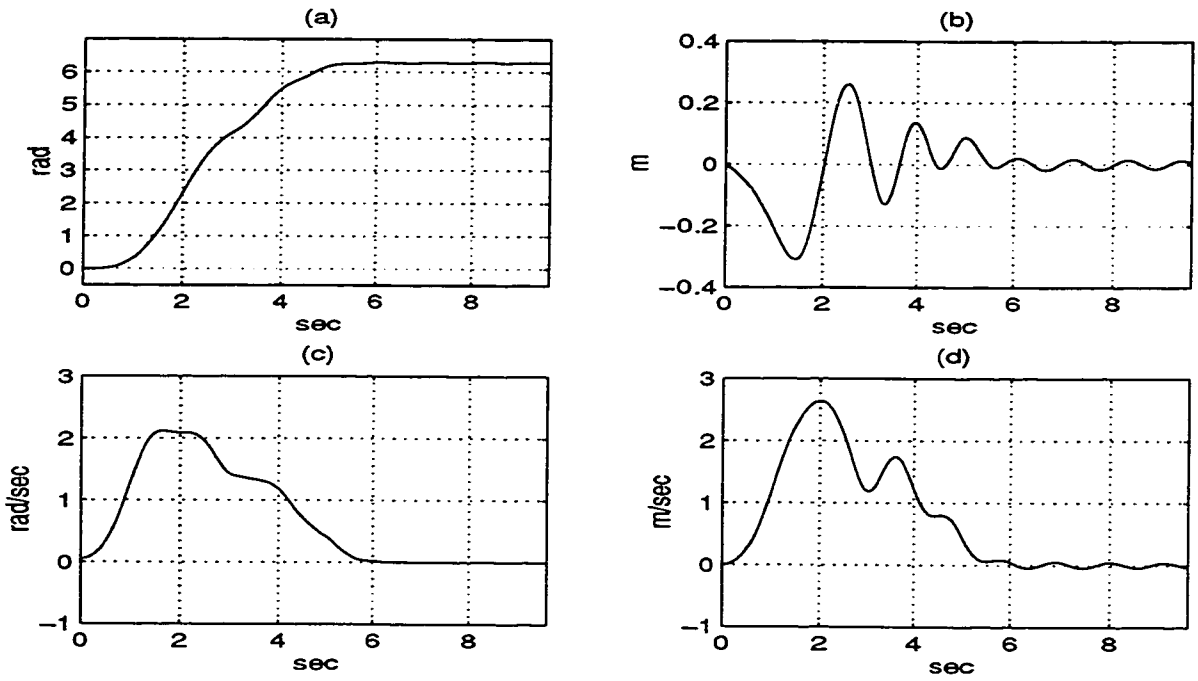

Figure 5.6: *Simulation results for a 2π amplitude step command using the third-order nonlinear controller. The linear controller results in instability: (a) tip position y, (b) tip deflection δ, (c) $\hat{\theta}_2$, and (d) $\hat{\delta}_2$.*

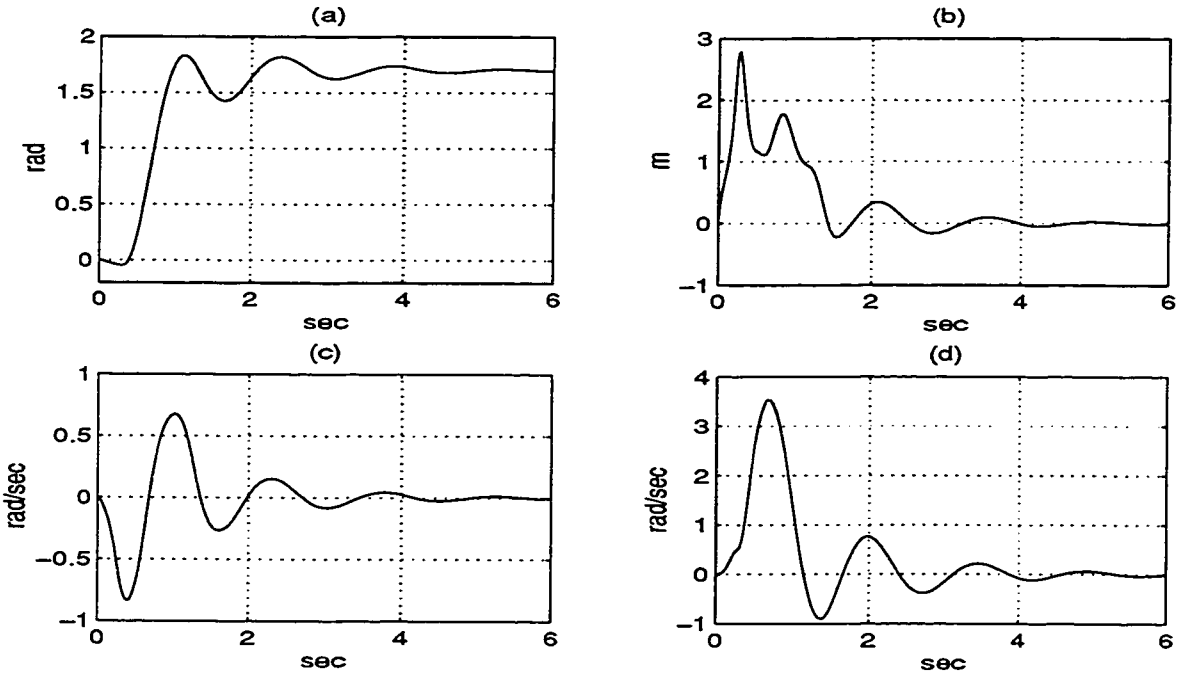

Figure 5.7: *Robustness of the third-order nonlinear controller in the presence of hub friction. The linear controller results in instability: (a) tip position y, (b) tip deflection δ, (c) $\hat{\theta}_2$, and (d) $\hat{\delta}_2$.*

Chapter 6

Robust Regulation of a Flexible-Link Manipulator Based on a New Modeling Approach

In this chapter, a new methodology for modeling a flexible link manipulator with an arbitrarily large number of deflection modes is presented where a part of dynamics representing flexibility is treated as *uncertainty*. The synthesis is performed based on only the *certain* dynamics of the manipulator. In other words, the proposed approach to modeling actually characterizes (in some sense) a reduced-order model of the system. It is shown that the *uncertainty* treated in this way is norm-bounded. Control of the tip position is pursued by utilizing the multi-objective H_∞ technique on the *certain* part of the dynamics. Robust regulation is obtained by minimizing the influence of the uncertainty on the tip position. The proposed strategy is applied to a single-link flexible arm and the simulation results verify the effectiveness of the analysis and design. Specifically, it is shown that using the proposed scheme, regulation of the tip position is achieved in a stable manner while using the standard approach, instability of the tip position occurs.

6.1 Introduction

In this chapter, a dynamical model for a flexible-link manipulator is presented such that a portion of the dynamics may be treated as norm-bounded uncertainty. In this view, the synthesis is performed for only the dominant or certain dynamics of the manipulator. This scheme, however, is significantly different from the conventional approaches of order reduction for linear/nonlinear systems [112] and in particular for flexible structures [113]. Specifically in this part, explicitly or implicitly, all the dynamics of the system are taken into consideration. In other words, the portion that is treated as perturbation is incorporated in the design by its maximum possible gain (in the L_2 sense) over different values of the inputs.

The main observation that can be made in support of the present methodology is the new insight and perspective that it provides by enabling a comparison between the mechanical behavior of flexible-link and rigid manipulators. Clearly the flexibility of a lightweight manipulator –when the compliance behavior itself is not the main objective– is not an inherent nor a desirable property of the arm; rather it is to be treated as an undesirable feature to be compensated for. The flexibility is basically due to the mechanical properties of the material used for building the robot and the dimensions of each link. From another point of view, even the common rigid robots, to a certain extent, are flexible. The only difference is that their flexibility may be ignored in modeling and control without introducing significant errors in the performance. In other words, for flexible arms, the flexibility may be interpreted as a perturbation acting on a rigid robot.

Since a flexible-link manipulator is a distributed parameter infinite dimensional system, the conventional approaches to control design truncate the model up to a certain number of deflection modes. This is also motivated by the fact that the impulse response of a truncated model based on two or three deflection modes, in general, is close to the impulse response of the actual arm. As a result, it might be tempting to suggest that in most applications, a model based on two modes should

be sufficient. However, the implication of ignoring the higher frequency modes which lie within the bandwidth of the sensors and actuators is that these modes could get amplified by the control system that could eventually lead to instability.

The modeling approach proposed in this section is motivated by representing a part of the original dynamical system as *unmodeled dynamics*. To clarify this point, consider the following system with the state vector $X := (x^T, v^T)^T$

$$\dot{x} = A_x\, x + A_{xv}\, v + B_x\, u, \tag{6.1}$$

$$\dot{v} = A_{vx}\, x + A_v\, v + B_v\, u, \tag{6.2}$$

where (6.2) is norm-bounded. It will be shown that it is possible to treat (6.2) as *unmodeled dynamics* interconnected to (6.1). In this way, one may synthesis a controller for the system (6.1)-(6.2) based on only (6.1) in which the coupling terms are treated as being unmodeled.

As pointed out above, in the standard way of modeling flexible-link manipulators, the system is assumed to be finite dimensional, and the synthesis is directly performed based on the corresponding model. In the modeling approach proposed in this chapter, however, the system may have arbitrarily large number of deflection modes. Although, the synthesis is performed on a finite-dimensional system, the controller designed may actually be applied to control the real system which is an infinite-dimensional system.

The objectives of this chapter are to provide a dynamical model for a flexible-link manipulator with an arbitrarily large number of deflection modes and to design a robust regulator based on the multi-objective H_∞ control technique. The outline of the remainder of the chapter is as follows. In Section 6.2, the new approach for modeling a flexible-link manipulator is introduced. Properties of the resulting model are investigated in Section 6.3. Section 6.4 presents the results of the multi-objective H_∞ control design. The framework for applying the proposed modeling approach to a flexible-link manipulator is given in Section 6.5. Simulation results

and conclusions are provided in Sections 6.6 and 6.7, respectively.

6.2 A New Approach to Modeling a Flexible-Link Manipulator

The dynamics of an n-link rigid robot arm may be expressed by a set of n differential equations [74],

$$M(\theta)\ \ddot{\theta} + n_1(\theta,\ \dot{\theta}) + F_c(\dot{\theta}) + F_h\dot{\theta} = u \tag{6.3}$$

where θ is an n-dimensional vector denoting the joint positions of the robot, n_1 represents the Coriolis and centrifugal forces, F_c denotes the Coulomb friction, F_h is the hub damping, and u is the vector of joint control torques.

Recall that in the case of a multi-link flexible-manipulator, the dynamic equations for a flexible-link arm can be derived following a Lagrangian approach [17]:

$$M(\delta,\theta)\begin{bmatrix}\ddot{\theta}\\ \ddot{\delta}\end{bmatrix} + \begin{bmatrix} n_1(\theta,\dot{\theta},\delta,\dot{\delta})\\ n_2(\theta,\dot{\theta},\delta)\end{bmatrix} + \begin{bmatrix} F_c(\dot{\theta}) + F_h\dot{\theta}\\ K_s\delta + F_s\dot{\delta}\end{bmatrix} = \begin{bmatrix} u\\ 0\end{bmatrix} \tag{6.4}$$

where $M(\delta,\theta)$ is the positive-definite symmetric inertia matrix. Let n and m_i ($i = 1\ \ldots\ n$) be the number of joints and deflection modes of the ith link, respectively. Then the inertia matrix $M(\theta,\delta)$ would be an $r \times r$ matrix, where $r = n + \sum_{i=1}^{n} m_i$, $\delta_i = [\delta_{i_1}\ \ \ldots\ \ \delta_{m_i}]^T$ is the vector of modal amplitudes, n_1 and n_2 are Coriolis and centrifugal terms, respectively, F_c denotes the Coulomb friction, F_h is the hub damping, K_s is the stiffness matrix, F_s is the structural damping matrix and u is the joint control torque.

A simple comparison between (6.3) and (6.4) reveals that the number of control inputs in a rigid manipulator, i.e., n is the same as the number of mechanical degrees of freedom, whereas this is not the case in a flexible manipulator where the number of mechanical degrees of freedom is $n + \sum_{i=1}^{n} m_i$. Hence, a flexible-link arm is

an under-actuated system in which the control is to be designed so that the rigid displacements as well as the flexible deflections have simultaneously certain desired behaviors. This limitation makes the control problem of a flexible-link manipulator significantly more complicated than the same problem for a rigid manipulator. The aim of this chapter is to provide new insight into the notion of *flexibility* of a flexible-link manipulator. In fact, we show that it is possible to treat a part of the flexible dynamics as being *uncertain.*

Towards this end, let us view some portions of the dynamics that could possibly include flexible modes as *unmodeled dynamics.* Although the term *unmodeled* refers to a subsystem whose dynamics are not known, it is used here to emphasize that the complete characteristics of this subsystem will not be utilized in the synthesis. If this is feasible, then the synthesis has to satisfy the design specifications for only the *known dynamics*, hereafter referred to as the *plant.* The *unmodeled dynamics*, on the other hand, may be considered as a subsystem that is connected to the *plant.* In this section, our objective is to apply the above concept to a single-link flexible manipulator. The extension to a multi-link flexible manipulator should in principle be feasible and is a topic for future work. The modeling approach is applicable to linear as well as nonlinear models of flexible-link manipulators. Since our proposed synthesis is based on a linear multi-objective control strategy, therefore we consider only the linearized model of a flexible-link manipulator in the modal coordinates. The model is given by [11, 80, 62]

$$\begin{aligned} \dot{X} &= A\,X + B\,u \\ y &= C\,X \end{aligned} \tag{6.5}$$

with

$$X = (x_0^T, x_1^T, \ldots, x_m^T)^T;\quad x_0 = (\theta, \dot{\theta})^T,\ x_i = (\delta_i, \dot{\delta}_i)^T,\quad i = 1, \ldots, m$$

$$A = \text{diag}\,(A_0, A_1, \ldots, A_m);\quad A_0 = \begin{pmatrix} 0 & 1 \\ 0 & -\alpha \end{pmatrix},\ A_i = \begin{pmatrix} 0 & 1 \\ -\omega_i^2 & -2\xi_i\omega_i, \end{pmatrix},$$

$$
\begin{aligned}
B &= (B_0^T, B_1^T, \ldots, B_m^T)^T; \quad B_0 = \beta \begin{pmatrix} 0 \\ 1 \end{pmatrix}, \quad B_i = \beta \begin{pmatrix} 0 \\ \phi_i'(L_0) \end{pmatrix}, \\
(\beta &= \frac{1}{I_0 + J_0 + J_L + M_L L_0^2}) \\
C &= (C_0, C_1, \ldots, C_m); \quad C_0 = \begin{pmatrix} L_0 & 0 \end{pmatrix}, \quad C_i = \begin{pmatrix} \phi_i(L_0) & 0 \end{pmatrix}, \qquad (6.6)
\end{aligned}
$$

where y is the tip position, m is the arbitrarily large number of flexible modes, α denotes the corresponding pole of the rigid dynamics, (ω_i, ξ_i) are the frequency and damping ratio of the ith deflection mode, I_0 is the hub inertia, J_0 is the inertia of the beam about the motor armature ($= \frac{1}{3}\rho L_0^3$), ρ is the mass per unit length, M_L is the payload mass, L_0 is the length of the link, J_L is payload inertia, $\frac{1}{\beta}$ is the total inertia about the armature, and ϕ_i represents ith mode shape.

Note that the design technique used in this chapter is state feedback. Consequently, for simplicity of design, the first state is taken as the output, i.e., the tip position. Taking the output as the first state implies that the first row of A should be changed and C is replaced by the first row of the identity matrix. The state-space model in this case is given by (6.5) with state vector defined as

$$
X = [y, \dot{\theta}, \delta_1, \dot{\delta}_1, \ldots, \delta_m^T, \dot{\delta}_m]^T \qquad (6.7)
$$

The transformation that transforms X in (6.5) to (6.7) is given in Appendix C.

Now, let $v = [\delta_i, \dot{\delta}_i, \ldots, \delta_m, \dot{\delta}_m]^T$, $(i \geq 1)$ denote the part of the state that is to be treated as *uncertainty* corresponding to unmodeled dynamics. The certain dynamics in this setting corresponds to the state vector $x = [y, \dot{\theta}, \delta_1, \dot{\delta}_1, \ldots, \delta_{i-1}, \dot{\delta}_{i-1}]^T$. Therefore, the state-space representation of the system is in the form (6.5) with

$$
\begin{aligned}
A &= \begin{pmatrix} A_x & A_{xv} \\ 0 & A_v \end{pmatrix}, \; B = \begin{pmatrix} B_x \\ B_v \end{pmatrix}, \; C = \begin{pmatrix} 1 & 0_{2\times m+1} \end{pmatrix}, \; X = (x^T, v^T)^T \qquad (6.8) \\
x &= [y, \dot{\theta}, \delta_1, \dot{\delta}_1, \ldots, \delta_{i-1}, \dot{\delta}_{i-1}]^T, \quad v = [\delta_i, \dot{\delta}_i, \ldots, \delta_m, \dot{\delta}_m]^T \qquad (6.9)
\end{aligned}
$$

where

$$A_x = \left[\begin{array}{cc|cccc} 0 & L_0 & 0 & \phi_1(L_0) & \cdots & 0 & \phi_{i-1}(L_0) \\ 0 & -\alpha & 0 & 0 & \cdots & 0 & 0 \\ \hline & & & A_1 & & 0 & \\ & 0 & & & \ddots & & \\ & & & 0 & & A_{i-1} & \end{array}\right], \quad A_{xv} = \left[\begin{array}{ccccc} 0 & \phi_i(L_0) & \cdots & 0 & \phi_m(L_0) \\ 0 & 0 & \cdots & 0 & 0 \\ \hline & & 0 & & \\ & & \vdots & & \\ & & 0 & & \end{array}\right]$$

$$A_v = \text{diag}\,(A_i, A_{i+1}, \ldots, A_m), \quad B_x = (B_0^T, B_1^T, \ldots, B_{i-1}^T)^T$$

$$B_v = (B_i^T, B_{i+1}^T, \ldots, B_m^T)^T \tag{6.10}$$

Therefore, the system can be represented in the form

$$\text{(plant)} \qquad \dot{x} = A_x\, x + A_{xv}\, v + B_x\, u, \quad y_x = x_1 = y \tag{6.11}$$

$$\text{(unmodeled dynamics)} \qquad \dot{v} = A_v\, v + B_v\, u, \quad y_v = C_v\, v \tag{6.12}$$

where C_v is the first row of A_{xv}. In the above partitioned form, the subsystem (6.12) may play the role of an uncertainty coupled to the certain subsystem (6.11) provided that the H_∞ norm of the uncertainty is bounded. The above representation is shown schematically in Figure 6.1. The plant has two inputs (v, u) and two outputs (z, X). The first input y_v represents the disturbances to be rejected. The second input is the *control input* u that is used for feedback design. The *controlled output* z represents a penalty variable, which may include a tracking error, as well as a cost of the control input needed to achieve the prescribed goal. Note that in the case of stabilization the first component of z may be the output itself whereas in the case of regulation the first component of z may be the difference between the output and the reference signal which we denote by e. The second output is the *measurement* x that is made on the system. This is used to generate the control input, which in turn is the tool we have to minimize the effect of the exogenous input on the controlled output. A constraint that is imposed is that the mapping from the *measurement* to the *control input* should be such that the closed loop system is internally stable. The effect of the *exogenous input* on the *controlled output* after closing the loop is measured in

terms of their energies and the worst-case disturbance of the closed-loop system. Our measure is the closed-loop H_∞ norm which is simply the L_2 induced norm. Suppose the objective is to only stabilize the system, i.e., the system has no exogenous input. By virtue of the small gain theorem, if the *plant* is stable, the overall system would remain stable if the product of the L_2 gains of the *plant* and *unmodeled dynamics* is less than one. It is clear that in the case of an unstable *plant*, one has to first stabilize the system by designing the control law u based on the available states and then apply the small gain theorem to ensure stability.

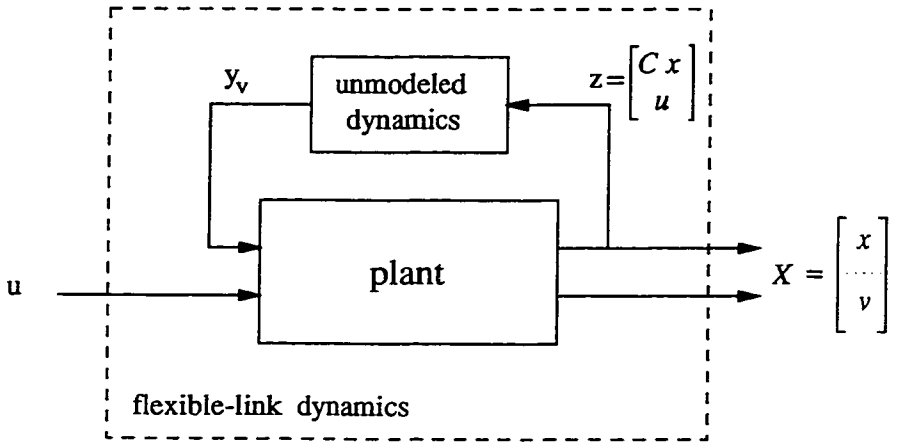

Figure 6.1: *Partitioning the flexible-link dynamics into two subsystems: plant and unmodeled dynamics where* $x = [y, \dot{\theta}, \delta_1, \dot{\delta}_1, \ldots, \delta_{i-1}, \dot{\delta}_{i-1}]^T$ and $v = [\delta_i, \dot{\delta}_i, \ldots, \delta_m, \dot{\delta}_m]^T$ $(i \geq 1)$.

The next section examines the properties of the proposed model of a flexible-link manipulator in view of the above discussion.

6.3 Properties of the Proposed Model of a Flexible-Link Manipulator

As pointed out earlier the model represented by equations (6.11)-(6.12) can be used to reformulate the problem in the framework of Figure 6.1. In this setting the state vector is partitioned into two parts. One part represents the *plant* dynamics,

while the remaining part represents the *unmodeled dynamics*. Consequently, only the *dominant* part of the states in the model (6.11)-(6.12) will be considered for the purpose of synthesis. Note that the *unmodeled dynamics* enter into the synthesis only through their maximum possible gain –in the L_2 sense– over different values of the inputs.

To show the boundedness of the *unmodeled dynamics*, recall the condition under which a linear system has a bounded H_∞ norm:

Theorem 6.1 [114] *The H_∞ norm of a linear system is finite if and only if its transfer function is proper and has no poles on the imaginary axis.*

From the structure of $A_v = \text{diag}\ (A_i, A_{i+1}, \ldots, A_m)$ it is easy to see that A_v is Hurwitz. This in turn shows that the dynamics represented by (6.12) are stable. Moreover, since there is no through-put between u and y_v, the input-output map is stable and proper. Consequently, according to Theorem 6.1, the *unmodeled dynamics* represented by (6.12) have finite H_∞ norm. Let the mapping induced by *unmodeled dynamics* be represented by Δ. The calculation of $\|\Delta\|_\infty$ is an iterative process. This process for a system given by equations

$$\begin{aligned} \dot{x} &= \bar{A}x + \bar{B}u \\ y &= \bar{C}x \end{aligned}$$

accounts for the search of that ν such that the matrix

$$R(\nu) = \begin{bmatrix} \bar{A} & \nu^{-2}\bar{B}\bar{B}^T \\ -\bar{C}^T\bar{C} & -\bar{A}^T \end{bmatrix}$$

has one or more eigenvalues on the imaginary axis. The procedure can begin with an upper bound for ν and search from there. It helps to realize that the matrix $R(\nu)$ is a *symplectic* matrix which has the property that its eigenvalues are symmetrically located with respect to the j-axis.

In the following section, however, we compute the H_∞ norm of the *unmodeled dynamics* by using a balancing technique for linear systems.

6.3.1 Balanced Realization

The dynamical system given in (6.12) has in fact the dynamics of a flexible structure that was studied in [115]. The H_∞ norm of a flexible structure may be computed from its balanced realization. In this section, we briefly review the definition of a balanced realization.

Consider the triple $(\bar{A}, \bar{B}, \bar{C})$ representing an nth order linear system (6.5). Let λ_i be the i-th eigenvalue of $\bar{A}$ and impose the condition $\lambda_i + \overline{\lambda}_j \neq 0$ for every $i, j = 1, \ldots, n$. The controllability and observability Grammians are defined as follows [116]

$$W_c = \int_0^t e^{\bar{A}\tau} \bar{B} \bar{B}^* e^{\bar{A}^*\tau} \, d\tau, \quad W_o = \int_0^t e^{\bar{A}\tau} \bar{C} \bar{C}^* e^{\bar{A}^*\tau} \, d\tau,$$

These Grammians satisfy the equations

$$\dot{W}_c = \bar{A} W_c + W_c \bar{A}^* + \bar{B} \bar{B}^*, \quad \dot{W}_o = \bar{A}^* W_o + W_o \bar{A} + \bar{C}^* \bar{C} \tag{6.13}$$

The stationary solutions of (6.13) such that $\dot{W}_c = \dot{W}_o = 0$ are determined from the Lyapunov equations

$$\bar{A} W_c + W_c \bar{A}^* + \bar{B} \bar{B}^* = 0, \quad \bar{A}^* W_o + W_o \bar{A} + \bar{C}^* \bar{C} = 0 \tag{6.14}$$

Note that stationary solutions exist for both stable and unstable systems with the difference that for stable systems, the solutions are positive definite. The system (6.5) is said to be balanced if its controllability and observability Grammians are equal and diagonal [116].

6.3.2 H_∞ Norm of the Unmodeled Dynamics

Using the similarity between the *unmodeled dynamics* and the dynamics of flexible structures, we exploit the relevant results from flexible structures to compute the H_∞ norm of the *unmodeled dynamics*. It is shown in [117] that the H_∞ norm of the dynamics of a flexible structure is approximately equal to $2\gamma_1^2$, where γ_1 is the

largest Hankel singular value of the system. Recall that the Hankel singular values for a system whose controllability and observability Grammians are W_c and W_o, respectively are defined as the square roots of the eigenvalues of W_cW_o. Since the Hankel singular values are in decreasing order, i.e., $\gamma_i \geq \gamma_{i+1}$, $(i = 1, \ldots, m-1)$, the H_∞ norm of the *unmodeled dynamics* can be determined by simply inspecting the block corresponding to mode # i, i.e., by computing the H_∞ norm of the system (A_i, B_i, C_i) where i is the index of the first state of the *unmodeled dynamics.* In the following theorem we show how the H_∞ norm of the unmodeled dynamics may be related to the parameters of the unbalanced system.

Theorem 6.2 *Let Δ be the operator that maps the input to the output of the* unmodeled dynamics *defined in Figure 6.1 with state vector $v = [\delta_i, \dot{\delta}_i, \ldots, \delta_m, \dot{\delta}_m]^T$ $(i \geq 1)$. Then an upper bound for the H_∞ norm of Δ is given by*

$$\|\Delta\|_\infty \leq \frac{|\beta\phi_i(L_0)'\phi_i(L_0)|}{\xi_i\omega_i^2} \tag{6.15}$$

Proof: As pointed out earlier, the H_∞ norm of Δ is approximately $2\gamma_1^2$, where γ_1 is the largest Hankel singular value of the system [117], i.e. $\|\Delta\|_\infty \approx 2\gamma_1^2$ where $\gamma_1 = \max_i \sqrt{\lambda_i(\Gamma^2)}$ and $\Gamma^2 = W_c = W_o$ in the balanced coordinates. Let the triple (A_i, B_i, C_i) be the system matrices corresponding to mode # i in modal coordinates, (see (6.6)), i.e.,

$$A_i = \begin{pmatrix} 0 & 1 \\ -\omega_i^2 & -2\xi_i\omega_i, \end{pmatrix}, \quad B_i = \beta \begin{pmatrix} 0 \\ \phi_i'(L_0) \end{pmatrix}, \quad C_i = \begin{pmatrix} \phi_i(L_0) & 0 \end{pmatrix}$$

It is shown in [118] that the balanced system is approximately given by

$$A_b = \begin{pmatrix} -\xi_i\omega_i & -\omega_i\sqrt{1-\xi_i^2} \\ \omega_i\sqrt{1-\xi_i^2} & -\xi_i\omega_i, \end{pmatrix}, B_b = \hat{\beta} \begin{pmatrix} 1 \\ -1 \end{pmatrix}, C_b = \mathrm{sgn}(\hat{\alpha})\hat{\beta} \begin{pmatrix} 1 & 1 \end{pmatrix} \tag{6.16}$$

where

$$\hat{\beta} = \sqrt{\frac{|\hat{\alpha}|}{2\omega_i}}, \quad \hat{\alpha} = \beta\phi_i'(L_0)\phi_i(L_0)$$

This follows from the results of [119] where the balanced and modal coordinates are almost the same if damping is small and all frequencies are widely separated. Referring to (6.14) and adding the left (right) sides of the equations together, we get

$$(A_b + A_b^T)\ \Gamma^2 + \Gamma^2\ (A_b + A_b^T) = -(B_b B_b^T + C_b^T C_b)$$

Noting that both Γ and $(A_b + A_b^T)$ are diagonal, we obtain

$$\begin{aligned} \|(A_b + A_b^T)\ \Gamma^2 + \Gamma^2\ (A_b + A_b^T)\| &= 2\|\Gamma^2\|\|A_b + A_b^T\| = 4\xi_i\omega_i\ \|\Gamma\|^2 \\ \|B_b B_b^T + C_b^T C_b\| &\leq B_b^T B_b + C_b C_b^T \end{aligned}$$

As a result

$$\|\Gamma\|^2 \leq \frac{B_b^T B_b + C_b C_b^T}{4\xi_i\omega_i}$$

Consequently, the inequality (6.15) follows by substituting the matrices B_b and C_b from (6.16) in the above expression. $\triangle$

Note that one may evaluate the H_∞ norm of the unmodeled dynamics by using any of the following three methods:

- By considering the full system matrix A_v consisting of sub-blocks $\#i, \ldots, \#m$ to compute the norm based on the general procedure given by, e.g., [98].
- By considering only the first sub-block of system matrix A_v, i.e., sub-block $\#i$ to compute the norm as in [117].
- By computing the upper bound using (6.15).

The first method is probably the most obvious way of computing the H_∞ norm. However, because of the large dimension of the full block matrix, the method is computationally very time consuming. In the second method, we need the balanced realization of the system, whereas in the third method, the H_∞ norm is computed

for the original model of the system that may be unbalanced. Figure 6.2 shows the H_∞ norms for the *unmodeled dynamics* of the flexible-link arm described in Tables A.1 and A.2 in Appendix A. by using the above three methods.

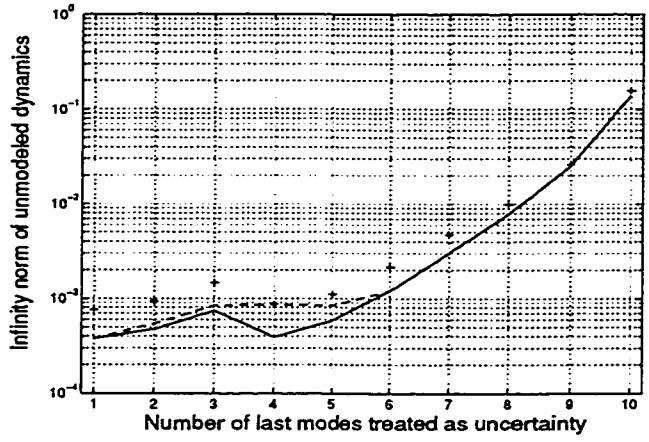

Figure 6.2: *Norm of the unmodeled dynamics of a flexible-link manipulator with ten eigenfrequences based on: block #i (solid), blocks #i,...,#10 (dashed), and the upper bound given by 6.15 (+).*

Two observations may be made from Figure 6.2. First, the relevant norms based on block #*i* and blocks #*i*,...,#10 are considerably close to each other implying that for computing the infinity norm of the *unmodeled dynamics*, it suffices to compute the norm based on only the first block. The second point is that this norm has an upper bound that can be easily computed by using the original model of the flexible-link arm.

6.4 The Design Technique

It is widely accepted that no mathematical representation can exactly model a physical system. Very often the plant to be controlled is not exactly known or more precisely is only known to belong to a certain class of systems. In this case, we say the plant is uncertain and denote the set which the plant belongs to as an uncertain set. For this reason, the designer must be aware of how modeling errors might adversely

affect the performance of a control system.

6.4.1 Multi-objective H_∞ Control

In this section, we review the results of [120, 111] concerning multi-objective H_∞ sub-optimal control with the controller constrained to achieve robust closed-loop regulation.

Let Δ denote the map from z to v and P_Δ be as shown in Figure 6.3. Assume that the L_2 norm of Δ is bounded by some positive number. The Problem of Robust Regulation in the presence of Gain-Bounded Uncertainty (RRGBU) may be stated as follows: Given a real number $\gamma_v > 0$, design a controller such that for all gain-bounded Δ with $\|\Delta\|_\infty < 1/\gamma_v$,

- the controller internally stabilizes P_Δ,
- the regulated output e converges to zero as $t \to \infty$,
- the convergence property holds for all plants in some neighborhood of P_Δ in the sense of the graph topology.

Throughout this chapter, the finite-dimensional linear time-invariant system

$$\begin{aligned} \dot{x} &= \mathbf{a}x + \mathbf{b_1}u_1 + \mathbf{b_2}u_2 \\ y_1 &= \mathbf{c_1}x + \mathbf{d_{11}}u_1 + \mathbf{d_{12}}u_2 \\ y_2 &= \mathbf{c_2}x + \mathbf{d_{21}}u_1 + \mathbf{d_{22}}u_2 \end{aligned}$$

is represented by

$$T_{yu} \sim \left[\begin{array}{c|cc} \mathbf{a} & \mathbf{b_1} & \mathbf{b_2} \\ \hline \mathbf{c_1} & \mathbf{d_{11}} & \mathbf{d_{12}} \\ \mathbf{c_2} & \mathbf{d_{21}} & \mathbf{d_{22}} \end{array}\right] \tag{6.17}$$

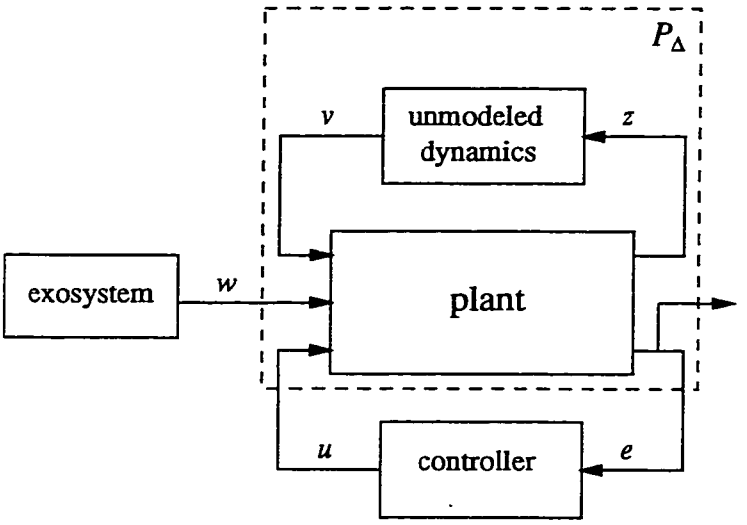

Figure 6.3: *Setup for the problem of robust regulation in the presence of gain-bounded uncertainty (RRGBU).*

where T_{yu} is the transfer function mapping input u to output y. According to this representation, the *plant* (6.11) may be expressed as follows:

$$P_l \sim \left[\begin{array}{c|ccc} A_x & A_{xv} & 0 & B_x \\ \hline C_1 & 0 & 0 & D_{12} \\ I & 0 & -I & 0 \end{array}\right] \tag{6.18}$$

where the controlled output z and the output e are defined by

$$\begin{aligned} z &= C_1\, x + D_{12}\, u := \begin{bmatrix} C_x \\ 0 \end{bmatrix} x + \begin{bmatrix} 0 \\ I \end{bmatrix} u = \begin{bmatrix} C_x\, x \\ u \end{bmatrix} \\ e &= x - x_{ref} \end{aligned} \tag{6.19}$$

where $C_x = [1 \;\; 0_{2\times m+1}]$.

Note that our proposed design technique is based on state feedback. However, since the first state was defined as the output, therefore, the x_{ref} is defined as $[y_{ref} \;\; 0_{2\times m+1}]$. By the Internal Model Principle [121], any controller that solves the output regulation problem, internally incorporates a model of the dynamical system generating the reference trajectories. In other words, a *copy of the exosystem* is

augmented as a subsystem in the compensator dynamics. In view of the above, the following definition characterizes the dynamics of the exosystem for incorporating in the synthesis. The frequencies $\omega_1, ..., \omega_N$ are associated with the reference input trajectory where $\omega = 0$ corresponds to a step input.

Definition 6.1 *(Internal model matrices)* [111]*:* $\tilde{A}$ and $\tilde{B}$ are internal model matrices associated with the robust regulation problem determined by $\omega_1, ..., \omega_N$ if these matrices satisfy

1. $\text{spec}(\tilde{A}) = \{\pm j\omega_1, ..., \pm j\omega_N\}$,
2. every eigenvalue of $\tilde{A}$ has multiplicity 1,
3. $\tilde{A}$ is diagonalizable, and
4. $(\tilde{A}, \tilde{B})$ is controllable.

As an example, if the regulation against say ω_1 is sought, we may set $\tilde{A}$ and $\tilde{B}$ as follows

$$\tilde{A} = \begin{bmatrix} 0 & \omega_1 \\ -\omega_1 & 0 \end{bmatrix}, \quad \tilde{B} = \begin{bmatrix} 0 \\ 1 \end{bmatrix}$$

We are now in a position to address the solution to the robust regulation problem for the setup shown in Figure 6.3. It is shown in [111] that this problem is equivalent to the problem of Robust Regulation with an H_∞ Constraint ($RRH_\infty C$). The setup for $RRH_\infty C$ is obtained from Figure 6.3 by removing the unmodeled dynamics block. The design of the robust regulator for both setups, i.e., RRGBU and $RRH_\infty C$ requires the results of the following theorem. The notation T_{zv} denotes the operator that maps v onto z.

Theorem 6.3 [111]*: Assume* (A_x, B_x) *is stabilizable and* (C_1, A_x, A_{xv}) *has no uncontrollable/unobservable modes on the imaginary axis. Assume also that* $D_{12}^T C_1 = 0$ *and* $D_{12}^T D_{12} = I$*. Then the following statements are equivalent*

- *There exists a controller that solves the robust regulation problem from w to e at the frequencies $\omega_1, ..., \omega_N$ while also making $\|T_{zv}\|_\infty < \gamma$ (the $RRH_\infty C$ problem).*

- *There exists a controller that renders $\|T_{zv}\|_\infty < \gamma$ and*

$$\gamma^2 T_k B_x B_x^T T_k^* > T_k A_{xv} A_{xv}^T T_k^* \tag{6.20}$$

for all $k = 1, \ldots, N$, where T_k and $\overline{A}$ are defined from

$$\begin{aligned} T_k : &= [1 \quad 0_{2\times m+1}](j\omega_k I - \overline{A})^{-1} \\ \overline{A} : &= A_x + (\frac{1}{\gamma^2} A_{xv} A_{xv}^T - B_x B_x^T)P \end{aligned} \tag{6.21}$$

and P is the stabilizing solution to

$$A_x^T P + P A_x + P(\frac{1}{\gamma^2} A_{xv} A_{xv}^T - B_x B_x^T)P + C_1^T C_1 = 0 \tag{6.22}$$

Moreover, if either of these conditions hold, then a controller that solves the robust regulation problem from w to e at the frequencies $\omega_1, ..., \omega_N$ is given by

$$K_c \sim \left[\begin{array}{c|c} \tilde{A} & \tilde{B}\begin{bmatrix} 1 & 0_{2\times m+1} \end{bmatrix} \\ \hline B_x^T L^T W^{-1} & -B_x^T P - B_x^T L^T W^{-1} L \end{array}\right]. \tag{6.23}$$

where L is the unique solution to

$$L\overline{A} - \tilde{A}L = \tilde{B}\begin{bmatrix} 1 & 0_{2\times m+1} \end{bmatrix}, \tag{6.24}$$

the internal model matrices $\tilde{A}$ and $\tilde{B}$ satisfy Definition 6.1, and W is a positive definite matrix that satisfies the Lyapunov inequality

$$\tilde{A}W + W\tilde{A}^T + \frac{1}{\gamma^2} L A_{xv} A_{xv}^T L^T - L B_x B_x^T L^T < 0. \tag{6.25}$$

Remark 6.1 The coupling condition (6.20) has an intuitive interpretation in the frequency domain. Referring to the definition of T_k, one finds that $T_k B_x$ and $T_k A_{xv}$

are the open-loop transfer functions from u to e and v to e, respectively (see Figure 6.3). Therefore, $T_k B_x B_x^T T_k^*$ and $T_k A_{xv} A_{xv}^T T_k^*$ may be considered as the square of the magnitude of the corresponding frequency responses. Consequently, the inequality (6.20) provides the ratio of the above magnitudes which in turn yields the attenuation provided by the controller.

To synthesize the controller (6.23), one must solve a Riccati equation for P, a linear matrix equation for L, and a linear matrix inequality (LMI) for W. A solution for L always exists, since $\overline{A}$ and $\widetilde{A}$ have no eigenvalues in common [111]. In the simple but important case where the only frequency of interest is $\omega_1 = 0$, W may be computed easily. Specifically, in this case, $\widetilde{A} = 0$ so any positive-definite matrix is an acceptable choice for W. The general case is also tractable, since the LMI is a finite-dimensional convex feasibility problem [122].

6.4.2 Robust Regulation Based on Partial State-Feedback

In Section 6.2 we observed that it is possible to partition the state equations of a flexible-link manipulator such that part of the state is treated as uncertainty. As seen from Figure 6.3, in this case the *plant* is interconnected to the *unmodeled dynamics*. In this section we study the problem of designing a robust regulator for a system that is interconnected to unmodeled dynamics.

By virtue of Theorem 6.3, the robust regulator is designed for a linear interconnected system described below. Specifically, consider the stable linear system

$$\begin{aligned} \dot{v} &= A_v\, v + B_v\, u, \\ y_v &= C_v\, v \end{aligned} \tag{6.26}$$

By assumption A_v is Hurwitz. According to Theorem 6.1, the H_∞ norm of the system is finite. This norm may be evaluated from the algebraic Riccati equation as shown in [123]. It is the smallest positive parameter γ_v such that the algebraic

Riccati equation below has a positive-definite solution

$$A_v^T P_v + P_v A_v + \frac{1}{\gamma_v^2} P_v B_v B_v^T P_v + C_v^T C_v = 0 \tag{6.27}$$

Furthermore, consider now a linear system

$$\begin{aligned} \dot{X} &= A\,X + B\,u \\ y &= C\,X \end{aligned} \tag{6.28}$$

where

$$X = \begin{pmatrix} x \\ v \end{pmatrix},\ A = \begin{pmatrix} A_x & A_{xv} \\ 0 & A_v \end{pmatrix},\ B = \begin{pmatrix} B_x \\ B_v \end{pmatrix},\ C = \begin{pmatrix} C_x & 0 \end{pmatrix} \tag{6.29}$$

with x as the state of a finite-dimensional linear system, v the state of system (6.26) and A_x, A_{xv}, B_x and C_x matrices with appropriate dimensions. Using the above definitions, the main result is now stated by the following theorem.

Theorem 6.4 *Consider the linear systems (6.26) and (6.28) with definitions given in (6.29). Let (A_x, B_x) be stabilizable and (C_1, A_x, A_{xv}) with C_1 defined in (6.19) have no uncontrollable/unobservable modes on the imaginary axis. Let the H_∞ norm of (6.26) be γ_v. Suppose the Riccati equation*

$$A_x P + P A_x + P(\frac{1}{\gamma^2} A_{xv} A_{xv}^T - B_x B_x^T) P + C_x^T C_x = 0 \tag{6.30}$$

has a positive definite solution P for some $\gamma < \frac{1}{\gamma_v}$. Then the controller K_c given by (6.23) solves the robust regulation problem for the system (6.28).

Proof: Let us first partition system (6.28) into a *plant* and an *unmodeled dynamics* as in (6.11) and (6.12) with the difference that the output here is $y_x = C_x\,x$. Let the dynamics of the *plant* be described by

$$\begin{aligned} \dot{x} &= A_x\,x + A_{xv}\,v + B_x\,u \\ y_x &= C_x\,x \end{aligned} \tag{6.31}$$

Consider the dynamics of v given by (6.26), represented in the form

$$\dot{v} = A_v\, v + B_v\, u = A_v\, v + \begin{bmatrix} 0 & B_v \end{bmatrix} \begin{bmatrix} C_x\, x \\ u \end{bmatrix}$$

Let the controlled output of (6.31) be given by (refer to (6.19))

$$z = C_1\, x + D_{12}\, u := \begin{bmatrix} C_x \\ 0 \end{bmatrix} x + \begin{bmatrix} 0 \\ I \end{bmatrix} u = \begin{bmatrix} C_x\, x \\ u \end{bmatrix} \tag{6.32}$$

Note that the above definition satisfies the conditions $D_{12}^T C_1 = 0$ and $D_{12}^T D_{12} = I$ in Theorem 6.3. Therefore, (6.26) may be represented by a system having a finite H_∞ norm that is

$$\dot{v} = A_v\, v + B_1\, z \tag{6.33}$$

where $B_1 = [0\ B_v]$ and $B_1 B_1^T = B_v B_v^T$. By invoking Theorem 6.1 it follows that (6.33) has a finite H_∞ norm denoted by γ_v. Therefore, system (6.33) may be treated as *unmodeled dynamics* to be coupled to system (6.31). Consequently, we might subsequently ignore this part of the dynamics in (6.28) and perform the design based on only the dynamics governed by (6.31). Towards this end, the only required knowledge from (6.33) is its H_∞ norm. Hence, by reformulating the problem into the framework of Figure 6.3, the result now follows by applying Theorem 6.3 to system (6.31). $\triangle$

Remark 6.2 Although the controller uses all the states of the system (6.31), i.e., x, with respect to the full order system (6.28), it utilizes partial state feedback of X. Therefore, robust regulation for (6.28) is actually achieved by only partial state feedback.

6.5 Framework for Application of the Proposed Modeling Technique

The multi-objective H_∞ control technique based on the modeling approach developed in this chapter may be applied to many physical systems. The principle behind the proposed methodology is that the system under control should possess a two-time scale separation, namely, low and high-frequency subsystems. The restriction imposed is that the high-frequency subsystem should be stable to result in the norm-bounded property. The design based on the multi-objective H_∞ technique proceeds by considering low-frequency subsystem while treating high-frequency subsystem as *unmodeled dynamics*. One of the practical applications that fits into this framework is the flexible-link manipulator which is studied in the next section. In fact the rigid dynamics that characterize the dominant motion of the joints correspond to the low-frequency subsystem and the deflection dynamics due to flexibility of the links correspond to the high-frequency subsystem. Assuming that all damping including the flexural damping, are positive and nonzero, the high-frequency subsystem is stable and hence norm-bounded.

6.5.1 Application to a Flexible-Link Manipulator

As discussed above the multi-objective H_∞ control technique can be applied to a flexible-link manipulator. The conventional use of H_∞ technique proceeds by first finding a mathematical description of the uncertainty set. The uncertainty set is constructed based on the nominal plant. Towards this end, one has to define the uncertainty set in such a way as to cover all possible plants in the corresponding topology. In the modeling approach of this chapter, the uncertainty arises from the plant itself. In fact, the plant is partitioned such that some of its dynamics are considered as being uncertain. Consequently, it is possible to show that a flexible-link manipulator may be represented by (6.11) and (6.12). The *uncertainty* constructed

in this way includes some of the deflection mode dynamics. However, what remains to be established is the dimension of the *uncertainty* dynamics so that the design conditions are satisfied. It appears that an infinite number of modes have to be considered for this purpose. This issue is addressed by the following corollary.

Corollary 6.1 *Let the flexible-link manipulator with m deflection modes be described by (6.11) and (6.12). Let also the deflection modes #i onward be considered as uncertainty, i.e.,* $v = [\delta_i, \dot{\delta}_i, \ldots, \delta_p, \dot{\delta}_p]^T$ *where the number of modes, p, can be arbitrarily large* ($p \to \infty$). *Consequently, the problem of multi-objective* H_∞ *design for system (6.11) based on* $v = [\delta_i, \dot{\delta}_i, \ldots, \delta_p, \dot{\delta}_p]^T$ *is equivalent to the same problem based on* $v_i = [\delta_i, \dot{\delta}_i]^T$ *in (6.12).*

Proof: In Section 6.3.2 it was shown that to compute the infinity norm of the *unmodeled dynamics* it suffices to compute the norm based on only the first block. Hence, based on the upper bound obtained in Theorem 6.2, it follows that to design a controller for compensating the deflection modes $\#i, \#(i+1), \#(i+2), \ldots$ it suffices to design a controller to compensate for only the deflection mode $\#i$. $\triangle$

For the purpose of design, we have to specify the value of i, i.e., the index of the state after which it is considered as uncertainty. It is clear that the smaller the i, the smaller is the size of *plant*, i.e., the dimension of x in (6.11). Therefore, it is desirable to choose the smallest possible value of i. From a physical point of view the problem is to determine the number of deflection modes that can be treated as uncertainty. Intuitively, for very flexible manipulators the first few modes should be taken into account in the *plant* representation. This is due to the fact that flexibility is an inherent feature of such manipulators and hence cannot be treated as uncertainty. Nevertheless, even for very flexible manipulators, it is always possible to treat some higher elastic modes as uncertainty. The following procedure illustrates the steps to be taken for finding the minimum value for i. The algorithm for designing a robust tip position regulator is based on the proposed model of a flexible-link manipulator described in Section 6.2. The procedure is as follows:

Step 1. Specify the dynamics of the exosystem based on Definition 6.1.

Step 2. Set $i = 1$.

Step 3. Construct equations (6.11) and (6.12).

Step 4. Find the upper bound of γ_v using (6.15).

Step 5. Check if (6.22) has a positive-definite solution for some $\gamma < \frac{1}{\gamma_v}$.

- If yes, go to Step 6.
- If no, set $i = i + 1$ and go to Step 3.

Step 6. Compute $\overline{A}$ from (6.21) and solve (6.24) for L.

Step 7. Solve inequality (6.25) for W, e.g., by means of MATLAB based softwares `lmitool` [124] and `SP` [125].

Step 8. Construct the controller (6.23) from the information obtained above.

Since the above procedure begins with $i = 1$, it will always result in the minimum value for i such that all the conditions of Theorem 6.3 are satisfied.

6.5.2 Presence of Parametric Uncertainty

In many applications of flexible-link manipulators, the system parameters are not known exactly *a priori*. For instance, the load may vary while performing a task, or the coefficients of friction and damping may change depending on the configurations. Thus, there may be significant uncertainty in a manipulator's dynamic model. To study the effects of this parametric uncertainty, consider the linearized model of (6.4) in configuration space

$$M \begin{bmatrix} \ddot{\theta} \\ \ddot{\delta} \end{bmatrix} + F \begin{bmatrix} \dot{\theta} \\ \dot{\delta} \end{bmatrix} + K \begin{bmatrix} \theta \\ \delta \end{bmatrix} = \begin{bmatrix} u \\ 0 \end{bmatrix} \tag{6.34}$$

where F and K are damping and stiffness matrices, respectively. Following [38], consider the following perturbations:

- uncertainty in the inertia matrix due to load changes (ΔM)
- uncertainty in the matrix F due to friction changes (ΔF)
- uncertainty in the matrix K due to configuration changes (ΔK)

In other words, the matrices in (6.34) may be represented by the sum of a nominal part and a perturbed part, specifically

$$M := M_0 + \Delta M, \quad F := F_0 + \Delta F, \quad K := K_0 + \Delta K$$

where M_0, F_0 and K_0 are the nominal matrices that are assumed to be known, whereas the parameter perturbation terms ΔM, ΔF and ΔK are assumed to be unknown. By considering the above perturbations, the dynamic equations for the manipulator become

$$(M_0 + \Delta M)\begin{bmatrix} \ddot{\theta} \\ \ddot{\delta} \end{bmatrix} + (F_0 + \Delta F)\begin{bmatrix} \dot{\theta} \\ \dot{\delta} \end{bmatrix} + (K_0 + \Delta K)\begin{bmatrix} \theta \\ \delta \end{bmatrix} = \begin{bmatrix} u \\ 0 \end{bmatrix} \tag{6.35}$$

Let $q_1 := [\theta^T, \delta^T]^T$. Therefore, $\tau := -(\Delta M\ \ddot{q} + \Delta F\ \dot{q} + \Delta K\ q)$ may be taken as the total disturbance due to parametric uncertainty. Therefore, using the above definition, the dynamic equation of the manipulator may be represented in the form

$$M_0\ \ddot{q_1} + F_0\ \dot{q_1} + K_0\ q_1 = Gu + \tau \tag{6.36}$$

where $G = [I \quad 0]^T$. Note that the dynamic structure of (6.36) is different from that of (6.11). As a matter of fact, the perturbations ΔM, ΔF and ΔK are more appropriately explained in terms of the mass-spring structure of (6.34). However, the model of a flexible-link manipulator used in this chapter is in the state-space form (6.11). There are two possibilities for representing the perturbations in state-space form, namely, independent and fractional representations. In the former, the perturbations appear as an independent exogenous input to the system. In the latter, the perturbations are stated in terms of the states and inputs.

6.5.3 Independent Representation

By defining $q = [q_1^T, \dot{q_1}^T]^T$ as the state vector, the following state-space representation of (6.36) is obtained

$$\dot{q} = \begin{pmatrix} 0 & I \\ -M^{-1}K & -M^{-1}F \end{pmatrix} q + \begin{pmatrix} 0 \\ -M^{-1}G \end{pmatrix} u + \begin{pmatrix} 0 \\ -M^{-1} \end{pmatrix} \tau \qquad (6.37)$$

The above system can be transformed into (6.11) by using an appropriate similarity transformation T such that $X = Tq$ (for details refer to Appendix C).

6.5.4 Fractional Representation

In view of (6.11) and (6.12), parametric uncertainty corresponds to the following structure

$$\dot{x} = (A_x^0 + \Delta A_x)\, x + (A_{xv}^0 + \Delta A_{xv})\, v + (B_x^0 + \Delta B_x)\, u \qquad (6.38)$$

$$\dot{v} = (A_v^0 + \Delta A_v)\, v + (B_v^0 + \Delta B_v)\, u \qquad (6.39)$$

where $(.)^0$ denotes the nominal value of $(.)$. Since the control is applied to only (6.38), any perturbations ΔA_v and ΔB_v that satisfy the conditions of Theorem 6.4 may be considered as admissible perturbations for the *uncertain* part of the dynamics. The *certain* part of the dynamics, i.e., (6.38) may be written as

$$\dot{x} = A_x^0\, x + A_{xv}^0\, v + B_x^0\, u + (\Delta A_x \vdots \Delta A_{xv} \vdots \Delta B_x) \begin{pmatrix} x \\ v \\ u \end{pmatrix} \qquad (6.40)$$

Note that $\Delta_{AB} := (\Delta A_x \vdots \Delta A_{xv} \vdots \Delta B_x)$ may be considered as a linear operator having a bounded norm. In fact, the $\infty-$norm of Δ_{AB} may be computed as $\|\Delta_{AB}\|_\infty = \max_i \sigma_i(\Delta_{AB})$, where σ_i denotes the singular values of Δ_{AB}. Since the elements of Δ_{AB} even for constant deviations of parameters are bounded, hence $\|\Delta_{AB}\|_\infty$ is bounded for constant parametric uncertainties. The representations (6.37) and (6.40)

both contain terms representing parametric uncertainty. There is, however, an important difference between these two representations. In (6.37), the exogenous input τ enters the system independent of the states and/or the control input of the system. If the H_∞ methodology is to be used as a design technique, then τ in (6.37) must be L_2 bounded. In other words the independent representation does not tolerate constant parametric deviations from nominal values. In the fractional representation (6.40), however, the uncertain part due to parametric uncertainty depends on the state $X = [x^T, v^T]^T$ and the control input u. Schematically one may modify Figure 6.1 to obtain Figure 6.4 where the parametric uncertainty may be treated as an extra block interconnected to the whole system. In terms of the results of Theorem 6.4, the stability of the closed-loop system may be ensured if the operator that maps Z to V (see Figure 6.4) is norm bounded. Consequently, for the purpose of design, the configuration shown in Figure 6.4 will be utilized.

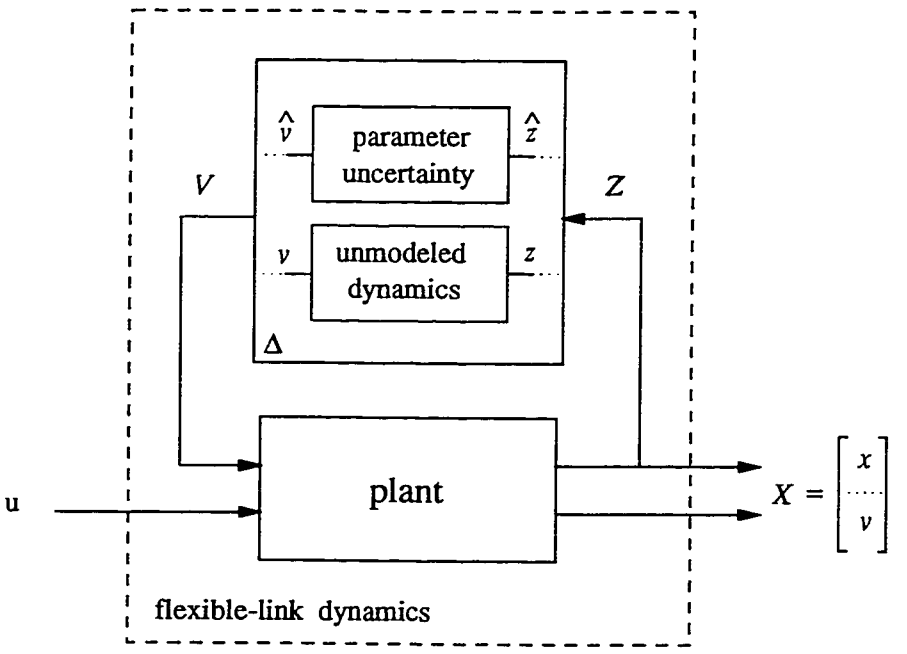

Figure 6.4: *Treating parametric uncertainty as unmodeled dynamics, where* $Z = (x^T, u^T, v^T)^T$, $\hat{z} = (x^T, u^T)^T$, $\hat{v} = \Delta_{AB}\ \hat{z}$, *and* $V = (\hat{v}^T, v^T)^T$. *The variables* z *and* v *are defined as in Figure 6.1* .

6.6 Simulation Results

In this section the methodology proposed in the previous sections is applied to a single-link flexible manipulator with six modes of deflection ($m_1 = 6$). The objective is to design a regulator so that the tip position robustly tracks a reference signal with a specified frequency ω_r. Note that set point regulation is included in the above formulation by setting $\omega_r = 0$. The design proceeds by utilizing the eight steps introduced in Section 6.5.1. The link parameters as well as the natural modes and the corresponding damping ratios used for design and simulation are given in Tables A.1 and A.2 in Appendix A. Table A.3 in Appendix A gives the pole-zero locations of the 14th-order model of the single-link flexible manipulator considered in [19]. By utilizing the procedure of section 6.5.1, the minimum value for i was found to be three. In other words, three deflection modes ($m_1 - i = 6 - 3 = 3$) are eligible to be considered as *uncertainty*. To verify and illustrate the effectiveness of the proposed method and to establish a comparison between the results of the design based on our approach and a standard modeling approach, the design is also performed for a 3-mode system, i.e., a system without *unmodeled dynamics*. In other words in our proposed method the controller is capable of handling the *unmodeled dynamics* as well as the uncertainty due to parametric deviations. In the standard modeling approach, however, the controller handles only the effects of parametric uncertainty. The details of the system and controller parameters for both the proposed and conventional methods are given in Appendix D. To represent the effects of parametric uncertainty, the elements of the system matrix were corrupted by randomly selected values. Specifically, if the perturbation matrix, denoted as Δ_A in Appendix D, is modified to 1.17 Δ_A, unlike the proposed scheme, the standard model becomes unstable. Figures 6.5–6.16 depict results that demonstrate the superior performance of the controller designed based on the proposed model as compared to the controller that is designed based on the standard model. By adjusting the weights on the controlled output and the controlled input, it is, in general, possible to tune

the controller to achieve a given set of desirable performance specifications. Consequently, for the sake of comparison, in both cases, all the weights are selected to be identical. Figures 6.5 and 6.6 depict the different states of the two controlled systems in response to a step input. The control inputs are shown in Figure 6.7. As can be seen, the controller that is designed based on the standard model requires higher effort as compared to the controller designed based on the proposed model. Let us define the value of the controlled output energy over the disturbance energy for the proposed model and the standard model by γ_1 and γ_2, respectively. A comparison of the attenuation levels may be made by evaluating their ratio, which is shown in Figure 6.8. It is clearly observed that the controller based on the proposed model has resulted in a higher attenuation of disturbances as compared to the controller designed based on the standard model. Figures 6.13–6.16 depict the simulation results for a sinusoidal reference trajectory with $\omega_r = 4$. It can be observed that the controller based on the standard model results in instability whereas the controller based on the proposed model has successfully ensured regulation in a stable manner.

6.7 Concluding Remarks

In this chapter, it was shown that for a flexible-link manipulator the dynamics corresponding to the high deflection modes may be treated as *uncertainty*. Using this methodology, one may robustly control the system where the order of the original model can be considered arbitrarily large. The controller design is performed for the known part of the model. A multi-objective H_∞ technique is utilized to design a robust regulator for the resulting system. The maximum number of deflection modes that should be taken into account in the *plant* is obtained through a well defined procedure. The proposed methodology is applicable to a manipulator with arbitrary flexibility. It was also shown that the effect of parametric uncertainty may be represented by a disturbance that is acting on the torque input. Throughout this

chapter it was assumed that all the states of the plant are available for measurement (cf. (6.5), (6.8), (6.11) and (6.12)). Obviously some of these states are available via standard sensors (such as hub angle, hub velocity and tip position). However, most of the states should be obtained in practice by means of sophisticated sensors or observers. Finally, simulation results illustrating the effectiveness of the proposed modeling and design methodologies were presented.

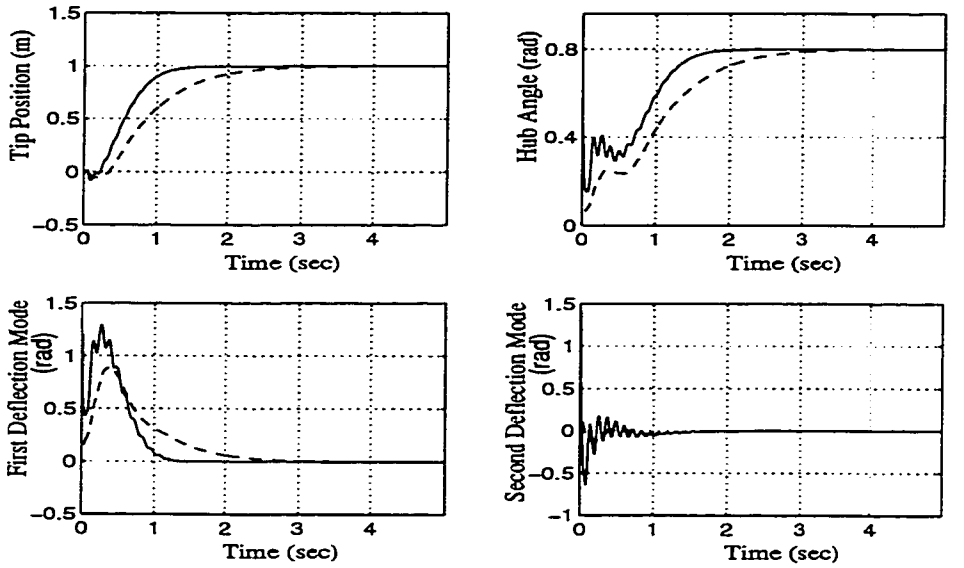

Figure 6.5: *Tip position along with other states of the system in response to a step input; (solid) proposed model, (dashed) standard model.*

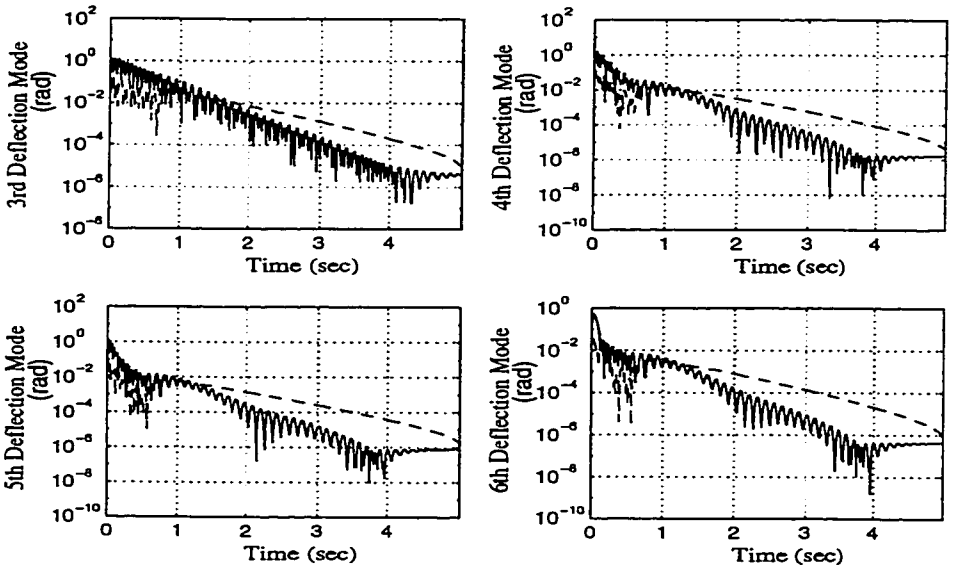

Figure 6.6: *Absolute values of the 3rd-6th deflection modes in response to a step input; (solid) proposed model, (dashed) standard model.*

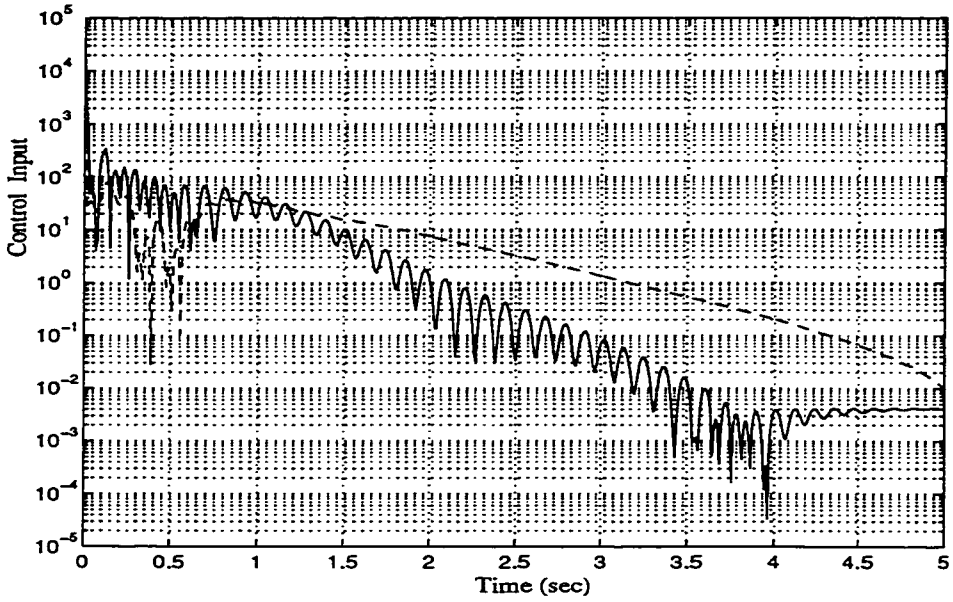

Figure 6.7: *Absolute values of control inputs for step input; (solid) proposed model, (dashed) standard model.*

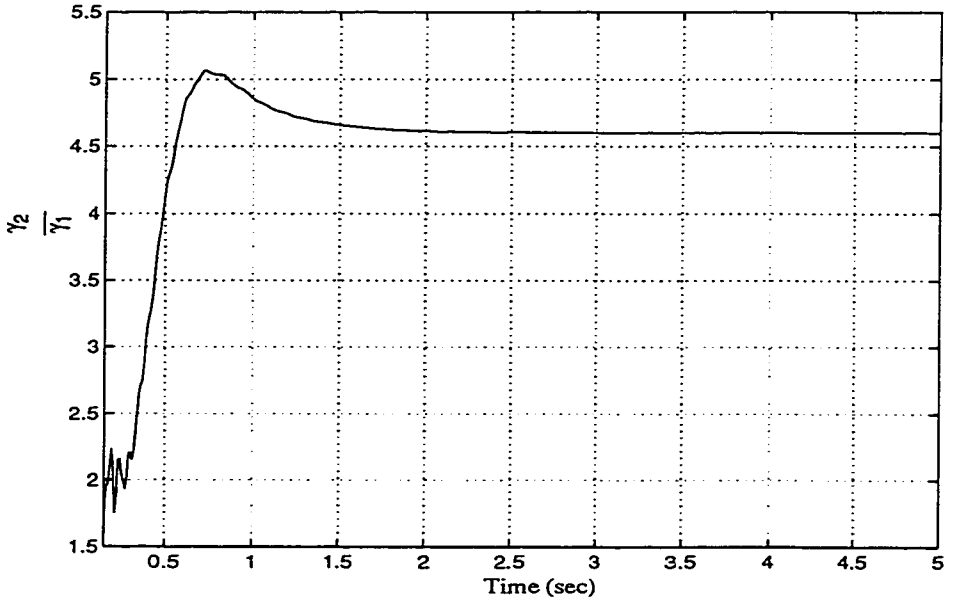

Figure 6.8: *Fraction of attenuation levels in the case of step input; (γ_1) proposed model, (γ_2) standard model.*

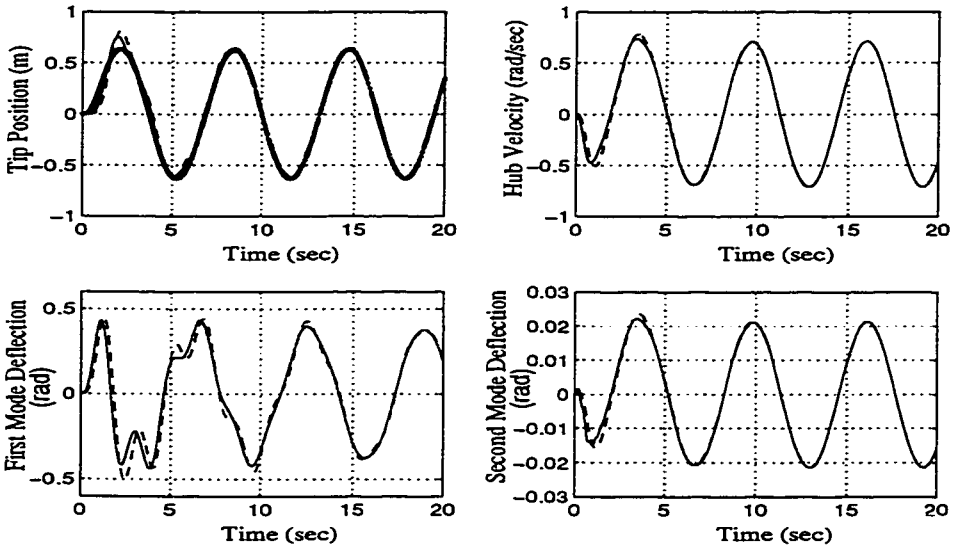

Figure 6.9: *Tip position along with other states of the system in response to a sine input ($\omega = 1$ rad/sec); (solid) proposed model, (dashed) standard model.*

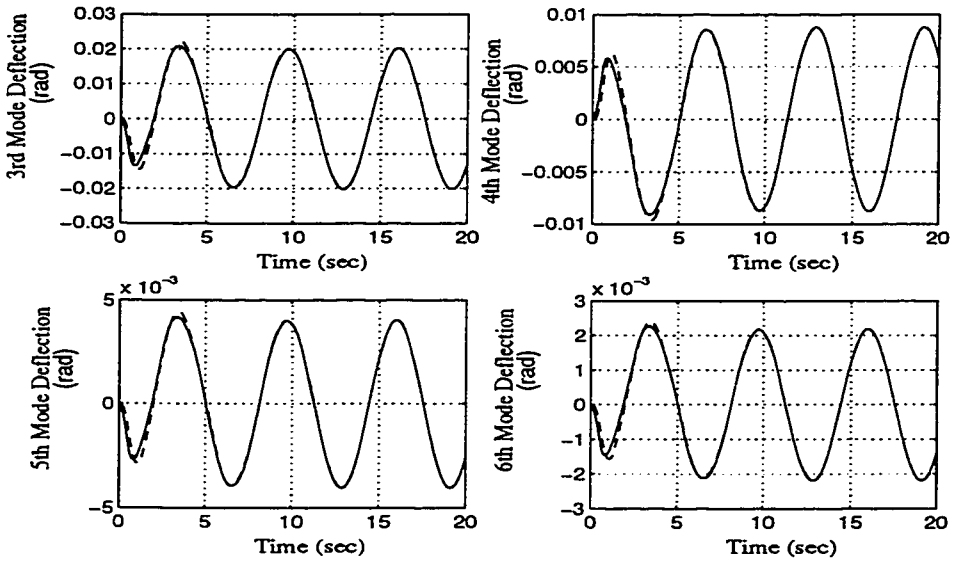

Figure 6.10: *3rd-6th deflection modes in response to a sine input ($\omega = 1$ rad/sec); (solid) proposed model, (dashed) standard model.*

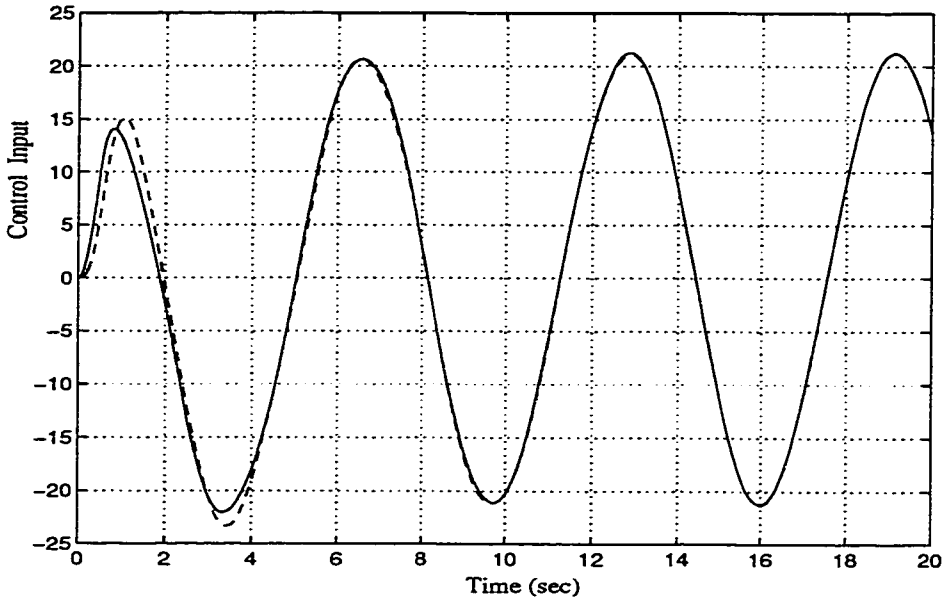

Figure 6.11: *Control input for a sine input ($\omega = 1$ rad/sec); (solid) proposed model, (dashed) standard model.*

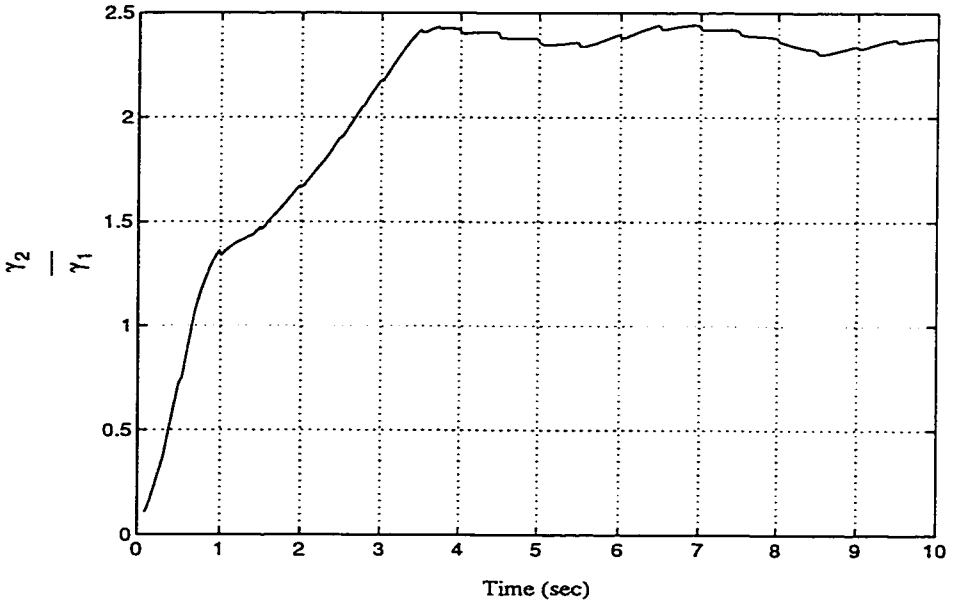

Figure 6.12: *Fraction of attenuation levels in the case of sine input ($\omega = 1$ rad/sec); (γ_1) proposed model, (γ_2) standard model.*

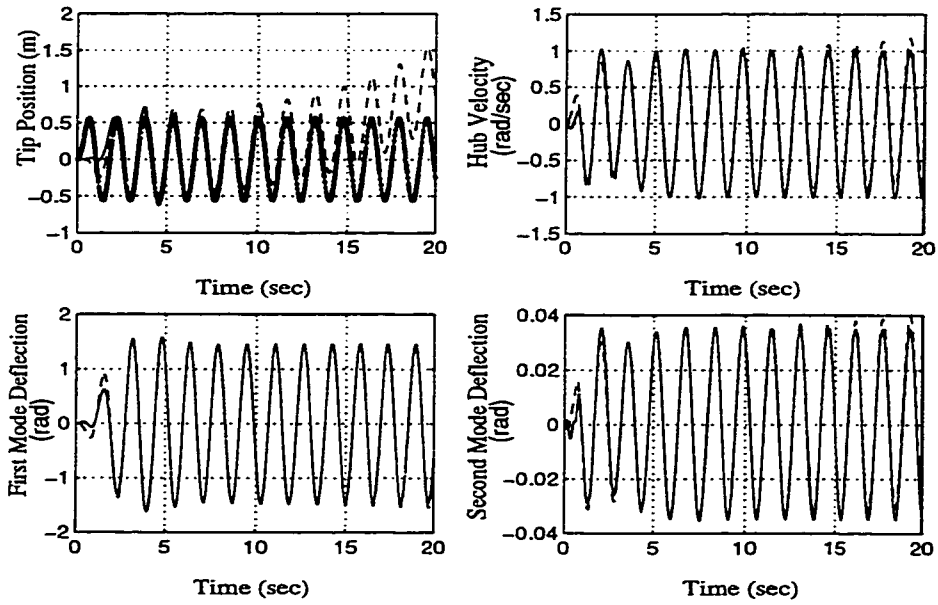

Figure 6.13: *Tip position along with other states of the system in response to a sine input ($\omega = 4$ rad/sec); (solid) proposed model, (dashed) standard model.*

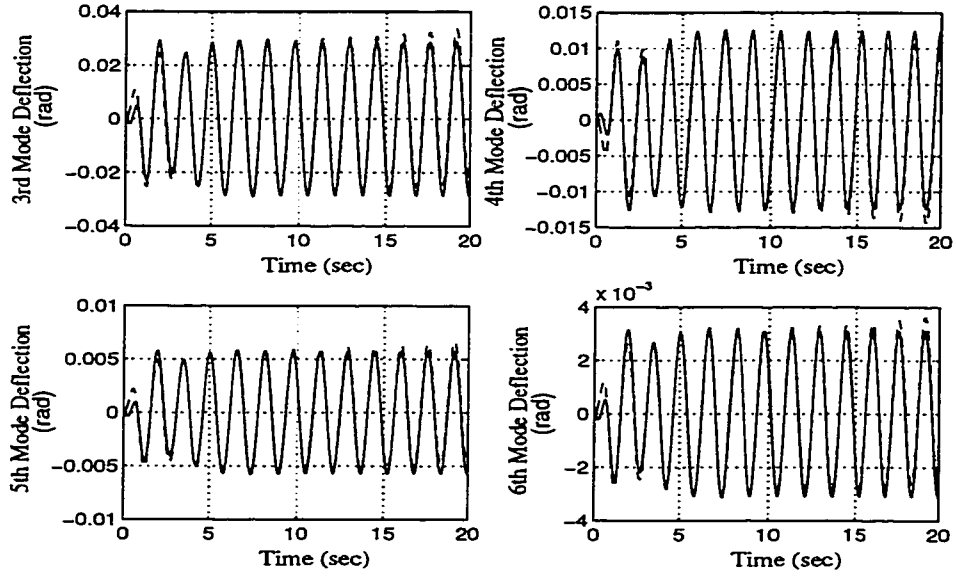

Figure 6.14: *Absolute values of the 3rd-6th deflection modes in response to a sine input ($\omega = 4$ rad/sec); (solid) proposed model, (dashed) standard model.*

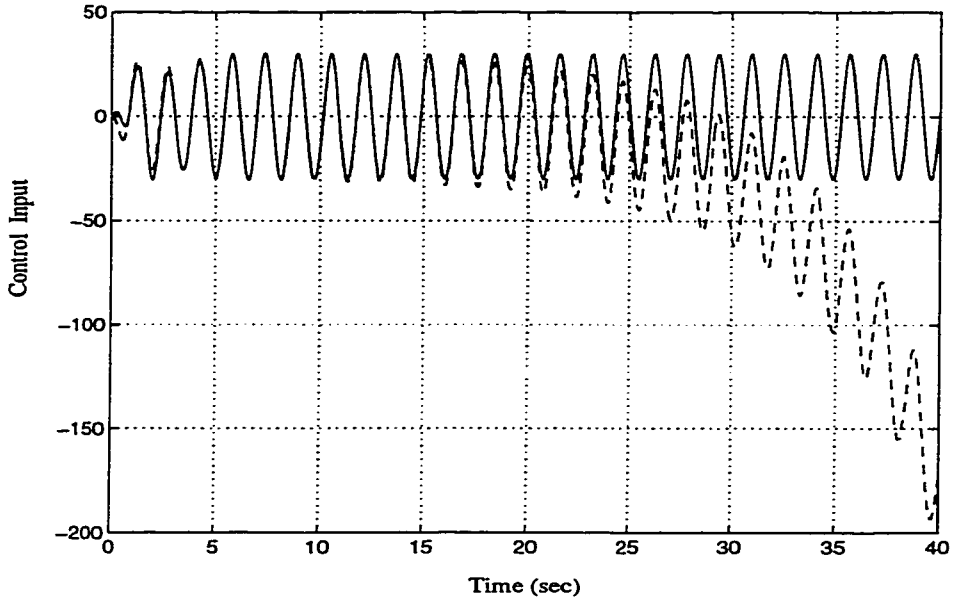

Figure 6.15: *Control input for a sine input ($\omega = 4$ rad/sec); (solid) proposed model, (dashed) standard model.*

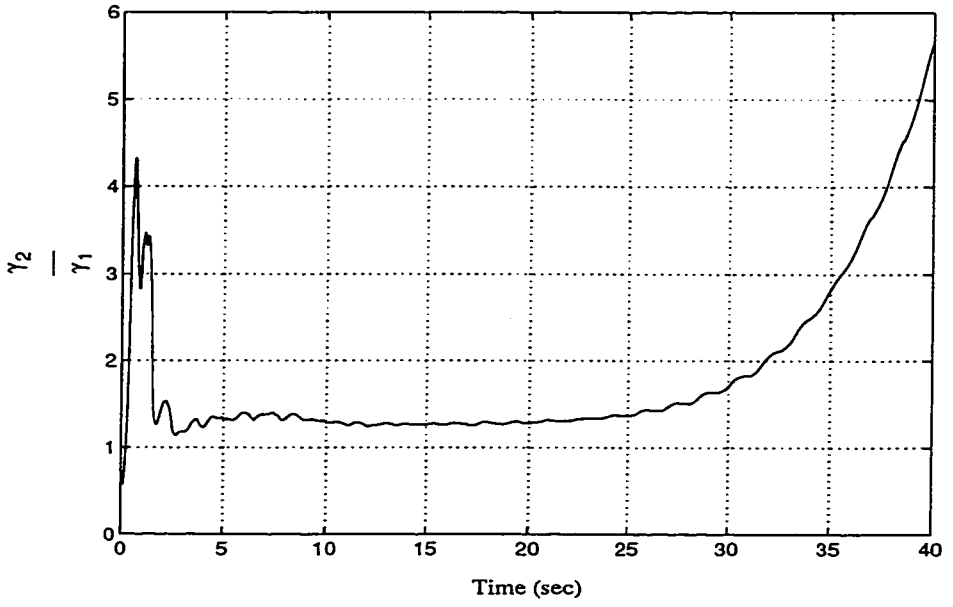

Figure 6.16: *Fraction of attenuation levels in the case of sine input ($\omega = 4$ rad/sec); (γ_1) proposed model, (γ_2) standard model.*

Chapter 7

Nonlinear Robust Regulation Based on the New Modeling Approach

The purpose of robust control is to design a controller so that the feedback system behaves in a desirable way for each possible plant in the uncertainty set. Although controller design is the ultimate goal, typical robust control progresses in three stages:

1. Description of uncertainty: Construct a mathematical description of the uncertainty set.

2. Robustness analysis: Determine if the feedback system behaves in a desirable way for each plant in the uncertainty set when a controller is given.

3. Robust controller design: Design a controller to satisfy the robustness requirement(s).

The robust control of a servomechanism problem for linear time-invariant multivariable systems was presented in [126, 127]. Two common ways for describing

uncertainty are parameter uncertainty and norm bounded uncertainty. The former embeds the uncertainty set into a Euclidean space by assuming that the uncertainty is caused by a collection of uncertain parameters in the system model. The latter characterizes uncertainty in terms of a norm bounded operator based on the assumption that the uncertainty is caused by a bounded operator perturbation that enters the system in an additive, multiplicative, or more generally fractional way [128].

This chapter begins with a treatment of two types of control problems based on which a multiobjective H_∞ control is defined. The problem of robust regulation for a general nonlinear system is then posed.

7.1 Nonlinear Multiobjective H_∞ Control

In this section, we study multiobjective H_∞ sub-optimal control with the controller constrained to achieve robust closed-loop regulation. The linear and time-invariant version of the following setup is addressed in [120, 111].

Consider the feedback system shown in Figure 7.1. Here the nonlinear plant

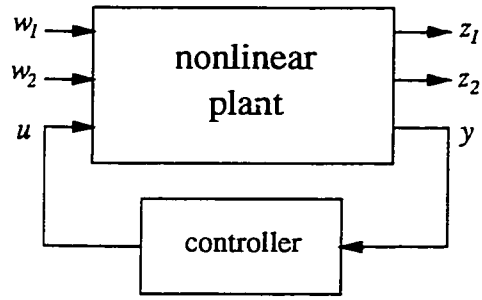

Figure 7.1: *Setup for the problem of robust regulation with an H_∞ constraint ($RRH_\infty C$).*

is assumed to be finite-dimensional and time-invariant, w_1 and w_2 are exogenous inputs, and z_1 and z_2 denote regulated or controlled outputs. The controller is said to be *admissible* for this plant if the resulting closed loop is well-posed and internally

(asymptotically) stable.

The controller synthesis problem addressed in this section is to design (if possible) an admissible controller that simultaneously solves the following two problems.

1. *The robust regulation problem.*

   Design (if possible) an admissible controller such that

   (a) For all inputs w_2 with $w_1 = 0$,

   $$\lim_{t\to\infty} z_2(t) = 0, \qquad \text{and,}$$

   (b) the above property holds for all plants in some neighborhood of the plant in the graph topology.

2. *The H_∞ constrained problem.*

   Design (if possible) an admissible controller such that with $w_2 = 0$, the H_∞ norm of the closed-loop map from w_1 to z_1, namely, $T_{z_1 w_1}$, is less than one, i.e.,

   $$\|T_{z_1 w_1}\|_\infty < 1.$$

The problem of simultaneously solving (1) and (2) will be called *the robust regulation problem with an H_∞ constraint* ($\mathrm{RRH}_\infty\mathrm{C}$). It is a multiple objective problem in which the controller is required to meet two separate design objectives simultaneously.

The *H_∞ constrained problem* in the linear setting is the standard problem of H_∞ control theory initiated by Zames [129]. The *robust regulation problem with an H_∞ constraint* ($\mathrm{RRH}_\infty\mathrm{C}$) is also equivalent to a particular *robust performance problem.* To make it more explicit, consider Figure 7.2 which is a rearrangement of Figure 7.1 after interconnecting an *unmodeled dynamics* block between w_1 and z_1.

Let Δ denote the map from z to v in Figure 7.2, and P_Δ be as shown in the same figure. Assume that the L_2 norm of Δ is bounded by some positive number. The

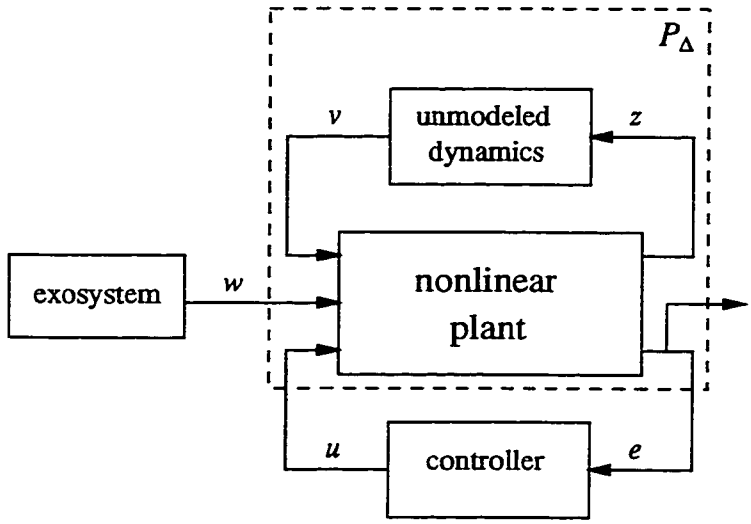

Figure 7.2: *Setup for the problem of robust regulation in the presence of gain-bounded uncertainty (RRGBU).*

problem of robust regulation in the presence of gain-bounded uncertainty (RRGBU) is as follows: Given a real number $\kappa > 0$, design a controller such that for all gain-bounded Δ with $\|\Delta\|_\infty < 1/\kappa$,

- the controller internally stabilizes P_Δ,
- the regulated output, e, converges to zero as time tends to infinity, i.e.,

$$\lim_{t\to\infty} e(t) = 0,$$

- the convergence property holds for all plants in some neighborhood of P_Δ in the graph topology.

It can be shown that the problems of $\text{RRH}_\infty\text{C}$ and RRGBU are equivalent. In other words, the H_∞ technique that is basically used to solve the $\text{RRH}_\infty\text{C}$ problem can simultaneously solve the RRGBU problem and vice versa. Therefore, if in the model shown in Figure 6.1 the L_2 gain of *unmodeled dynamics* is bounded, then we may design a robust regulator for the flexible-link manipulator by posing the corresponding RRGBU problem whose solution is the same as the $\text{RRH}_\infty\text{C}$ problem.

7.2 Nonlinear Robust Regulation for a General Nonlinear System with Gain-Bounded Uncertainty

In this section we study the problem of robust regulation for a general nonlinear system, i.e. non-affine with respect to control and exogenous inputs, in the presence of L_2 gain-bounded perturbations. The linear and time-invariant version of this problem is addressed and solved in [120, 111]. The nonlinear version, but affine with respect to both control and exogenous inputs, was recently addressed in [130]. Here we pose this problem for a general nonlinear system. Consider a nonlinear system modeled by equations of the form (see Figure 7.2)

$$\begin{aligned} \dot{x} &= f(x,\ u,\ v,\ w) \\ z &= h_1(x,\ u,\ w) \\ e &= h_2(x,\ v,\ w) \end{aligned} \tag{7.1}$$

with state $x \in \mathbb{R}^n$, where $u \in \mathbb{R}^m$ is the control input, $w \in \mathbb{R}^r$ is a disturbance input generated by an exosystem

$$\dot{w} = Sw \tag{7.2}$$

while $e \in \mathbb{R}^p$ is a regulated output. The additional input $v \in \mathbb{R}^{\hat{r}}$ and the additional output $z \in \mathbb{R}^{\hat{p}}$ represent the effect of perturbing *unmodeled dynamics*, namely a nonlinear system of the form

$$\begin{aligned} \dot{\xi} &= a(\xi,\ z) \\ v &= c(\xi) \end{aligned} \tag{7.3}$$

with unknown dimension and unknown parameters and whose L_2 gain, however, is known to be bounded by some positive number ρ.

It is assumed that the system is well-posed along trajectory x, i.e., for every $t \geq 0$, f is well defined. Without loss of generality, we assume that $f(0,\ 0,\ 0,\ 0) = 0,\ h_1(0,\ 0,\ 0) = 0,\ h_2(0,\ 0,\ 0) = 0,\ a(0,\ 0) = 0,\ c(0) = 0$. For this system we study the problem of robust regulation. In other words we want to find a feedback law which in general is a dynamical system modeled by equations of the form

$$\begin{aligned} \dot{\eta} &= \psi(\eta,\ e) \\ u &= \beta(\eta,\ e) \end{aligned}$$

with state $\eta \in \mathbb{R}^{\nu}$ and in which $\psi(0,\ 0) = 0,\ \beta(0,\ 0) = 0$. This controller is to yield a closed-loop system which has a locally exponentially stable equilibrium at $(x, \xi, \eta) = (0,\ 0,\ 0)$ and is such that, for every initial condition $(x(0),\ \xi(0),\ \eta(0),\ w(0))$ in a neighborhood of $(0,\ 0,\ 0,\ 0)$, the regulated output converges to zero as time tends to infinity, i.e. $\lim_{t\to\infty} e(t) = 0$. As discussed earlier, the problem in question can be recast as a problem of robust stabilization, in the presence of norm-bounded uncertainties, for a suitable *augmented* plant, in which the regulated output e drives an appropriate *internal model* of exosystem (7.2). This approach leads to the study of the problem of robustly (and locally exponentially) stabilizing an augmented plant described by equations of the form

$$\begin{aligned} \dot{x} &= f(x,\ v,\ u,\ 0) \\ \dot{\eta} &= F\eta + Gh_2(x,\ v,\ 0) \\ z &= h_1(x,\ u,\ 0) \end{aligned} \tag{7.4}$$

(in which F and G are appropriate matrices depending on the exosystem) in the presence of unmodeled dynamics of the form (7.3). Robust stabilization will be pursued, using a version of the *small gain theorem* presented in [131], by seeking a feedback law which solves a suboptimal problem of disturbance attenuation, in the sense of an L_2 gain, for the augmented plant thus introduced.

7.3 Output Regulation

In this section we review some basic principles underlying the design of a feedback law for the purpose of achieving output regulation in the presence of plant uncertainties. The analysis of this problem for an affine nonlinear system can be found in [132]. Consider a system modeled by equations of the form

$$\begin{aligned} \dot{x} &= f(x,\ u,\ w) \\ e &= h(x,\ w) \\ y &= k(x,\ w) \end{aligned} \tag{7.5}$$

with state $x \in \mathbb{R}^n$, in which $u \in \mathbb{R}^m$ is the control input, $w \in \mathbb{R}^r$ is a disturbance input, generated by an exosystem

$$\dot{w} = Sw \tag{7.6}$$

while $e \in \mathbb{R}^p$ is a regulated output and $y \in \mathbb{R}^s$ is a measured output. All the mappings involved are assumed to be smooth and $f(0,\ 0,\ 0) = 0$, $h(0,\ 0) = 0$, $k(0,\ 0) = 0$. We assume that the matrix S is a skew symmetric matrix, which is equivalent to assuming that the exogenous inputs generated by (7.6) are linear combinations of a finite number of fixed sinusoidal functions of time. The problem of output regulation is to find a feedback law, which in general is a dynamical system modeled by equations of the form

$$\begin{aligned} \dot{\eta} &= \psi(\eta,\ e) \\ u &= \beta(\eta,\ e) \end{aligned} \tag{7.7}$$

in which $\eta \in \mathbb{R}^\nu$, yields a closed-loop system which has a locally exponentially stable equilibrium at $(x,\ \eta) = (0,\ 0)$ and in which, for every initial condition $(x(0),\ \eta(0),\ w(0))$ in a neighborhood of $(0,\ 0,\ 0)$, the regulated output converges to zero as time tends to infinity, i.e.

$$\lim_{t\to\infty} e(t) = 0 \tag{7.8}$$

It should be noted that the results of [132] cannot be directly used to deal with the presence of plant uncertainties which is the problem addressed in the previous section.

7.3.1 State and Error Feedback

In this subsection we consider the case in which both the full state x of the controlled plant and the full regulated output e are available for feedback. We then examine the problem of when a controller of the form

$$\begin{aligned} \dot{\eta} &= F\eta + Ge \\ u &= \beta(\eta,\ x) \end{aligned} \tag{7.9}$$

(where $F \in \mathbb{R}^{\nu \times \nu}$ is a matrix playing the role of an internal model of the exogenous inputs) induces robust regulation.

The basic principles underlying output regulation can be summarized as follows. Suppose F and G in (7.9) are fixed matrices and there exists a feedback law $u = \beta(\eta,\ x)$ which locally exponentially stabilizes the equilibrium $(x,\ \eta) = (0,\ 0)$ of the corresponding closed-loop system (when $w = 0$).

In this case each (sufficiently small) exogenous input produces a well-defined steady-state response. In fact, following [132], observe that system (7.5), controlled by (7.9) and driven by the exosystem (7.6), is the composite system

$$\begin{aligned} \dot{x} &= f(x,\ \beta(\eta,\ x),\ w) \\ \dot{\eta} &= F\eta + Gh(x,\ w) \\ \dot{w} &= Sw \end{aligned} \tag{7.10}$$

which has a center manifold at $(x,\ \eta,\ w) = (0,\ 0,\ 0)$. The latter can be expressed in the form

$$\mathcal{M}_c = \{(x,\ \eta,\ w) :\ x = \pi(w),\ \eta = \sigma(w)\}$$

i.e., in the form of the graph of a map $w \mapsto \{\pi(w),\ \sigma(w)\}$ where $\pi(w)$ and $\sigma(w)$ satisfy certain partial differential equations. The manifold in question is invariant and locally exponentially attractive for the composite system (7.10), which means that for every initial condition $(x(0),\ \eta(0),\ w(0))$ in a neighborhood of $(0,\ 0,\ 0)$ the response of (7.10) converges, as time tends to infinity, to a uniquely defined steady-state response which is determined only by the trajectory $w(t)$ of the exosystem and has the form $x(t) = \pi(w(t)),\ \eta(t) = \sigma(w(t))$. Consequently, the regulated output converges toward a steady-state response of the form

$$e(t) = h(\pi(w(t),\ w(t)).$$

In particular, asymptotic output regulation occurs if and only if the map $h(x,\ w)$ vanishes on $\mathcal{M}_c$. It is deduced from this analysis that the main problem of achieving robust regulation is to choose F and G in (7.9) in such a way that the mapping $\pi(w)$ associated with the invariant manifold $\mathcal{M}_c$ renders

$$h(\pi(w(t),\ w(t)) = 0. \tag{7.11}$$

As discussed earlier, it is usually quite difficult to have this condition met in the presence of plant uncertainties for a nonlinear system. Thus, it is more practical to seek approximate versions of the latter, for instance, to require that only the first few terms of a polynomial approximation of the left-hand side of (7.11) vanish. This yields the concept of approximate regulation of order k, introduced in [133] and [134] to deal with the case of plant uncertainties.

In the (robust) approximate output regulation problem the objective is to choose matrices F and G (and subsequently the stabilizing feedback $u = \beta(\eta,\ x)$) in such a way that the identity (7.11) holds *modulo* a residual function of w which vanishes at $w = 0$ together with all partial derivatives of order less than or equal to a fixed integer k. To describe how the matrices in question can be determined, some auxiliary notations are needed. Let k be a fixed integer and let $\mathcal{P}_k$ denote the set of all polynomials of degree less than or equal to k in the variables $w_1,\ w_2, ...,\ w_r$ with

coefficients in $\mathbb{R}$. $\mathcal{P}_k$ indeed is a finite-dimensional vector space over $\mathbb{R}$. Consider the map

$$\begin{aligned} D_k : \mathcal{P}_k &\rightarrow \mathcal{P}_k, \\ \mathbf{p} &\mapsto \frac{\partial \mathbf{p}}{\partial w} S w. \end{aligned} \tag{7.12}$$

Let μ denote the degree of the minimal polynomial of D_k, and let $M_k \in \mathbb{R}^{\mu \times \mu}$ be a matrix having the same minimal polynomial as D_k. It can be shown that it is always possible to choose M_k to be a skew-symmetric matrix [130]. Moreover, it is possible to find a vector $g_k \in \mathbb{R}^{\mu \times 1}$ such that the pair $(M_k,\ g_k)$ is controllable. Using the pair $(M_k,\ g_k)$ thus determined, set

$$\eta = \begin{pmatrix} \eta_1 \\ \eta_2 \\ . \\ \eta_p \end{pmatrix}, \quad F = \begin{pmatrix} M_k & 0 & ... & 0 \\ 0 & M_k & ... & 0 \\ . & . & ... & . \\ 0 & 0 & ... & M_k \end{pmatrix}, \quad G = \begin{pmatrix} g_k & 0 & ... & 0 \\ 0 & g_k & ... & 0 \\ . & . & ... & . \\ 0 & 0 & ... & g_k \end{pmatrix} \tag{7.13}$$

in which $\eta_i \in \mathbb{R}^{\mu \times 1}$ for $i = 1, ...,\ p$ (recall that p denotes the number of the regulated output e).

Then it can be shown that if the feedback law $u = \beta(\eta,\ x)$ locally exponentially stabilizes the equilibrium $(x,\ \eta) = (0,\ 0)$ of the closed-loop system, then the desired property of approximate regulation of order k is achieved.

Proposition: [130] Suppose $u = \beta(\eta,\ x)$ locally exponentially stabilizes the equilibrium $(x,\ \eta) = (0,\ 0)$ of (7.5)-(7.9), and let $\pi(w)$, $\sigma(w)$ define a center manifold for (7.10) at $(x,\ \eta,\ w) = (0,\ 0,\ 0)$. Then the map $\pi(w)$ is such that

$$h(\pi(w)) + q(\pi(w))w = R_k(w)$$

where $R_k(w)$ is a residual function of w which vanishes at $w = 0$ together with all partial derivatives of order less than or equal to k. If in particular, $h(\pi(w)) + q(\pi(w))w$ is a polynomial of degree less than or equal to k, then necessarily $R_k(w) = 0$ and the steady-state response of (7.10) to any exogenous input $w(t)$ generated by the exosystem (7.2) is identically zero.

7.3.2 Pure Error Feedback

The results of the previous subsection can be extended to the case in which the measured output y coincides with the regulated output e. To this end, it suffices to consider a feedback law having the form

$$\begin{aligned} \dot{\eta}_0 &= F\eta_0 + Ge \\ \dot{\eta}_1 &= \psi_1(\eta_0,\ \eta_1,\ e) \\ u &= \beta(\eta_0,\ \eta_1,\ e) \end{aligned} \tag{7.14}$$

where F and G are exactly as defined in the previous subsection, and $\psi_1(\eta_0,\ \eta_1,\ e)$ and $\beta(\eta_0,\ \eta_1,\ e)$ are such as to locally exponentially stabilize the corresponding closed-loop system.

7.4 Nonlinear Robust Regulation Against Gain-Bounded Perturbations

As shown in the previous section a controller of the form (7.9) (respectively of the form (7.14), in the case of pure error feedback) is able to induce asymptotic regulation so long as the feedback $\beta(\eta, x)$ (respectively, the additional dynamics $\dot{\eta}_1 = \psi_1(\eta_0,\ \eta_1,\ e)$ and the feedback law $u = \beta(\eta_0,\ \eta_1,\ e)$, in the case of pure error feedback) locally exponentially stabilizes the equilibrium $(x,\ \eta) = (0,\ 0)$ of the corresponding closed-loop system. Thus, to achieve robust regulation for the class perturbed systems described earlier, it suffices to solve a problem of robust (local exponential) stabilization for a system of the form

$$\begin{aligned} \dot{x} &= f(x,\ v,\ u,\ 0) \\ \dot{\eta} &= F\eta + Gh_2(x,\ v,\ 0) \\ z &= h_1(x,\ u,\ 0) \end{aligned} \tag{7.15}$$

in the presence of unmodeled dynamics of form (7.3). Robust stabilization will be achieved, as suggested in [108], by computing and imposing the feedback law which solves a (suboptimal) problem of disturbance attenuation. The Hamiltonian function associated with the *unmodeled dynamics* is defined as

$$H(\xi,\ p_{um},\ v,\ u) = p_{um}^T a(\xi,\ z) + c^T(\xi)c(\xi) - \rho^2 z^T z \tag{7.16}$$

where $p_{um} = U_\xi^T$ and $U(\xi)$ is a functional of ξ. By invoking the version of the small gain theorem presented in [131] and the notion of L_2 gain of a nonlinear system studied in [90], it is assumed that the perturbation (7.3) is such that an equality of the form

$$H_*(\xi,\ p_{um}) := H(\xi,\ z_*,\ p_{um}) = U_\xi a(\xi,\ z_*) + c^T(\xi)c(\xi) - \rho^2 z_*^T z_* < 0 \tag{7.17}$$

has a positive definite proper solution $U(\xi)$, where ρ is a given number and z_* is the solution of the equation

$$\frac{\partial H}{\partial z} = \frac{\partial a^T(\xi,\ z)}{\partial z} U_\xi^T - 2\rho^2 z^T = 0. \tag{7.18}$$

Then a feedback law will be sought which attenuates in the sense of the L_2 gain the effect of the input v on the output z of system (7.15) by a factor $(1/\rho)$. If, in addition, the other hypotheses involved in the analysis of asymptotic and local exponential stability are satisfied, a feedback law of this type renders the corresponding closed-loop system robustly stable for any perturbation whose L_2 gain is bounded by ρ and the regulation properties outlined in the previous section holds.

7.5 Disturbance Attenuation for a Class of Interconnected Nonlinear Systems

Motivated by the analysis illustrated so far, we now focus our attention on the solution of problems of disturbance attenuation with internal stability for the class

of nonlinear systems which can be modeled by equations of the form

$$\begin{aligned}\begin{pmatrix}\dot{x}\\ \dot{\eta}\end{pmatrix} &= \hat{F}(x,\ \eta,\ v,\ u)\\ z &= h_1(x,\ u)\\ y &= h_2(x,\ v)\end{aligned} \tag{7.19}$$

with state $(x,\ \eta) \in \mathbb{R}^{n\times\nu}$, where $u \in \mathbb{R}^m$ is the control and $v \in \mathbb{R}^{\hat{r}}$ is the disturbance input, while $z \in \mathbb{R}^{\hat{p}}$ is the controlled output and $y \in \mathbb{R}^p$ is the measured output. The matrix F in (7.15) is a skew-symmetric matrix. The class of systems thus defined includes, in particular, composite systems in which the output

$$e = h_2(x,\ v)$$

of a nonlinear system of the form

$$\dot{x} = f(x,\ v,\ u) \tag{7.20}$$

drives a linear system of the form

$$\dot{\eta} = F\eta + Ge$$

i.e., those interconnected structures considered in the previous section [see (7.4)].

The Hamiltonian function for this problem is a function $H : \mathbb{R}^n \times \mathbb{R}^\nu \times \mathbb{R}^{\hat{r}} \times \mathbb{R}^m \to \mathbb{R}$ defined as

$$H(x,\ \eta,\ p,\ v,\ u) = p^T\hat{F}(x,\ \eta,\ v,\ u) + z^Tz - \gamma^2v^Tv. \tag{7.21}$$

Suppose the system described by (7.19) satisfies the following hypothesis.

Assumption 7.1 The penalty map $h_1(x,\ u)$ is such that the matrix

$$D_1 = \frac{\partial h_1}{\partial u}(0,\ 0)$$

has rank m.

Then it turns out that in a neighborhood of the point $(x,\ \eta,\ p,\ v,\ u) = (0,\ 0,\ 0,\ 0,\ 0)$, the function $H(x,\ \eta,\ p,\ v,\ u)$ has a unique local saddle point in $(v,\ u)$ for each $(x,\ \eta,\ p)$. More precisely, there exist unique smooth functions $v_*(x,\ \eta,\ p)$ and $u_*(x,\ \eta,\ p)$, defined in a neighborhood of $(0,\ 0,\ 0)$, satisfying

$$\begin{aligned}
\frac{\partial H}{\partial v}(x,\ \eta,\ p,\ v_*(x,\ \eta,\ p),\ u_*(x,\ \eta,\ p)) &= 0, \\
\frac{\partial H}{\partial u}(x,\ \eta,\ p,\ v_*(x,\ \eta,\ p),\ u_*(x,\ \eta,\ p)) &= 0, \\
v_*(0,\ 0,\ 0) = 0, \qquad\qquad u_*(0,\ 0,\ 0) &= 0.
\end{aligned}$$

and such that

$$\begin{aligned}
H(x,\ \eta,\ p,\ v,\ u_*(x,\ \eta,\ p)) &\leq H(x,\ \eta,\ p,\ v_*(x,\ \eta,\ p),\ u_*(x,\ \eta,\ p)) \\
&\leq H(x,\ \eta,\ p,\ v_*(x,\ \eta,\ p),\ u) \qquad (7.22)
\end{aligned}$$

for each $(x,\ \eta,\ p,\ v,\ u)$ in a neighborhood of the point $(x,\ \eta,\ p,\ v,\ u) = (0,\ 0,\ 0,\ 0,\ 0)$. The existence of these functions and (7.22) can be deduced from the observation that $H(x,\ \eta,\ p,\ v,\ u)$, viewed as a function of $(v,\ u)$, has a Hessian matrix which at $(x,\ \eta,\ p,\ v,\ u) = (0,\ 0,\ 0,\ 0,\ 0)$ is equal to

$$\begin{pmatrix} -2\gamma^2 I & 0 \\ 0 & 2D_1^T D_1 \end{pmatrix}$$

where $D_1^T D_1$ is positive definite by hypothesis.

Let $W : \mathbb{R}^n \times \mathbb{R}^\nu \to \mathbb{R}$ be a smooth function defined in a neighborhood of $(x,\ \eta) = (0,\ 0)$ and such that $W(0,\ 0) = 0$ and $W_{(x,\ \eta)} = 0$, set

$$\begin{aligned}
H_*(x,\ \eta,\ p) &= H(x,\ \eta,\ p,\ v_*(x,\ \eta,\ p),\ u_*(x,\ \eta,\ p)) \\
\alpha_1(x,\ \eta) &= v_*(x,\ \eta,\ W_{(x,\ \eta)}^T), \quad \alpha_2(x,\ \eta) = u_*(x,\ \eta,\ W_{(x,\ \eta)}^T) \qquad (7.23)
\end{aligned}$$

and observe that (7.22) implies in particular

$$H(x,\ \eta,\ W_{(x,\ \eta)}^T,\ v,\ \alpha_2(x,\ \eta)) \leq H_*(x,\ \eta,\ W_{(x,\ \eta)}^T). \qquad (7.24)$$

Now, suppose that the function $W(x,\ \eta)$ is nonnegative (in which case $W(0,\ 0) = 0$ implies $W_{(x,\ \eta)}(0,\ 0) = 0$) and renders the inequality

$$H_*(x,\ \eta,\ W^T_{(x,\ \eta)}) \leq 0 \tag{7.25}$$

satisfied for each $(x,\ \eta)$ in a neighborhood of zero. This shows that the system (7.19) has the dissipative property.

Inequality (7.25) is the Hamilton-Jacobi-Isaacs inequality. If $W(x,\ \eta)$ is positive definite and satisfies a strict inequality, i.e., the left hand side of (7.25) is negative for each $(x,\ \eta) \neq (0,0)$, it can be shown that the feedback law $u = \alpha_2(x,\ \eta)$ is also locally asymptotically stabilizing.

7.6 Application to a Flexible-Link Manipulator

The procedure described in the previous sections may be utilized for the purpose of nonlinear robust output regulation of a flexible link manipulator. The output usually consists of the tip position of the manipulator.

7.6.1 Nonlinear Modeling Based on the New Approach

The state-space equations for a flexible-link manipulator are given by (2.10). By applying the transformations introduced in Appendix C and similar to (6.5), the nonlinear model of a flexible-link manipulator may be represented by

$$\begin{aligned} \dot{X} &= F_o(X) + G_o(X)u \\ y &= C\ X \end{aligned} \tag{7.26}$$

where X and C are defined as in (6.6). Using (7.26), one may write the nonlinear version of the equations (6.11) and (6.12) in the form

$$\text{(nonlinear plant)} \qquad \dot{x} = F_x(x,v) + G_x(x,v)u,\ \ y_x = x_1 = y \tag{7.27}$$

$$\text{(unmodeled dynamics)} \qquad \dot{v} = F_v(x,v) + G_v(x,v)u,\ \ y_v = C_v\ v \tag{7.28}$$

where C_v is defined as in (6.12). In other words, (6.11) and (6.12) represent the first order approximations of (7.27) and (7.28).

Now, consider the setup shown in Figure 7.2. Define

$$\begin{aligned} z &= C_1\, x + D_{12}\, u := \begin{bmatrix} C_x \\ 0 \end{bmatrix} x + \begin{bmatrix} 0 \\ I \end{bmatrix} u = \begin{bmatrix} C_x\, x \\ u \end{bmatrix} \\ e &= y - y_{ref} = [1\ 0_{2\times m+1}]\, x - y_{ref} \end{aligned} \tag{7.29}$$

where C_x is defined as in (6.19) and y and y_{ref} are defined as in (5.10). Note that the definition of z in (7.29) satisfies the condition of Assumption 7.1. In order to design a nonlinear multi-objective H_∞ controller we have to compute the H_∞ norm of the unmodeled dynamics which was introduced above.

7.6.2 Boundedness of the Unmodeled Dynamics

In this section we show that the boundedness of the unmodeled dynamics defined in (7.28) is related to the boundedness of its linearized model. Consider a nonlinear system with the input $u \in \mathbb{R}^m$ and the output $y \in \mathbb{R}^p$ of the form:

$$\begin{aligned} \dot{x} &= f_1(x,u) \qquad ; f_1(0,\ 0) = 0 \\ y &= h_1(x) \qquad ; h_1(0) = 0 \end{aligned} \tag{7.30}$$

The L_2 gain of this system is related to the L_2 gain of its linearization at $x = 0$, i.e.,

$$\begin{aligned} \dot{\bar{x}} &= F_1\bar{x} + G_1\bar{u} \\ \bar{y} &= H_1\bar{x} \end{aligned} \tag{7.31}$$

where $F_1 = \frac{\partial f_1}{\partial x}(0,\ 0)$, $G_1 = \frac{\partial f_1}{\partial u}(0,\ 0)$ and $H_1 = \frac{\partial h_1}{\partial x}(0)$. The following result is from [99].

Theorem 7.1 *Consider the nonlinear system (7.30) with its linearization (7.31). Assume F_1 is asymptotically stable. Then the following statements are equivalent:*

- *The linearization (7.31) has L_2 gain $< \gamma$.*
- *The nonlinear system (7.30) has locally L_2 gain $< \gamma$.*

The condition under which a linear system has bounded H_∞ norm was stated in Theorem 6.1.

In the light of the above results, the boundedness of a nonlinear system is determined by observing whether or not its linearization is bounded. Consequently, we may turn our attention to the linearized dynamics of (7.28), i.e., (6.12). In Section 6.3, however, it was shown that the *unmodeled dynamics* represented by (6.12) have finite H_∞ norm. Consequently, the *nonlinear unmodeled dynamics* represented by (7.28) have also finite H_∞ norm. Based on Theorem 7.1, this norm may be computed by the approach presented in Section 6.3.2.

7.6.3 Design of Internal Model of the Exogenous Input

In order to design a regulator based on a particular exosystem, it is necessary to compute matrices F and G introduced in Sections 6 and 7.3. Based on the first or linear approximation, these matrices can be realized as follows. Suppose that we are interested in regulating against signals with frequencies $\omega_1, \ldots, \omega_N$. With every frequency ω_k to be regulated against, associate system matrices F_k and G_k. If $\omega_k = 0$, choose integrator dynamics

$$F_k = 0 \in \mathbb{R}^{p \times p} \quad \text{and} \quad G_k = I \in \mathbb{R}^{p \times p}.$$

If $\omega_k \neq 0$, choose the dynamics

$$F_k = \begin{bmatrix} 0 & \omega_k I \\ -\omega_k I & 0 \end{bmatrix} \in \mathbb{R}^{2p \times 2p} \quad \text{and} \quad G_k = \begin{bmatrix} 0 \\ I \end{bmatrix} \in \mathbb{R}^{2p \times 2p}$$

Now set

$$F = \begin{bmatrix} F_1 & & \\ & \ddots & \\ & & F_N \end{bmatrix} \quad \text{and} \quad G = \begin{bmatrix} G_1 \\ \vdots \\ G_N \end{bmatrix}$$

After computing matrices F and G, we may easily form equations (7.4), where

$$\begin{aligned} x &= [y, \dot{\theta}, \delta_1, \dot{\delta}_1, \ldots, \delta_{i-1}, \dot{\delta}_{i-1}]^T \\ v &= [\delta_i, \dot{\delta}_i, \ldots, \delta_m, \dot{\delta}_m]^T \\ z &= C_1\, x + D_{12}\, u := \begin{bmatrix} C_x \\ 0 \end{bmatrix} x + \begin{bmatrix} 0 \\ I \end{bmatrix} u = \begin{bmatrix} C_x\, x \\ u \end{bmatrix} \end{aligned}$$

and f is taken from (7.27). The resulting equation thus formed from (7.4) will be referred to as the augmented system.

7.6.4 Disturbance Attenuation for the Augmented System

In this subsection a robust controller is designed so that the tip position tracks the exogenous input. The controller is supposed to minimize the influence of the disturbance, i.e. $v = [\delta_i, \dot{\delta}_i, \ldots, \delta_m, \dot{\delta}_m]^T$ $(i \geq 1)$ on the controlled output z given by (7.29). The design procedure is similar to the one presented in Chapters 3 and 5. In fact, one has to find the control (u_*) in such a way that the HJI inequality (7.25) in its strict sense $(<)$ holds. To this end, the approximation technique presented in Section 3.5 may be utilized and an approximate solution in the form of a polynomial up to a prescribed order can be computed. The important difference in this case is that the attenuation level of γ in (7.21) must satisfy two constraints. First, it should be such that (7.21) or its linear counterpart in the form (3.7) has a positive-definite solution. The second constraint was discussed in Chapter 6, i.e., it should satisfy the relation $\gamma < 1/\rho$. Consequently, the design procedure begins with that given in Section 5.5 yielding the linear part of the controller. The higher order terms can also be found by utilizing a polynomial approximation technique.

7.7 Simulation Results

In this section the methodology proposed in the previous sections is applied to a single-link flexible manipulator with six modes of deflection ($m_1 = 6$). The objective is to design a nonlinear regulator so that the tip position robustly tracks a reference signal with a specified frequency ω_r. Note that set point regulation is included in the above formulation by setting $\omega_r = 0$. Since the regulation for nonzero frequencies was considered in Chapter 6, in this section we only consider set point regulation. In fact the simulation results in this section will show that using the new modeling approach for a flexible-link manipulator it is possible to get a larger domain of validity compared to the corresponding linear framework. The link parameters as well as the natural modes and the corresponding damping ratios used for design and simulation are the same as in Section 6.6. The nonlinear controller was computed approximately up to the third-order. Similar to the design results in Chapter 5, the second order controller did not improve the performance considerably. The third-order controller, however, did have a significant effect on the performance. The advantage of the third-order nonlinear controller over its linear counterpart becomes apparent from the results shown in Figures 7.3 and 7.4. These simulations correspond to a π *rad* rotation of the hub. Simulation results in Figures 7.5 and 7.6 reveal that the third-order controller, in this application, has the ability of performing a complete rotation of the hub in a stable manner. The linearized controller, however, results in instability.

7.8 Concluding Remarks

The objective of this chapter was to design a nonlinear regulator to robustly control the tip position of a flexible-link manipulator. Based on a new modeling approach, the original dynamic equations were shown to be partitionable into two sub-systems,

namely, *plant* and *unmodeled dynamics*. It was shown that for a flexible-link manipulator the dynamics corresponding to the high deflection modes may be treated as norm-bounded *uncertainty*. Using this methodology, one may design a robust nonlinear controller where the order of the original model can be considered arbitrarily large (infinite). A nonlinear multi-objective H_∞ technique was utilized to design a robust nonlinear regulator for the resulting system. It was shown that the maximum number of deflection modes that should be taken into account in the *plant* can be obtained from the linear version of the problem which was studied in Chapter 6. It is worth noting that similar to the scenario in Chapter 6, the effect of parametric uncertainty may also be represented by a disturbance that is acting on the torque input. In fact all issues posed in the previous chapter can also be extended to the nonlinear case. The main objective of designing a nonlinear regulator, however, is to enlarge the domain of attraction of the controller. Consequently, only this direction was followed in this chapter. Throughout this chapter it was assumed that all the states of the *plant* are available for measurement. Some of these states are available via standard sensors (such as hub angle, hub velocity and tip position). However, most of the states should be obtained in practice by means of sophisticated sensors or nonlinear observers. The simulation results illustrating the effectiveness of the proposed modeling and design methodologies were presented.

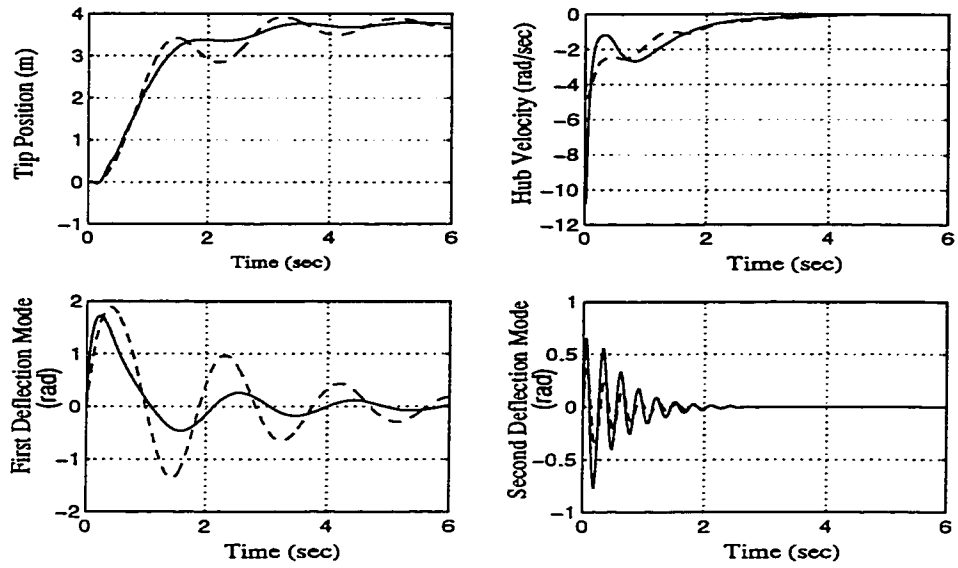

Figure 7.3: *Tip position along with other states of the system in response to a π rad rotation of hub; (solid) nonlinear controller, (dashed) linear controller.*

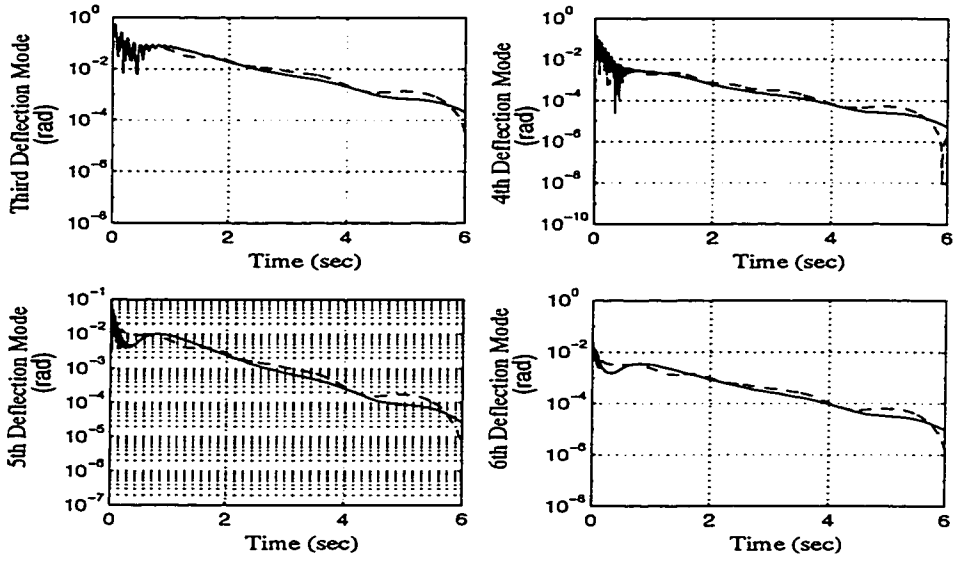

Figure 7.4: *Absolute values of the 3rd-6th deflection modes in response to π rad rotation of hub; (solid) nonlinear controller, (dashed) linear controller.*

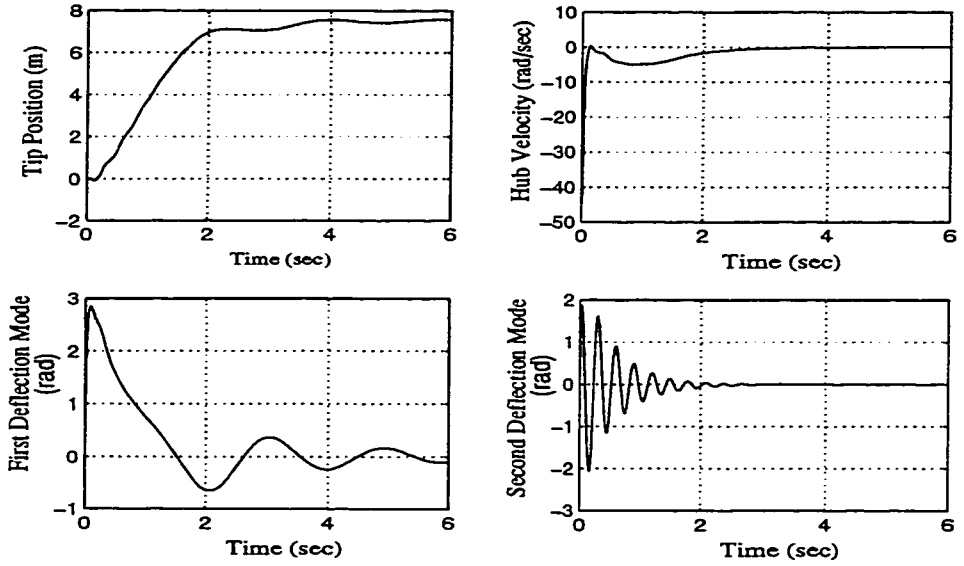

Figure 7.5: *Tip position along with other states of the system in response to a 2π rad rotation of hub. The linear controller results in instability.*

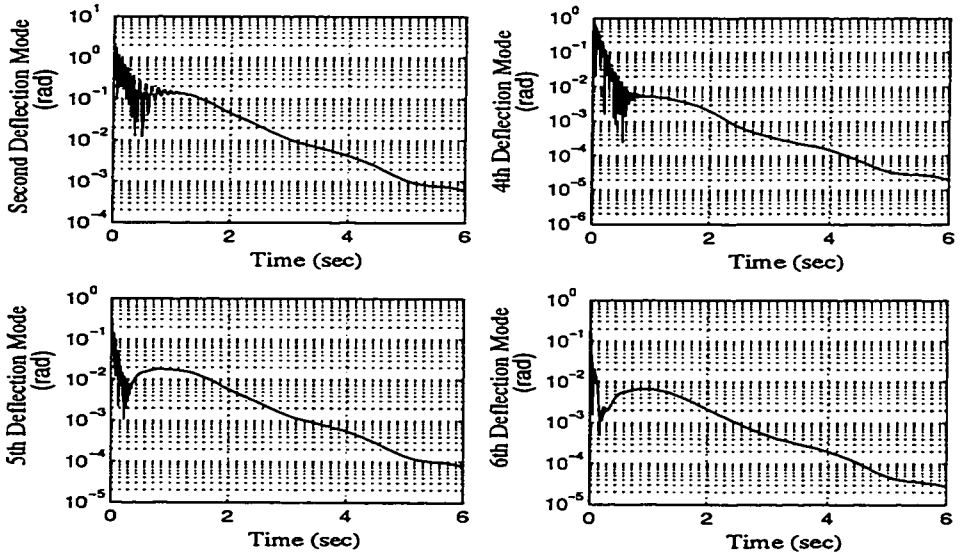

Figure 7.6: *Absolute values of the 3rd-6th deflection modes in response to 2π rad rotation of hub. The linear controller results in instability.*

Chapter 8

Conclusion and Directions for Future Research

For the purpose of robust control of a flexible-link manipulator, two types of modeling were studied. In the first type, the uncertainty is due to parameter variations of the manipulator while performing a task or when its configuration is changing. The uncertainties considered in this regard are due to deviations of parameters from their nominal values. These deviations may be L_2-bounded and/or constant. By using a nonlinear transformation, a dynamical model which has a constant *input vector field* (g in $\dot{x} = f(x) + g(x)\ u$) was obtained. This coordinate change was shown to be effective in designing nonlinear controllers that are normally complicated in nature.

To compensate the above mentioned uncertainties nonlinear H_∞ control techniques were employed. It was shown that this method provides the attenuation of disturbance effects on the penalty variable with a prescribed level of attenuation (γ). The maximum attenuation, i.e., the smallest possible γ, is not arbitrary and may be computed from the corresponding linear Riccati equation. The relationships between the problem in question to some basic notions like dissipativeness, differential games, and the Hamiltonian function were discussed. For designing the nonlinear H_∞ controller, the approximate polynomial solution of the Hamilton-Jacobi-Isaacs

(HJI) inequality for a general nonlinear system was derived.

By exploiting the stability properties of perturbed systems, the qualitative behaviors of nonlinear H_∞ controllers were considered. The effects of (i) the approximate solutions, (ii) attenuation level, and (iii) weighting the controlled output on the domain of validity of the HJI inequality were investigated. It was shown that (i) utilizing lower order approximations, (ii) increasing the attenuation level, and (iii) weighting the controlled output may result in a smaller domain of validity.

In the second type of modeling, uncertainty appears as in a norm-bounded perturbation. Based on this interpretation, flexible structures exhibit two kinds of behavior, one of which may be treated as a disturbance acting on the modeled dynamics. The principle behind the methodology proposed in this thesis is that the system under control should possess a two-time scale separation, namely, low and high-frequency subsystems. The restriction imposed is that the high-frequency subsystem should be stable in order to result in the norm-bounded property. The design based on the multi-objective H_∞ technique proceeds by considering the low-frequency subsystem while treating the high-frequency subsystem as *unmodeled dynamics*. One of the practical applications that fits into this framework is the flexible-link manipulator. In fact the rigid dynamics that characterize the dominant motion of the joints correspond to the low-frequency subsystem and the deflection dynamics due to flexibility of the links correspond to the high-frequency subsystem.

To design a robust controller for the model whose high-frequency subsystem is treated as uncertainty, the problem of multi-objective H_∞ control was posed. It is composed of two separate problems. The first problem is the robust regulation in which the tracking of the reference input for the disturbance-free system is sought. The second one is the H_∞ constraint problem where the goal is the attenuation of disturbances on the penalty variable. The problem of simultaneously solving these two problems is called the robust regulation problem with an H_∞ constraint. In the case of linear systems, the problem in question can be recast as a problem

of robust stabilization in the presence of norm-bounded uncertainties for a suitable augmented plant in which the regulated output drives an appropriate internal model of the exosystem. In the present work, the problem was approached in a similar way.

The above generalizations to the case of nonlinear systems were shown to be valid. The formulation leads to the study of the problem of robustly (and locally exponentially) stabilizing an augmented plant in the presence of unmodeled dynamics whose L_2 gain is bounded. It was shown that for the proposed model, the *nonlinear unmodeled dynamics* are norm-bounded. After designing the internal model, the problem of disturbance attenuation for the resulting augmented plant was considered. The synthesis proceeds through the solution of a Hamilton-Jacobi-Isaacs (HJI) inequality for the augmented plant.

In this dissertation we investigated both theoretical as well as simulation results for robust control of a flexible-link manipulator. Based on the knowledge and the experience gained in this respect, the following routes may be pursued for further enhancement of the analytical results and control design strategies.

Mixed singular perturbation/multi-objective H_∞ control

The methodology of modeling proposed in this thesis was based on the fact that the system under control possesses a two-time scale separation property, namely, low- and high-frequency subsystems. In this connection, one may exploit the method of *singular perturbations* for modeling the system possessing the two-time scale behavior. Application of *singular perturbation* theory [135] to such a system results in the following set of equations:

$$\dot{x} = F_s(x,\ z,\ u,\ \epsilon) \tag{8.1}$$

$$\epsilon\dot{z} = F_f(x,\ z,\ u,\ \epsilon) \tag{8.2}$$

where x is the state of the *slow* subsystem, z is the state of the *fast* subsystem, and ϵ is a singular perturbation parameter of the system. Now, it might be observed

that the strategy of adaptively controlling the system (8.1) by just neglecting the flexible dynamics (8.2) and considering z as a disturbance to the system is likely to fail, since no assumption on the boundedness of the disturbance can be made. This is due to the fact that, the synthesis in the present setting is only based on the *slow* subsystem and in fact the *fast* subsystem is neglected. In the composite control strategy of the form $u = u_s + u_f$, however, the control has a partitioned structure. Part of the control (u_f) has to take the *fast* states towards an equilibrium boundary layer, and the other part of control (u_s) works on the *slow* manifold to provide the desired behavior. The idea of multi-objective H_∞ control can be used in designing the controller for the *slow* subsystem, i.e., u_s where z is treated as *uncertainty*. It now becomes apparent that the other part of the control, i.e., u_f only has to stabilize the *fast* subsystem yielding the norm-boundedness property.

Real domain of validity of nonlinear H_∞ control

Our approach for qualitatively analyzing the behavior of the H_∞ control based closed-loop system uses a Lyapunov technique. Given that, in general, Lyapunov methods can only provide an estimate of the domain of attraction for a nonlinear system, it is not feasible to explicitly obtain the *exact* domain of validity of a nonlinear system by using this technique. In other words the purpose of Chapter 3 is *not* to explicitly *compute* the *exact* domain of validity; rather, the objective is to provide a methodology for comparing the *estimates* of domains of validity obtained by using different approximations of the nonlinear system. A more comprehensive treatment of the subject would require the comparison of the *real* domains of validity instead of their estimates. One possible approach in this regard might be incorporation of Zubov's theory [102]. This is due to the fact that for studying the stability property of a dynamical system, Zubov's theorem considers the exact domain of attraction.

Rate of convergence of nonlinear H_∞ control

In addition to the domain of validity which is essential in the field of nonlinear H_∞ control, there are some other issues that are related to the performance of the controllers designed using H_∞ techniques. One of the important issues that needs to be investigated is the rate of convergence. By applying the Gronwall-Bellman inequality it might be possible to construct a relationship between a Lyapunov function of the system and its time derivative.

Extension to a multi-link flexible manipulator

The new modeling approach proposed in this thesis was applied to a single-link flexible manipulator. A possible extension of the results is to consider a multi-link flexible manipulator and treat the dynamics of the higher frequency modes of each link as *uncertainty*.

Design based on measurement feedback

Throughout this dissertation, it was assumed that all the states of the plant are available for measurement. Obviously some of these states are available via standard sensors (such as hub angle, hub velocity and tip position). However, most of the states should be obtained in practice by means of sophisticated sensors or observers. Control of flexible-link manipulators based on measurement feedback should then use strategies similar to the ones presented in [91] and [92].

Appendix A

Link Data

L_0	1.2 m
A_0	.000976 m^2
m_b	1.356 Kg
ρ	1 Kg/m
I_0	0.27 $Kg.m^2$
J_0	0.109 $Kg.m^2$
M_L	45 g
J_L	0.00852 $Kg.m^2$
EI	2.44 $N.m^2$
F_c	0.59 $N.m.s$
C_{coul}	4.77 $N.m$
$\hat{\kappa}$	15

Table A.1: *Link parameters*

ω_1	3 rad/s	ξ_1	0.1125
ω_2	21 rad/s	ξ_2	0.0863
ω_3	60 rad/s	ξ_3	0.0833
ω_4	118 rad/s	ξ_4	0.0827
ω_5	196 rad/s	ξ_5	0.0828
ω_6	293 rad/s	ξ_6	0.0832

Table A.2: *Frequencies and damping ratios of the first six deflection modes*

Poles	Zeros
0	-8.3334
-135.71	-117.27
$-0.37745 \pm 3.334j$	20.187
$-1.8337 \pm 21.169j$	30.308
$-4.9834 \pm 59.624j$	$-69.519 \pm 32.394j$
$-9.7455 \pm 117.37j$	$73.184 \pm 96.891j$
$-16.186 \pm 194.83j$	$-112.53 \pm 194.17j$
$-24.391 \pm 292.22j$	$93.015 \pm 225.37j$

Table A.3: *Pole-zero locations of the 14^{th}–order model*

Appendix B

Monotonicity of Function $\hat{k}_0(s)$

Lemma B.1 *Suppose $k_0 < 1$. Then $\hat{k}_0(s)$ defined in (4.28) is a monotonic function of s.*

Proof: For notational simplicity we write k_1 instead of $\frac{k_1}{a}$. Since $k_0 < 1$, then

$$\sum_{j=s-2}^{\infty} k_0^j = \frac{k_o^{s-2}}{1-k_o} > 0, \quad s \geq 2$$

For any value of s_0, we now show that $\hat{k}_0(s_0) < \hat{k}_0(s_0+1)$. Towards this end, we have to obtain the least upper bound on the values of y_0 and z_0 satisfying the following inequalities:

$$0 < \frac{y_0^{s_0-2}}{1-y_0} < k_1 \quad \text{and} \quad 0 < \frac{z_0^{s_0-1}}{1-z_0} < k_1 \tag{B.1}$$

or

$$\begin{aligned} y_0^{s_0-1} &< k_1\ y_0(1-y_0) < k_1\ y_0 := k_2 < k_1 \\ z_0^{s_0-1} &< k_1(1-z_0) < k_1 \end{aligned}$$

As a result,

$$y_0 < k_2^{\frac{1}{s_0-1}} \quad \text{and} \quad z_0 < k_1^{\frac{1}{s_0-1}}$$

which implies that $\sup\{y_0\} < \sup\{z_0\}$. This completes the proof of the Lemma. $\triangle$

Appendix C

State-Space Transformations

Transformation for setting the first state as the output

The transformation that transforms X in (6.5) to (6.7) is given by

$$T_X = \begin{bmatrix} l & 0 & \phi_1(l) & 0 & \cdots & \phi_m(l) & 0 \\ 0 & & & & & & \\ \vdots & & & I_{(2m+1)} & & & \\ 0 & & & & & & \end{bmatrix}$$

Note that $T_X\ A\ T_X^{-1} = T_X A$ and $T_X\ B = B$.

Transformation between configuration-space and state-space

The transformation T that transforms the state-space equations from q defined in (6.37) to X defined in (6.6) coordinates may be obtained as follows. Let n and m_i $(i = 1 \ ... \ n)$ denote the number of joints and deflection modes of the ith link,

respectively. Let $r := n + m$ where $m = \sum_{i=1}^{n} m_i$. Suppose e_i is the $i-$th row of a $2r$th order identity matrix. Define

$$E_i = \begin{pmatrix} e_i \\ e_{r+i} \end{pmatrix}, \qquad \hat{E}_i = \begin{pmatrix} e_{n+i} \\ e_{n+i+r-1} \end{pmatrix}$$

Then, the matrix T is given by $T = T_2 T_1$ where

$$T_1 = \left[E_1^T, E_2^T, \ldots, E_n^T, \hat{E}_1^T, \hat{E}_2^T, \ldots, \hat{E}_m^T \right]^T$$

and T_2 is a matrix that diagonalizes the resulting representation.

Appendix D

Simulation Data

System data

$$A_x = \begin{bmatrix} 0 & 0.0015 & 0.5204 & -1.5131 & 0.1341 & 1.4687 & 1.0600 & -0.8021 \\ 0 & -135.5185 & 0.0000 & 0.0000 & 0.0000 & 0.0000 & 0.0000 & 0.0000 \\ 0 & 0.0000 & -0.3774 & 3.3346 & 0.0000 & -0.0000 & -0.0000 & -0.0000 \\ 0 & 0.0000 & -3.3346 & -0.3774 & -0.0000 & -0.0000 & 0.0000 & 0.0000 \\ 0 & -0.0000 & -0.0000 & -0.0000 & -1.8338 & 21.1698 & -0.0000 & 0.0000 \\ 0 & -0.0000 & -0.0000 & -0.0000 & -21.1696 & -1.8338 & 0.0000 & 0.0000 \\ 0 & 0.0000 & -0.0000 & -0.0000 & 0.0000 & -0.0000 & -4.9862 & 59.6315 \\ 0 & -0.0000 & -0.0000 & -0.0000 & -0.0000 & 0.0000 & -59.6316 & -4.9862 \end{bmatrix}$$

$$A_{xv} = \begin{bmatrix} 0.8268 & 0.8514 & -1.0557 & -0.0335 & 0.8783 & -0.2318 \\ 0.0000 & -0.0000 & 0.0000 & -0.0000 & -0.0000 & -0.0000 \\ 0.0000 & -0.0000 & -0.0000 & -0.0000 & -0.0000 & -0.0000 \\ -0.0000 & 0.0000 & -0.0000 & 0.0000 & -0.0000 & -0.0000 \\ 0.0000 & 0.0000 & 0.0000 & -0.0000 & -0.0000 & -0.0000 \\ 0.0000 & -0.0000 & 0.0000 & -0.0001 & 0.0000 & 0.0000 \\ 0.0000 & 0.0000 & 0.0000 & -0.0000 & -0.0000 & -0.0000 \\ 0.0000 & 0.0000 & 0.0000 & -0.0000 & -0.0000 & -0.0000 \end{bmatrix}, \quad B_x = \begin{bmatrix} 0.0000 \\ -4.5272 \\ 0.0639 \\ 0.0122 \\ 0.0632 \\ -0.0077 \\ 0.0226 \\ 0.0560 \end{bmatrix}$$

$$A_v = \begin{bmatrix} -9.7598 & 117.4250 & -0.0000 & -0.0000 & -0.0000 & -0.0000 \\ -117.4250 & -9.7599 & -0.0000 & 0.0000 & 0.0000 & 0.0000 \\ -0.0000 & 0.0000 & -16.2488 & 195.0503 & 0.0000 & 0.0000 \\ 0.0000 & 0.0000 & -195.0501 & -16.2487 & 0.0000 & -0.0000 \\ -0.0000 & 0.0000 & 0.0000 & 0.0000 & -24.5282 & 292.7370 \\ 0.0000 & 0.0000 & 0.0000 & -0.0000 & -292.7361 & -24.5287 \end{bmatrix}, \quad B_v = \begin{bmatrix} 0.0501 \\ -0.0100 \\ 0.0303 \\ -0.0242 \\ 0.0141 \\ -0.0142 \end{bmatrix}$$

$$C_v = \begin{bmatrix} 0.8268 & 0.8514 & -1.0557 & -0.0335 & 0.8783 & -0.2318 \end{bmatrix}$$

Perturbation on matrix A (same for both cases), $\Delta_A = \text{diag}\left(\Delta_{A_x} \quad \Delta_{A_v} \right)$ with

$$\Delta_{A_x} = \text{diag}\left(2.2822 \quad 0.5262 \quad 2.3847 \quad 1.3504 \quad 1.3570 \quad 1.7491 \quad 0.5164 \quad 2.0552 \right)$$

$$\Delta_{A_v} = \text{diag}\left(2.9595 \quad 2.0654 \quad 3.3439 \quad 1.9465 \quad 0.5185 \quad 3.4416 \right)$$

Controller data for the proposed model

$$A_{c_p} = \left[0 \right], \quad B_{c_p} = \left[1 \quad 0 \quad 0 \quad 0 \quad 0 \quad 0 \quad 0 \quad 0 \right]$$

$$C_{c_p} = \left[-19.1391 \right], \quad D_{c_p} = 10^4 \left[-4.5852 \quad -0.0000 \quad -1.7261 \quad 3.8459 \quad 0.2997 \quad 0.6245 \quad -0.1226 \quad 0.1580 \right]$$

Controller data for the standard model

$$A_{c_s} = \left[0 \right], \quad B_{c_s} = \left[1 \quad 0 \quad 0 \quad 0 \quad 0 \quad 0 \quad 0 \quad 0 \right]$$

$$C_{c_s} = \left[-3.3333 \right], \quad D_{c_s} = 10^3 \left[-3.6022 \quad -0.0000 \quad -3.3549 \quad 6.0303 \quad -1.6145 \quad 0.6905 \quad -0.0661 \quad -0.0666 \right]$$

Bibliography

[1] Sobel, K.M., Banda, S.S., and Shapiro, E.Y., "Robust Modalized Observer with Flight Control Application," in *Proceedings of the 27th IEEE Conference on Decision and Control*, pp. 1018–1019, 1988.

[2] Petkovski, D.B., "Iterative Algorithm for Improved Measures of Stability Robustness for Linear State-Space Models," *International Journal of Systems Science*, vol. 20, pp. 1565–1573, Aug 1989.

[3] Engelberger, J.F., ed., *"Robotics in Practice"*. London: Kogan Page, 1980.

[4] Book, W.J., "Modeling, Design, and Control of Flexible Manipulator Arms : A Tutorial Review," in *Proceedings of the 29th IEEE Conference on Decision and Control*, December 1990.

[5] Moudgal, V.G., Passino, K.M., and Yurkovich, S., "Rule-Based Control for a Flexible-Link Robot," *IEEE Trans. on Control Systems Technology*, vol. 2, pp. 392–405, December 1994.

[6] Gevarter, W.B., "Basic Relations for Control of Flexible Vehicles," *AIAA Journal*, April 1970.

[7] Isidori, A., *"Nonlinear Control Systems: An Introduction"*. Springer-Verlag, 2nd ed., 1989.

[8] Banavar, R.N. and Dominic, P., "An LQG/H_∞ Controller for a Flexible Manipulator," *IEEE Trans. on Control Systems Technology*, vol. 3, pp. 409–416, December 1995.

[9] Tarn, T.J., Bejcky, A.K., and Ding, X., "Nonlinear Feedback in Robot Arm Control," Robot. Lab. Rep. SSM–RL–88–11, Washington Univ., St. Louis, MO, 1988.

[10] Rattan, K.S. and Feliu, V., "Feedforward Control of Flexible Manipulators," in *Proceedings of IEEE Int. Conference on Robotics and Automation*, May 1992.

[11] Cannon, R.H. and Schmitz, E., "Initial Experiments on the End-Point Control of a Flexible One-Link Robot," *Int. J. of Robotics Research*, vol. 18, pp. 62–75, Fall 1984.

[12] Book, W.J., "Recursive Lagrangian Dynamics of Flexible Manipulator Arms," *Int. J. of Robotics Research*, vol. 3, pp. 87–101, Fall 1984.

[13] Kanoh, H., "Distributed Parameter Models of Flexible Robot Arms," *Advanced Robotics*, vol. 5, pp. 87–99, 1991.

[14] Bayo, E., "A Finite-Element Approach to Control the End-Point Motion of a Single-Link Flexible Robot," *J. of Robotic Systems*, vol. 4, no. 1, 1987.

[15] Usoro, P.B., Nadira, R., and Mahil, S.S., "A Finite Element/Lagrange Approach to Modeling Lightwight Flexible Manipulators," *ASME J. of Dynamic Systems, Measurement and Control*, vol. 110, pp. 198–205, September 1988.

[16] Chedmail, P. and Michel, G., "Modelisation of Plane Flexible Robots," in *Proceedings of the 15th ISIR*, (Tokyo, Japan), pp. 1083–1090, 1992.

[17] De Luca, A. and Siciliano, B., "Trajectory Control of a Nonlinear One-Link Flexible Arm," *Int. J. Control*, vol. 50, no. 5, 1989.

[18] Cetinkunt, S. and Book, W.J., "Symbolic Modeling and Dynamic Simulation of Robotic Manipulators with Compliant Links and Joints," *Int. J. Robotics Comput. Integrated Manuf.*, vol. 5, no. 4, pp. 301–310, 1989.

[19] Geniele, H., Patel, R.V., and Khorasani, K., "Control of a Flexible-Link Manipulator," in *Proceedings of the Fourth Int. Symp. on Robotics and Manufacturing*, (Sante Fe, New Mexico), pp. 567–572, November 1992.

[20] Geniele, H., Patel, R.V., and Khorasani, K., "Control of a flexible-link manipulator," in *Proceedings of the IEEE Int. Conf. on Robotics and Automation*, pp. 1217–1222, 1995.

[21] Kwon, D.S. and Book, W.J., "An Inverse Dynamic Method Yielding Flexible Manipulator State Trajectories," in *Proceedings of the American Control Conference*, 1993.

[22] Hennessey, M.P., Priebe, J.A., Huang, P.C., and Grommes, R.J., "Design of a Lightweight Robotic Arm and Controller," in *Proceedings of IEEE Int. Conference on Robotics and Automation*, (Raleigh, NC), pp. 779–785, 1987.

[23] Serna, A.M. and Bayo, E., "Trajectory Planning for Flexible Manipulators," in *Proceedings of IEEE Proceedings of IEEE Int. Conference on Robotics and Automation*, pp. 910–915, 1990.

[24] Singhose, E.W., Seering, W.P., and Singer, N.C., "Shaping Inputs to Reduce Vibration: A Vector Diagram Approach," in *Proceedings of IEEE Int. Conference on Robotics and Automation*, pp. 915–920, 1990.

[25] Farsi, M., Finch, J.S., Warwick, K., Tzafestas, S.G., and Stasinopoulos, G., "Simplified PID Self-Tuning Controller for Robotic Manipulators," in *Proceedings of the 25th IEEE Conference on Decision and Control*, pp. 1886–1890, December 1986.

[26] Karkkainen, P., "Compensation of Manipulator Flexibility Effects by Modal Space Techniques," in *Proceedings of IEEE Int. Conference on Robotics and Automation*, 1985.

[27] Lambert, M., *"Adaptive Control of Flexible Systems"*. PhD thesis, Oxford, 1987.

[28] Siciliano, B., Yuan, B., and Book, W.J., "Model Reference Adaptive Control of a One-Link Flexible Arm," in *Proceedings of the 25th IEEE Conference on Decision and Control*, 1986.

[29] Balas, M.J., "Feedback Control of Flexible Systems," *IEEE Trans. on Automatic Control*, vol. 23, pp. 673–679, August 1978.

[30] Khorasani, K., "Adaptive Control of Flexible-Joint Robots," *IEEE Trans. on Robotics and Automation*, vol. 8, pp. 250–267, April 1992.

[31] Siciliano, B., Book, W.J., and De Maria, G., "An Integral Manifold Approach to Control a One-Link Flexible Arm," in *Proceedings of the 25th IEEE Conference on Decision and Control*, 1986.

[32] Aoustin, Y. and Chevallereau, C., "The Singular Perturbation Control of a Two-Flexible-Link Robot," *IEEE Trans. on Robotics and Automation*, pp. 737–742, May 1993.

[33] Bouaziz, B., Dochain, D., Piedboeuf, J.C., and Hurteau, R., "Singular Perturbation Approach to Modeling and Control of Flexible Manipulators," in *Second IEEE Conference on Control Applications*, September 1993.

[34] Khorasani, K. and Spong, M.W., "Invariant Manifolds and Their Application to Robot Manipulators with Flexible Joints," in *Proceedings of IEEE Int. Conference on Robotics and Automation*, March 1985.

[35] Siciliano, B. and Book, W.J., "A Singular Perturbation Approach to Control of Lightweight Flexible Manipulators," *Int. J. of Robotics Research*, vol. 7, pp. 79–90, August 1988.

[36] Gauthier, J.P., "H_∞ Control of a Distributed Parameter System with Non-Minimum Phase," *Int. J. Control*, vol. 53, no. 1, pp. 45–79, 1991.

[37] Lin, L.C., "State Feedback H_∞ Control of Manipulators with Flexible Joints and Links," in *Proceedings of IEEE Int. Conference on Robotics and Automation*, April 1991.

[38] Chen, B.S., Lee, T.S., and Feng, J.H., "A Nonlinear H_∞ Control Design in Robotic Systems Under Parameter Perturbation and External Disturbance," *Int. J. Control*, vol. 59, no. 2, pp. 439–461, 1994.

[39] Meressi, T. and Paden, B., "Gain Scheduled H_∞ Controllers for a Two-Link Flexible Manipulator," *AIAA J. Guidance, Control and Dynamics*, vol. 17, pp. 537–543, May-June 1994.

[40] Doyle, J.C., "Guaranteed Margins for LQG Regulators," *IEEE Trans. on Automatic Control*, vol. 34, pp. 831–847, 1981.

[41] Maciejowski, J.M., *Multivariable Feedback Design.* Addison-Wesley, 1989.

[42] Hashtrudi–Zaad, K. and Khorasani, K., "Control of Nonminimum Phase Singularly Perturbed Systems with Applications to Flexible Link Manipulators," *International Journal of Control*, vol. 63, pp. 679–701, March 1996.

[43] Hashtrudi–Zaad, K. and Khorasani, K., "An Integral Manifold Approach to Tracking Control for a class of Non-minimum Phase Linear Systems Using Output Feedback," *Automatica*, vol. 32, pp. 1533–1552, March 1996.

[44] Moallem, M., Khorasani, K., and Patel, R.V., "Tip Position Tracking of Flexible Multi–Link Manipulators: An Integral Manifold Approach," in *Proceedings of the 1997 IEEE International Conference on Robotics and Automation*, IEEE, 1997.

[45] Panzieri, S. and Ulivi, G., "Design and Implementation of a State Observer for a Flexible Robot," *IEEE Trans. on Robotics and Automation*, May 1993.

[46] Alder, L.J. and Rock, S.M., "Adaptive Control of a Flexible-Link Robotic Manipulator with Unknown Payload Dynamics," in *Proceedings of the American Control Conference*, June 1993.

[47] Rokui, M.R. and Khorasani, K., "Adaptive Tracking Control of a Flexible Link Manipulator Based on the Discrete-time Nonlinear Model," in *Proceedings of the American Control Conference*, vol. 3, (Albuquerque, New Mexico), June 1997.

[48] Garcia-Benitez, E., Watkins, J., and Yurkovich, S., "Nonlinear Control with Acceleration Feedback for a Two-Link Flexible Robot," *Contr. Eng. Practice, IFAC Journal*, vol. 1, no. 6, pp. 987–989, 1993.

[49] Tzes, A.P. and Yurkovich, S., "Application and Comparison of On-Line Identification Methods for Flexible Manipulator Control," *J. of Robotic Res.*, vol. 10, no. 5, pp. 515–527, 1991.

[50] Yurkovich, S., Pacheo, F.E., and Tzes, A. P., "On-Line Frequency Domain Information for Control of a Flexible-Link Robot with Varying Payload," in *Proceedings of the 28th IEEE Conference on Decision and Control*, 1989.

[51] Yurkovich, S. and Pacheco, F.E., "On Controller Turning for a Flexible-Link Manipulator with Varying Load," *J. of Robotic Systems*, vol. 6, pp. 233–254, 1989.

[52] Yurkovich, S., Tzes, A.P., and Hillsley, K.L., "Identification and Control for a Manipulator with Two Flexible Links," in *Proceedings of the 29th IEEE Conference on Decision and Control*, December 1990.

[53] Moallem, M., Patel, R.V., and Khorasani, K., "An Inverse Dynamics Control Strategy for Tip Position Tracking of Flexible Multi–Link Manipulators," in *Proceedings of the International Federation of Automatic Control 13th World Congress*, pp. 85–90, 1996.

[54] Moallem, M., Patel, R.V., and Khorasani, K., "An Observer–Based Inverse Dynamics Control Strategy for Flexible Multi–Link Manipulators," in *Proceedings of the 35th IEEE Conference on Decision and Control*, (Kobe, Japan), 1996.

[55] Moallem, M., Patel, R.V., and Khorasani, K., "Experimental Results for Nonlinear Decoupling Control of Flexible Multi–Link Manipulators," in *Proceedings of IEEE International Conference on Robotics and Automation*, 1997.

[56] Moallem, M., Khorasani, K., and Patel, R.V., "Inverse Dynamics Sliding Control of Flexible Multi–Link Manipulators," in *Proceedings of the American Control Conference*, vol. 4, (Albuquerque, New Mexico), June 1997.

[57] Aoustin, Y., Chevallereau, C., and Moog, C.H., "Experimental Results for the End-Effector Control of a Single Flexible Robot Arm," *IEEE Trans. on Control Systems Technology*, vol. 2, pp. 371–381, December 1994.

[58] Gross, E. and Tomizuka, M., "Experimental Flexible Beam Tip Tracking Control with a Truncated Series Approximation to Uncancelable Inverse Dynamics," *IEEE Trans. on Control Systems Technology*, vol. 2, pp. 382–391, December 1994.

[59] Yurkovich, S., "Motion and Vibration Control Using Command Shaping Methods," in *Proceedings of the American Control Conference*, June 1993.

[60] Hillsley, K.L. and Yurkovich, S., "Vibration Control of a Two-Link Flexible Robot Arm," in *Proceedings of IEEE Int. Conference on Robotics and Automation*, April 1991.

[61] Magee, D.P. and Book, W.J., "Eliminating Multiple Modes of Vibration in a Flexible Manipulator," in *Proceedings of IEEE Int. Conference on Robotics and Automation*, pp. 474–479, 1993.

[62] Tzes, A. and Yurkovich, S., "An Adaptive Input Shaping Control Scheme for Vibration Suppression in Slewing Flexible Structures," *IEEE Trans. on Control Systems Tehnology*, vol. 1, pp. 114–121, June 1993.

[63] Meckl, P.H. and Kinceler, R., "Robust Motion Control of Flexible Systems Using Feedforward Forcing Functions," *IEEE Trans. on Control Systems Technology*, vol. 2, pp. 245–254, September 1994.

[64] Kubica, E. and Wang, D., "A Fuzzy Control Strategy for a Flexible-Link Robot," in *Proceedings of IEEE Int. Conference on Robotics and Automation*, pp. 236–241, 1993.

[65] Moudgal, V.G., Kwong, W.A., Passino, K.M., and Yurkovich, S., "Fuzzy Learning Control for a Flexible-Link Robot," in *Proceedings of the American Control Conference*, pp. 563–567, June 1994.

[66] Garcia-Benitez, E., Yurkovich, S., and Passino, K.M., "A Fuzzy Supervisor for Flexible Manipulator Control," in *Proc. 1991 IEEE Int. Symp. Intel. Contr.*, (Arlington, VA), pp. 37–42, 1991.

[67] Garcia-Benitez, E., Yurkovich, S., and Passino, K.M., "Rule-Based Supervisory Control of a Two-Link Flexible Manipulator," *J. Intell. Robotic Syst.*, vol. 7, pp. 195–213, 1993.

[68] Moudgal, V.G., Passino, K.M., and Yurkovich, S., "Expert Supervisory Control for a Two-Link Flexible Robot," in *Proceedings of IEEE Int. Conference on Robotics and Automation*, pp. 236–241, 1993.

[69] Mahmmood, N. and Walcott, B.L., "Neural Network Based Adaptive Control of a Flexible Link Manipulator," in *Proceedings of the IEEE National Aerospace and Electronics Conference*, (Piscataway, NJ), pp. 851–857, 1993.

[70] Yesildirek, A., Vandegrift, M.W., and Lewis, F.L., "Neural Network Controller for Flexible-Link Robots," in *Proceedings of IEEE International Symposium on Intelligent Control*, (Piscataway, NJ), pp. 63–68, 1994.

[71] Nemir, D.C., Koivo, A.J. , and Kashyap, R.L., "Pseudolinks and the Self-Tuning Control of a Nonrigid Link Mechanism ," *IEEE Trans. Systems, Man and Cybernetics*, vol. 18, pp. 40–48, Feb. 1988.

[72] King, J.O., Gourishankar, V.G., and Rink, R.E., "Composite Pseudolink End-Point Control of Flexible Manipulators," *IEEE Trans. on Systems, Man and Cybernetics*, vol. 20, pp. 969–977, October 1990.

[73] Talebi, H.A., Khorasani, K., and Patel, R.V., "Experimental Evaluation of Neural Network–based Controllers for Tip Position Tracking of a Flexible-Link Manipulator," in *Proceedings of the IEEE International Conference on Robotics and Automation*, vol. 4, pp. 3300–3305, 1997.

[74] Craig, J.J., *Introduction to Robotics: Mechanics and Control.* Addison-Wesley, 2nd ed., 1989.

[75] Meirovitch, L., *Elements of Vibration Analysis.* McGraw-Hill, 1986.

[76] Meirovitch, L., *Analytical Methods in Vibrations.* The Macmillan Company, 1967.

[77] Wang, D. and Vidyasagar, M., "Transfer Functions for a Single Flexible Link," in *Proceedings of the 28th IEEE Conference on Decision and Control*, 1989.

[78] Geniele, H., "Control of a Flexible-Link Manipulator," Master's thesis, Concordia University, Montreal, Canada, 1994.

[79] Yazdanpanah, M.J., "Utilizing MAPLE and MATLAB for Modeling A Single-Link Flexible Manipulator and Designing A Nonlinear H_∞ Controller." Internal report, Dept of Electrical Eng. and Computer Science, Concordia University, 1995.

[80] Fraser, A.R. and Daniel, R.W., *Perturbation Techniques for Flexible Manipulators.* Kluwer Academic Publishers, 1991.

[81] Cetinkunt, S. and Book, W.J., "Performance Limitations of Joint Variable-Feedback Controllers Due to Manipulator Struactural Flexibility," *IEEE Trans. on Robotics and Automation*, vol. 6, April 1990.

[82] Sunada, W.H. and Dubowsky, S., "On the Dynamic Analysis and Behavior of Industrial Robotic Manipulators With Elastic Members," *Trans. of the ASME; Journal of Mechanical Design*, vol. 104, pp. 42–51, 1983.

[83] Luh, J.Y.S., "Conventional Controller Design for Industrial Robots–A Tutorial," *IEEE Trans. on Systems, Man and Cybernetics*, vol. SMC-12, pp. 298–316, May/June 1983.

[84] Stoorvogel, A., *H_∞ Control Problem.* Prentice Hall, 1992.

[85] Hill, D. and Moylan, P., "Dissipative Dynamical Systems: Basic Input-Output and State Properties," *Journal of the Franklin Instiute*, vol. 309, pp. 327–357, May 1980.

[86] van der Schaft, A.J., "On a State Space Approach to Nonlinear H_∞ Control," *Systems & Control Letters*, vol. 16, pp. 1–8, 1991.

[87] Basar, T. and Bernhard, P., *H_∞ Optimal Control and Related Minimax Design Problems, A Dynamic Game Approach.* Birkhauser, 1991.

[88] Ball, J. A. and W. Helton, "Factorization of Nonlinear Systems: Toward a Theory for Nonlinear H_∞ Control ," in *Proceedings of the 27th IEEE Conference on Decision and Control*, December 1988.

[89] Ball, J.A. and Helton, W., "H_∞ Control for Nonlinear Plants: Connections with Differential Games," in *Proceedings of the 28th IEEE Conference on Decision and Control*, December 1989.

[90] van der Schaft, A. J., "L_2-Gain Analysis of Nonlinear Systems and Nonlinear State Feedback H_∞ Control," *IEEE Trans. on Automatic Control*, vol. 37, pp. 770–784, June 1992.

[91] Isidori, A. and Astolfi, A., "Disturbance Attenuation and H_∞-Control via Measurement Feedback in Nonlinear Systems ," *IEEE Trans. on Automatic Control*, vol. 37, pp. 1283–1293, September 1992.

[92] Isidori, A. and Tarn, T.J., "Robust Regulation for Nonlinear Systems with Bounded Uncertainties," *IEEE Trans. on Automatic Control*, vol. 40, pp. 1744–1754, October 1995.

[93] Isidori, A. and Kang, W., "H_∞ Control via Measurement Feedback for General Nonlinear Systems," *IEEE Trans. on Automatic Control*, vol. 40, pp. 466–472, March 1995.

[94] Nijmeijer, H. and Van der Schaft, A., *Nonlinear Dynamical Control Systems.* Springer-Verlag, 1990.

[95] Basar, T. and Oldser, G.J., *Dynamic Noncooperative Game Theory.* Academic Press, 1982.

[96] Friedman, A., *Differential Games.* Wiley-International, 1971.

[97] Lukes, D.L., "Optimal Regulation of Nonlinear Dynamical Systems," *SIAM J. Control*, vol. 7, pp. 75–100, February 1969.

[98] Li, X.P. and Chang, B.C., "Properties of H_∞ Riccati Solutions," in *Control of Uncertain Dynamic Systems* (Bhattacharyya, S.P. and Keel, L.H., eds.), (San Antonio, Texas), pp. 77–94, CRC Press, 1991.

[99] van der Schaft, A.J., "Nonlinear H_∞ State Space Control Theory," in *Essays on Control: Perspectives in the Theory and its Applications*, pp. 153–190, Birkhauser, 1993.

[100] Isidori, A., "H_∞ Control via Measurement Feedback for Affine Nonlinear Systems," *International Journal of Robust and Nonlinear Control*, vol. 4, pp. 553–574, 1994.

[101] Isidori, A., "Feedback Control of Nonlinear Systems," in *European Control Conference*, (Grenoble, France), pp. 1001–1012, July 1991.

[102] Kang, W., "Zubov's Theorem and Domain of Attraction for Controlled Dynamical Systems," in *Nonlinear Control Systems Design* (Krener, A.J. and Mayne, D.Q., eds.), pp. 143–146, IFAC, June 1995.

[103] Kang, W., De, P.K., and Isidori, A., "Flight Control in a Windshear via Nonlinear H_∞ Methods," in *Proceedings of the 31st IEEE Conference on Decision and Control*, December 1992.

[104] Khalil, H.K., *Nonlinear Systems.* Macmillan Publishing Company, 1992.

[105] Willems, J.L., *Stability Theory of Dynamical Systems.* Nelson, 1970.

[106] Astolfi, A. and Lanari, L, "Disturbance Attenuation and Set-Point Regulation of Rigid Robots via H_∞ Control," in *Proceedings of the 33rd IEEE Conference on Decision and Control*, December 1994.

[107] Vidyasagar, M., *Nonlinear Systems Analysis.* Prentice Hall, 2nd ed., 1993.

[108] Astolfi, A. and Guzzella, L., "Robust Control of Nonlinear Systems: An H_∞ Approach," in *Proceedings of the 12th IFAC Triennial World Congress*, (Sydney, Australia), pp. 281–284, 1993.

[109] Isidori, A. and Tarn, T.J., "Dissipation Inequalities for a Class of Composite Nonlinear Systems, with Application to Constrained Disturbance Attenuation," in *Proceedings of the 32nd IEEE Conference on Decision and Control*, December 1993.

[110] Byrnes, C.I., Isidori, A., and Willems, J.C., "Passivity, Feedback Equivalence, and the Global Stabilization of Minimum Phase Nonlinear Systems," *IEEE Trans. on Automatic Control*, vol. 36, pp. 1228–1240, November 1991.

[111] Abedor, J., Nagpal, K., Khargonekar, P P., and Poolla, K., "Robust Regulation in the Presence of Norm-Bounded Uncertainty," *IEEE Trans. on Automatic Control*, vol. 40, pp. 147–153, January 1995.

[112] Pernebo, L. and Silverman, L.M., "Model Reduction via Balanced State Space Representations," *IEEE Trans. on Automatic Control*, vol. 27, pp. 382–387, April 1982.

[113] Gawronski, W., "Balanced LQG Compensator for Flexible Structures," in *Proceedings of the American Control Conference*, June 1993.

[114] Doyle, J.C., Francis, B.A., and Tannenbaum, A.R., *"Feedback Control Theory"*. Macmillan Publishing Company, 1992.

[115] Gawronski, W., *Balanced Control of Flexible Structures.* Springer, 1996.

[116] Moore, B.C., "Principal Component Analysis in Linear Systems: Controllability, Observability, and Model Reduction," *IEEE Trans. on Automatic Control*, vol. 26, pp. 17–32, February 1981.

[117] Gawronski, W., "Computation of H_∞ Norm for Flexible Structures," in *Proceedings of the American Control Conference*, June 1993.

[118] Jonckheere, E.A., "Principal Component Analysis of Flexible Systems–Open-Loop Case," *IEEE Trans. on Automatic Control*, vol. 29, pp. 1095–1097, December 1984.

[119] Gregory, C.Z. Jr., "Reduction of Large Flexible Spacecraft Models Using Internal Balancing Theory," *AIAA J. Guidance, Control and Dynamics*, vol. 17, no. 6, pp. 725–732, 1984.

[120] Abedor, J., Nagpal, K, Khargonekar, P.P., and Poola, K., "Robust Regulation with an H_∞ Constraint," in *Control of Uncertain Dynamic Systems* (Bhattacharyya, S.P. and Keel, L.H., eds.), (San Antonio, Texas), pp. 95–110, 1991.

[121] Francis, B.A. and Wonham, W.M., "The Internal Model Principle of Control Theory," *Automatica*, vol. 12, pp. 457–465, 1976.

[122] Boyd,S., El Ghaoui, L., Feron, E., and Balakrishnan, V., *Linear Matrix Inequalites in Systems and Control Theory.* SIAM : Society for Industrial and Applied Mathematics, 1994.

[123] Doyle, J.C., Glover, K., Khargonekar, P.P., and Francis, B.A., "State-Space Solutions to Standard H_∞ and H_2 Control Problems," *IEEE Trans. on Automatic Control*, vol. 34, pp. 123–132, August 1989.

[124] El Ghaoui, L., Delebecque, F., and Nikoukhah, R., `LMITOOL`*: A User Friendly Interface for LMI Optimization, User's Guide.* ENSTA, Paris, Beta Version ed., 1995.

[125] Vandenberghe, L. and Boyd, S., `SP`*: Software for Semidefinite Programming : User's Guide.* Stanford University, Beta Version ed., 1994.

[126] Davison, E.J., "The Robust Control of a Servomechanism Problem for Linear Time-Invariant Multvariable Systems," *IEEE Trans. on Automatic Control*, vol. 21, pp. 25–34, February 1976.

[127] Patel, R.V. and Munro, N., *Multivariable System Theory and Design.* Pergamon Press, 1982.

[128] Vidyasagar, H., *Control System Synthesis: A Factorization Approach.* Cambridge, Massachusetts: The MIT Press, 1985.

[129] Zames, G., "Feedback and Optimal Sensitivity: Model Reference Transformation, Multiplicative Seminorms and Approximate Inverse," *IEEE Trans. on Automatic Control*, vol. 26, pp. 301–320, 1981.

[130] Isidori, A. and Tarn, T.J., "Robust Regulation for Nonlinear Systems with Gain-Bounded Uncertainties," *IEEE Trans. on Automatic Control*, vol. 40, pp. 1744–1754, October 1995.

[131] Hill, D. and Moylan, P., "Stability Results for Nonlinear Feedback Systems," *Automatica*, vol. 13, pp. 377–382, 1977.

[132] Isidori, A. and Byrnes, C., "Output Regulation of Nonlinear Systems," *IEEE Trans. on Automatic Control*, vol. 35, pp. 131–140, Feb. 1990.

[133] Huang, J. and Rugh, W., "An Approximation Method for Nonlinear Servomechanism Problem," *IEEE Trans. on Automatic Control*, vol. 37, pp. 1395–1398, 1992.

[134] Huang, J. and Lin, C.F., "On a Robust Nonlinear Servomechanism Problem," in *Proceedings of the 30th IEEE Conference on Decision and Control*, December 1991.

[135] Saksena, V.R., O'Reilly, J., and Kokotovic, P.V., "Singular Perturbations and Time-Scale Methods in Control, Theory: Survey 1976-1983 ," *Automatica*, vol. 20, pp. 273–293, May 1984.